UNIVERSIDAD COMPLUTENSE DE MADRID
FACULTAD DE CIENCIAS QUÍMICAS
Departamento de Bioquímica y Biología Molecular

TESIS DOCTORAL

Domesticating predatory bacteria for biotechnological tools

Bacterias depredadoras para ser aplicadas en procesos biotecnológicos

MEMORIA PARA OPTAR AL GRADO DE DOCTOR

PRESENTADA POR

Cristina Herencias Rodríguez

Directora

Mª Auxiliadora Prieto Jiménez

Madrid
Ed. electrónica 2019

UNIVERSIDAD COMPLUTENSE DE MADRID

Facultad de Ciencias Químicas

Departamento de Bioquímica y Biología Molecular

DOMESTICATING PREDATORY BACTERIA FOR BIOTECHNOLOGICAL TOOLS

BACTERIAS DEPREDADORAS PARA SER APLICADAS EN PROCESOS BIOTECNOLÓGICOS

Tesis doctoral

Cristina Herencias Rodríguez

Directora

Mª Auxiliadora Prieto Jiménez

Madrid, 2019

UNIVERSIDAD COMPLUTENSE DE MADRID

Facultad de Ciencias Químicas

Departamento de Bioquímica y Biología Molecular

DOMESTICATING PREDATORY BACTERIA FOR BIOTECHNOLOGICAL TOOLS

BACTERIAS DEPREDADORAS PARA SER APLICADAS EN PROCESOS BIOTECNOLÓGICOS

Tesis doctoral

Cristina Herencias Rodríguez

Directora

María Auxiliadora Prieto Jiménez

Consejo Superior de Investigaciones Científicas – CSIC

Centro de Investigaciones Biológicas - CIB

Madrid, 2019

And those who were seen dancing were thought to be insane by those who couldn't hear the music.

Aquellos que eran vistos bailando, eran considerados locos por quienes no podían escuchar la música.

F. Nietzsche

ACKNOWLEDGEMENTS

First and foremost, I would like to express my wide and sincere gratitude to my research supervisor, Dr. Mª Auxiliadora Prieto Jiménez, for giving me the opportunity to research and providing invaluable guidance throughout this thesis. Her dynamism, vision, and motivation have deeply inspired me during these years.

I would like to acknowledge Dr. Aljoscha Wahl for accepting me into his research group in TUDelft and leading me to work on the fascinating field of metabolism.

I would also like to thank Prof. José Luis García, Dr. Eduardo Díaz, Dr. Pedro García, and Prof. Ernesto García for their constructive advice during these years.

Thanks to Virginia Martínez and Juan Nogales for introducing me to the interesting fields of predatory bacteria and metabolism. I would also like to thank to Rosa del Campo for her enthusiasm with which she understands the microbiology and for her fruitful advices.

I am indebted to the institutions that have financially supported this work: Ministerio de Economía y Competitividad and EMBO which supported over FPI fellowship the accomplishment of this Ph.D. Thesis at CIB and the short stay at Delft University of Technology.

I appreciate the work of CIB facilities such as microscopy, photography and technical support team, as well as ICTP facilities (SEM).

I would like to give special thanks to Natalia, Vir, Sergio, Gonn, Fran and Roberto, without whom it would not be possible. To Elena and Edu for their inconditional support whatever happens. Wilson, thanks for listening to my music and making me dance.

Lastly, I would like to thank my family for all the support during my whole life. Special thanks to Jose, who design the beautiful cover of this book.

To my mum and my grandfather who always encourage me to get my dreams.

INDEX

I. ABBREVIATIONS

ATP	Adenosine Triphosphate
BALOs	*Bdellovibrio* and like organisms
TCA	Tricarboxylic acid cycle
CoA	Coenzyme A
DNA	Deoxyribonucleic acid
Dnase	Deoxyribonuclease
RNA	Ribonucleic acid
h	Hour
min	Minute
s	Second
l	Liter
cfu	Colony forming units
pfu	Plaque forming units
HI	Host Independent
HD	Host Dependent
bp	Base pair
PHA	Polyhydroxyalkanoate
PHB	Polyhydroxybutyrate
AP	Attack phase
GP	Intraperiplasmic growth phase
PYE	Peptone and Yeast extract medium
m	Meter
LPS	Lipopolysaccharide

hit	Host independent locus
qPCR	Quantitative PCR
M	Molar
Km	Kanamycin
OD	Optical density
ORF	Open Reading Frame
FBA	Flux Balance Analysis
g CDW	Grams of Cell Dry Weight
mcl-PHA	Medium chain length PHA
scl-PHA	Short chain length PHA
Mw	Weight-average molecular weight
Mn	Number-average molecular weight
PDI	Polydispersity index
scv	Small colony variant
ST	Sequence Typing
CF	Cystic fibrosis
GEM	Genome-scale Metabolic Model
HPLC	High-Performance Liquid Chromatography
GC	Gas Chromatography
MS	Mass-spectrometry
TOF	Time of flight
Q	Quadrupole

II. SUMMARY

As with many findings in science, the *Bdellovibrio* group of predatory bacteria and like organisms (*Bdellovibrio* and like organisms, BALOs) was discovered by serendipity (Stolp and Starr, 1963). Since they were identified, the scientific community has striven to describe their biphasic growth cycle, investigating and characterizing the predation mechanism. Prey selectivity and the ecological role of the predators in their natural niches have also been studied. Another crucial factor to be addressed involves an understanding of the genotypic and phenotypic changes giving rise to host-independent (HI) mutant development (Jurkevitch, 2006; Sockett, 2009a). Progress made in the last few decades in the field of predatory bacteria involves both classical molecular genetics and biochemical characterization, such as central metabolism and TCA cycle (Hespell et al., 1973). Analyses at system level have also been performed, including -omic techniques, such as transcriptomic and proteomic analyses (Barabote et al., 2007; Karunker et al., 2013).

Due to its lifestyle and its capacity for lysis against prey cells, *Bdellovibrio bacteriovorus* has been proposed for several applications. However, the difficulty involved in handling it in the laboratory and its obligate predatory condition make *B. bacterivorous* difficult to investigate, and several factors therefore remain uncertain.

During Chapter 1 of the present Ph.D. thesis, we reconstructed a genome-scale metabolic model of the predatory bacterium *B. bacteriovorus* HD100. This tool was used to study the metabolism of the predator, as well as to analyze the different phases of development: the attack phase (AP) and the intraperiplasmic growth phase (GP). The *in silico* simulation obtained with the metabolic model reiteratively suggested that the predator is capable of growing in the absence of prey, as a HI strain. Such growth was simulated in an amino acid-based defined medium.

The available transcriptomic data for AP and GP facilitated the differential analyses of the two phases, based upon the construction of condition-specific models, *i*CHAP and *i*CHGP. Prediction of the carbon flux distribution in each phase revealed crucial features of the metabolic abilities of the predator. Integration and contextualization of these datasets into the model provided more reliable information and a deeper comprehension of the metabolic network, compared with the sole analysis of the genome sequence (Rendulic et al., 2004).

Although AP did not show any particular metabolic feature, during GP the metabolism of the predator was completely oriented towards production of biomass building blocks, such as nucleotides and lipids. Interestingly, the decarboxylative phase of the TCA cycle was completely inactivated, α-ketoglutarate constituting the main fuel for the TCA. Remarkably, pyruvate is channeled directly to the gluconeogenesis, while the acetyl-CoA is redirected for the biosynthesis of fatty acids.

It is also worth mentioning that, although *B. bacteriovorus* HD100 possesses a relatively large genome, it bears several auxotrophies. In this sense, the metabolic model, *i*CH457, enables us to perform a reaction essentiality analysis. In order to analyze the lifestyle of the predatory bacteria, the essential reactions of a free-living organism, such as *Pseudomonas putida* KT2440, were used for comparison.

Although *B. bacteriovorus* HD100 has been described as an obligate predator, the reiterative evidence of its potential ability to grow in the absence of prey prompted us to experimentally verify this hypothesis in Chapter 2. Consequently, the incubation of *B. bacteriovorus* HD100 in a rich medium mainly comprising a protein hydrolysate, such as PYE (peptone and yeast extract), promoted ATP production, an increase in biomass and the biosynthesis of nucleotides, measured as genome number.

These results led us to further examine the medium composition with the aim of elucidating which metabolites were being taken up. Chromatographic analyses were employed to detect amino acids as the preferred carbon source. We performed targeted GC-MS analysis to quantify consumption. Growth of *B. bacteriovorus* in a rich defined medium comprising a mixture of the 20 amino acids highlighted glutamate as the favorite substrate. Once this metabolite is depleted, aspartate, threonine and valine constituted the main fuels for the cell.

Considering the lytic activity of *B. bacteriovorus*, this predator could be considered as a highly useful tool for the extraction of intracellular bio-products. As a proof of concept, during Chapter 3 we described the development of the predator as a biological lytic agent for the extraction of polyhydroxyalkanoates (PHA). PHA is a biopolymer synthetized by certain microorganisms such as gram-negative bacteria susceptible to predation by *B. bacteriovorus* HD100. This polymer accumulates in the cytoplasm of the PHA-producing bacteria, and represents an effective substitute to the traditional petrochemical-based plastics. The results of our research in this chapter, published in the journal *Scientific Reports* (Martínez et al., 2016), reported the use of predatory bacteria as biological lytic agents for recovering high-value products from the cytoplasm of the cell. The genome of the HD100 strain contains two PHA

depolymerase genes, whose corresponding proteins are responsible for partial degradation. Construction of two mutant strains in these genes improved the extraction of the polymer and made this biological lytic tool more efficient.

Finally, the lytic ability highlights *B. bacteriovorus* as an interesting agent for biocontrol of clinical and environmental pathogens (Jurkevitch et al., 2000). Evaluation of the predation susceptibility of different pathogenic bacteria would constitute a significant step forward with regard to establishing the range of applicability of the predator, and to elucidating some key factors involved in the predatory mechanism. The ability of *B. bacteriovorus* HD100 to prey upon different bacteria is explained in Chapter 4.

III. RESUMEN

Como otros muchos descubrimientos en ciencia, las bacterias depredadoras del grupo *Bdellovibrio and like organisms* (BALOs) fueron halladas por serendipia (Stolp and Petzold, 1962 (Stolp and Starr, 1963). Desde su descubrimiento, la comunidad científica ha invertido un esfuerzo considerable en describir su ciclo de vida bifásico, investigar y caracterizar el mecanismo de depredación y la selectividad de presa, comprender los cambios genotípicos y fenotípicos que lideran la conversión de mutantes independientes de presa (HI), así como la relevancia ecológica que presentan estos microorganismos en su nicho natural (Jurkevitch, 2007; Sockett, 2009b). De esta forma, a lo largo de los años se han realizado numerosos avances en el campo, tanto a nivel bioquímico, por ejemplo la descripción de rutas del metabolismo central como el ciclo de Krebs (Hespell et al., 1973) y nivel sistémico con la implementación de las técnicas –ómicas, como por ejemplo análisis de transcriptómica o proteómica (Barabote et al., 2007; Karunker et al., 2013).

Por otro lado, debido a su estilo de vida y a la capacidad lítica que presenta sobre células presa, se han propuesto numerosas aplicaciones para este microorganismo. Sin embargo, debido a las limitaciones que presentan estos depredadores relacionadas con su ciclo de vida bifásico dependiente de presa, numerosas preguntas quedan todavía sin respuesta.

Durante el primer capítulo de esta tesis doctoral, se ha llevado a cabo la reconstrucción de un modelo metabólico a escala genómica de la bacteria depredadora *B. bacteriovorus* HD100. Esta herramienta se ha utilizado para facilitar el estudio del metabolismo del depredador, permitiendo el análisis de las diferentes fases de crecimiento: fase extracelular (AP) y fase intracelular (GP). Mediante este estudio, se han obtenido reiteradas evidencias del potencial crecimiento de *B. bacteriovorus* HD100 como un microorganismo independiente de presa, únicamente suplementando el medio con aminoácidos.

Por otro lado, la disponibilidad de datos de transcriptómica en la literatura para las fases AP y GP, ha permitido el análisis diferencial del metabolismo, gracias a la obtención de modelos específicos de condición. Mediante el análisis de la distribución de flujo de carbono a lo largo de la red metabólica en cada uno de los modelos específicos, *i*CHAP e *i*CHGP, se ha podido comparar el comportamiento metabólico del depredador en cada una de las fases. Estos análisis han proporcionado información más fiable, así como una visión global y profunda comparada con la obtenida a partir de los datos obtenidos del análisis de la secuencia del genoma (Rendulic et al., 2004).

Por un lado, durante AP no se ha encontrado ninguna característica destacable. Sin embargo, durante la fase de crecimiento intraperiplásmico, GP, el metabolismo se encuentra claramente dirigido a la producción de macromoléculas como nucleótidos o lípidos. Curiosamente, se puede apreciar que la fase descarboxilativa del ciclo de Krebs se encuentra completamente desactivada, siendo el α-cetoglutarato el primer metabolito de la ruta. Además, es importante resaltar que el piruvato se dirige directamente a la gluconeogénesis, mientras que el acetil-Coa se destina íntegramente a la biosíntesis de ácidos grasos.

Es importante recalcar que, aunque *B. bacteriovorus* contiene un genoma considerablemente grande, presenta numerosas auxotrofías. En este contexto, el modelo metabólico *i*CH457, ha permitido realizar un análisis de reacciones esenciales. Con el objetivo de comprender el estilo de vida de este depredador obligado, se han comparado estas reacciones con las propuestas como esenciales en un organismo de vida libre como *P. putida* KT2440.

A pesar de la condición de depredador obligado de *B. bacteriovorus* HD100, la reiterada predicción del crecimiento independiente de presa propuesta por el modelo, promovió su comprobación experimental durante el Capítulo 2. De esta forma, se ha determinado que la incubación del depredador en un medio rico principalmente constituido por hidrolizado de proteínas, como es el PYE (extracto de levadura con peptona) y en ausencia de presa, conlleva la producción de ATP, el incremento de biomasa y la biosíntesis de nucleótidos, medida como número de genomas.

Este resultado nos animó a examinar la composición del medio con el objetivo de elucidar los metabolitos que estaban siendo utilizados. Mediante análisis cromatográficos se determinó que los aminoácidos representaban el grupo de metabolitos preferido por el depredador, por lo que utilizando análisis dirigidos a este tipo de compuesto se determinó que, bajo el crecimiento en una mezcla homogénea de los 20 aminoácidos, el glutamato es el sustrato preferente y, una vez éste se ha agotado, el aspartato, la treonina y la valina son los metabolitos consumidos en primer lugar.

Teniendo en cuenta la capacidad de lisar las células presa una vez completado el ciclo de vida, *B. bacteriovorus* se presenta como una eficiente herramienta de lisis para la extracción de bioproductos intracelulares. Como prueba de concepto, a lo largo del capítulo 3 se describe el desarrollo de *B. bacteriovorus* como herramienta lítica biológica para la extracción de polihidroxialcanoatos (PHA), polímeros naturales acumulados en el citoplasma de algunas bacterias, que representa una excelente alternativa para los plásticos de origen petroquímico.

Durante este estudio, publicado en la revista *Scientific Report* (Martínez et al., 2016), se ha puesto de manifiesto no solo el uso de bacterias depredadoras como agentes líticos para la recuperación de productos de interés, sino que también se han construido mutantes en las enzimas despolimerasas de PHA encontradas en el genoma de *B. bacteriovorus* HD100. La generación de estos mutantes ha supuesto una mejora en el rendimiento de recuperación, ya que la acción de las despolimerasas también supone la degradación del polímero y, por tanto, la disminución de la calidad de éste.

Por otro lado, la habilidad lítica de *B. bacteriovorus* HD100 le confiere un atractivo como potencial agente de biocontrol que puede ser utilizado contra diferentes bacterias, nocivas tanto para la salud humana como medioambiental (Jurkevitch et al., 2000). De esta manera, la evaluación de la capacidad depredadora de *B. bacteriovorus* HD100 contra diferentes cepas patógenas supondría un gran avance para conocer el rango de presa de este depredador, así como identificar el factor que determina un evento de depredación efectivo. Este estudio se ha llevado a cabo durante el cuarto capítulo de esta tesis doctoral, donde se evalúa la susceptibilidad a la depredación de diferentes bacterias patógenas.

IV. GENERAL INTRODUCTION

1. PREDATION: A GENERAL OVERVIEW

Individual organisms in a community interact in many different ways. An interaction may either benefit both individuals or just one organism to the detriment of the other. The latter process is known as “antagonistic interactions”, which includes predation, grazing, and parasitism (Czárá et al., 2002).

Predation is a biological interaction whereby an individual (the predator) kills and feeds on another (the prey) to survive. It is a very common biological interaction in nature and its role is crucial in shaping ecosystem structure and ecological function (Berger et al., 2001; Hawlena and Schmitz, 2010). Several examples of predators among animals can be found in a wide range of taxa. On the microscopic scale, protozoa, bacteria, and bacteriophages also consume prey organisms (Clarholm, 1984). They play an important role in maintaining population sizes in microbial communities, which promotes the diversity of microorganisms and contributes to a stable community structure, linking the production and removal of biomass (Fuhrman and Caron, 2016; Thompson, 1999).

Many evolutionary biologists currently consider that predation has played a major role in defining patterns in the history of life, such as the increase in maximum complexity of organisms (Vermeij, 1994). Predator and prey are natural enemies, and they have developed and improved many physical, morphological and metabolic adaptations, and have altered their behavior to counter each other. This evolutionary reciprocity is the basis of coevolution, where adaptation by one player not only promotes change in its opponent, but the opponent's adaptation likewise generates selection as an evolutionary response in the first player (Gallet et al., 2009). However, it is difficult to ascertain whether specific adaptations are strictly the consequence of coevolution, whereby a prey adaptation gives rise to a predator adaptation, which in turn is countered by further adaptation in the prey. Interestingly, and according to the alternative proposal to coevolution suggested by Vermeij, the Escalation Hypothesis (Vermeij, 1994), most predators are generalists in their prey preference, in contrast to the coevolutionary system, where most predators are assumed to be specialists. This option reduces the impact of a given prey adaption and represents a response to its own enemies (competition with other predators and abiotic factors that reduce the prey population) (Brodie, 1999).

Predators limit the growth of the prey by consuming them as well as by altering their behavior (Nelson et al., 2004). Proliferations or reductions of the prey population can also give rise to increases or decreases in the number of predators. These cyclical fluctuations in their simplest form (one predator population, one prey population) have been described in the Lotka-Volterra model. This model is based on a pair of first order non-linear differential equations that determine an ecological predator-prey interaction. It makes a number of assumptions considering the development of the prey and predator populations: the growth rate of prey, the rate at which predators kill prey, the death rate of predators and the rate at which predators reproduce by consuming prey. Figure 1 illustrates a linearized solution of the evolution of predator and prey populations using the non-linear Lotka-Volterra equations.

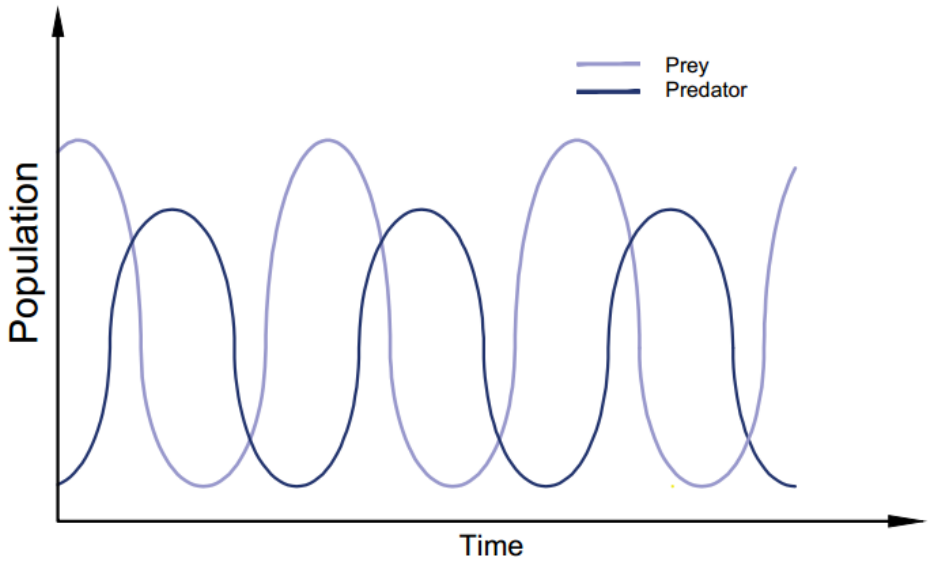

Figure 1. Linearized version of the Lotka-Volterra equation describing the dynamics of a biological system in which one predator and one prey interact.

2. BACTERIAL PREDATION

Predation, which is considered a top-down control for bacterial growth and survival in the environment, has been described as the major mortality and selection factors for bacteria in many aquatic and terrestrial systems, impacting their abundance, composition, and activity (Thingstad, 2000). There are different bacterial predator groups, including a size range of more than eight orders of magnitudes, from viruses to large bivalves, which all might feed on similar-sized bacterial prey (Figure 2). One can expect enormous dissimilarities in the type of predatory relations with bacteria, in the regulating mechanisms thereof and in the impact of predation upon different environments (Corno and Jürgens, 2006). The main groups of bacterial predators

in nature are metazoans, protists, bacteriophages and predatory bacteria. The structure and composition of an ecosystem will depend on the abundance and the presence of the predators. In the case of microbial predators (protists, prokaryotes, phages), it is not easy to establish whether the number of isolated cells is representative of most of the natural network due to the existence of unculturable strains (Khaled K Mahmoud et al., 2007). At the lower end of the scale (viruses and bacteria), predators are usually smaller than their prey, while at the upper scale, phagocytosis of smaller prey is the common predatory mechanism (i.e. protozoa). However, a small predatory cell could attach more efficiently to the prey cell surface than a bigger organism and take advantage of the larger size of the prey to provide a sufficiently abundant food supply for replication and growth (Corno and Jürgens, 2006).

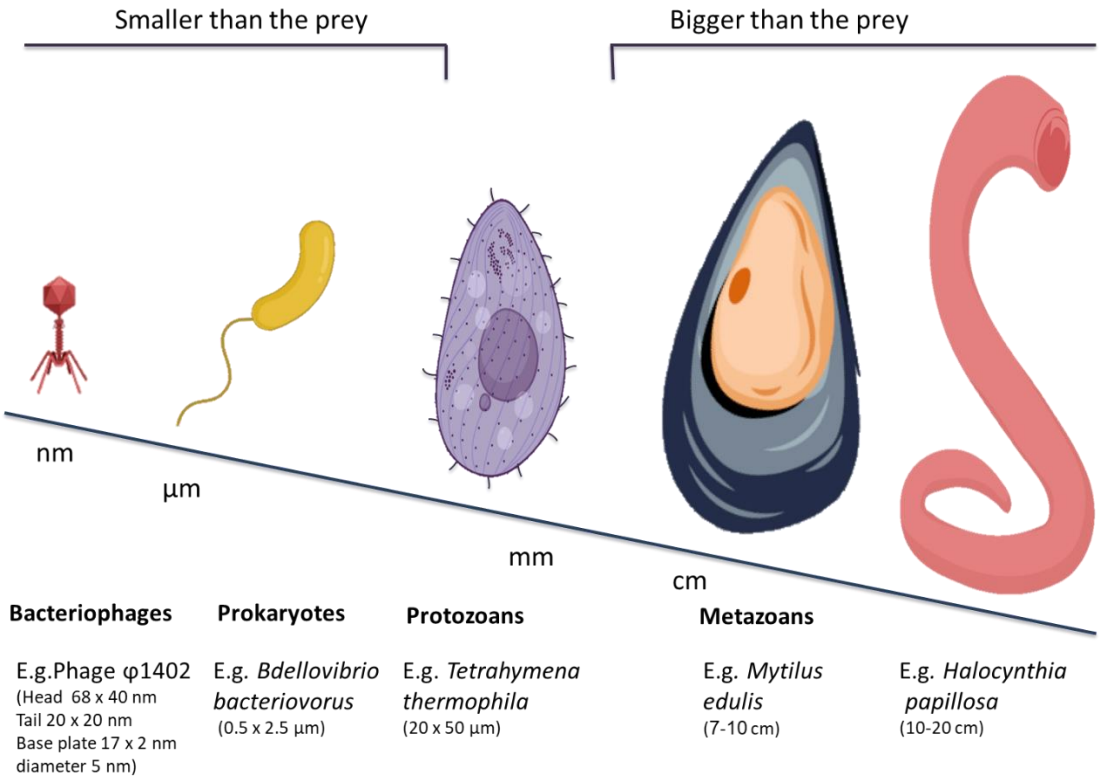

Figure 2. Relative size of bacterial predators. There is a wide variability, as well as an overlap, in the size of bacterial consumers of different groups, from bacteriophages to metazoans.

Predatory bacteria are phylogenetically diverse and ubiquitous in terrestrial and aquatic environments. They are distributed along different proteobacterial classes (alpha, beta, gamma, and delta-proteobacteria). These bacteria, which possess different phenotypes and metabolic traits, can be classified as obligate predators (they need the prey cell to replicate and complete their lifecycle) and facultative predators (they are not dependent on the prey to conclude their growth cycle) (Davidov and Jurkevitch, 2004).

The objective of predatory microbes is simple: to use energy and biosynthetic monomers and polymers collected by and contained within other organisms. To this end, predators have developed different predatory strategies (Figure 3) (Martin, 2002):

- "Wolfpack" group predation (Figure 3A): A group of predator cells can jointly produce a variety of hydrolytic enzymes to degrade nearby bacteria. The nutrients derived from the prey become available to the food web population. *Myxococcus* sp. and *Lysobacter* sp. are examples of this type of predation (Jurkevitch and Davidov, 2006).
- Epibiosis (Figure 3B): The predator cell attaches to the outer surface of the prey cell and begins to degrade and take up nutrients. *Vampirococcus* sp. exhibits typical epibiotic predation (Guerrero et al., 1986).
- Direct invasion of the cytoplasm (Figure 3C): the predator cell directly enters the prey cell by diacytosis, growing and dividing inside the cytoplasm; one example of this is *Daptobacter* sp. (Guerrero et al., 1986).
- Periplasmic invasion (Figure 3D): the periplasm is the compartment in which the predator cell grows and divides. This strategy is the most studied and *Bdellovibrio bacteriovorus* is the best characterized member (Sockett, 2009b).

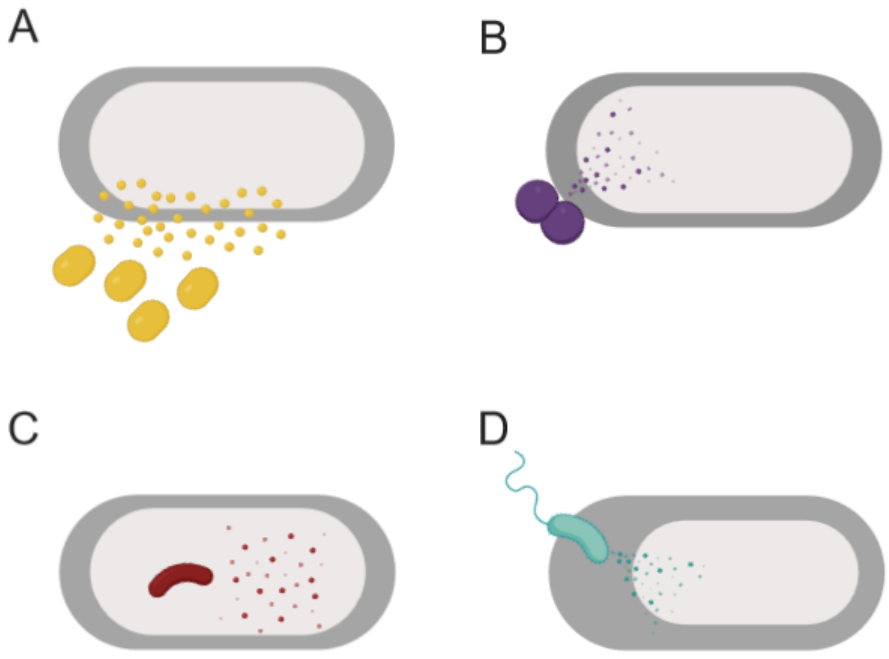

Figure 3. Different strategies of predation by microorganisms, as described in the text. A) Wolfpack group predation (*Myxococcus* sp. and *Lysobacter* sp.) B) Epibiotic attachment (*Vampirococcus* sp.). C) Direct invasion of the cytoplasm (*Daptobacter* sp.). D) Intraperiplasmic predation (*B. bacteriovorus*).

However, this theoretical classification is difficult to apply in the field, because more than one of these strategies can be employed (or perhaps even a different one). For instance, *Myxococcus* and *Lysobacter* strains are able to use another strategy differing from "wolfpack predation" (Kobayashi et al., 2005; McBride et al., 1996). Moreover, within *Bdellovibrio* spp., it is possible to find different strains that exhibit diverse strategies (epibiotic or periplasmic) (Shemesh and Jurkevitch, 2003). Consequently, the predatory strategy must be ecologically contextualized, including resource allocation, environmental conditions, spatial and temporal influences, and genetic evolution (Davidov and Jurkevitch, 2004).

The study of predatory bacteria almost inevitably leads to the study of the evolution of predation itself. The antagonistic relationships in microbial ecosystems likely evolved several times in different groups of gliding bacteria to finally reach the present predatory microbial networks (McBride, 2004). Interestingly, the spontaneous occurrence of host-independent (HI) variants of predatory bacteria suggests that the transition from a facultative to an obligate predatory lifestyle may only be involved in a limited adaptive sequence (Cotter and Thomashow, 1992). From an evolutionary point of view, since predation represents a method by which prokaryotes can penetrate other prokaryotes, this interaction could account for the endosymbiotic association (Guerrero et al., 1986) and, furthermore, for the origin of the eukaryotic cell (Margulis, 1996).

3. *BDELLOVIBRIO* AND LIKE ORGANISMS

These prokaryotic predators have been known since 1962, when Stolp, Petzold, and Starr discovered, named and isolated a *Bdellovibrio* strain for the first time at the University of California, Davis (California, EE.UU.) in experiments designed for the isolation of bacteriophages from soil samples (Stolp and Starr, 1963). The group of "*Bdellovibrio* and like organisms" (BALOs) includes the obligate predators *Bdellovibrio* spp., *Bacteriovorax* spp. and *Peridibacter* spp. (δ-proteobacteria) and *Micavibrio* (α-proteobacteria).

BALOs are small vibrioids to rod-shaped gram-negative aerobic and mesophilic bacteria (0.2-0.5 µm wide, 0.5-2.5 µm long) which present high motility, reaching velocities of 160 µm s^{-1} (Thomashow and Rittenberg, 1978), they are propelled by a single sheathed flagellum. Although they were first isolated in soil, they are ubiquitous in nature and can be found in aquatic and terrestrial environments, including hypersaline systems (Piñeiro et al., 2008), biofilms (Kadouri and O'Toole, 2005), mammalian guts (Hobley et al., 2012; Schwudke et al., 2001) and cystic fibrosis lung microbiota (Caballero et al., 2017).

In the last few decades, BALOs have attracted the attention of the scientific community, which can be seen in the greater number of publications (Figure 4). Research on predatory bacteria presents two clearly different milestones, involving on the one hand, the development of the biochemical and molecular biology tools (1960-80), and on the other, the emergence of the -omic technologies (2001-2019). In addition, the potential applicability of predatory bacteria has aroused further interest in recent years.

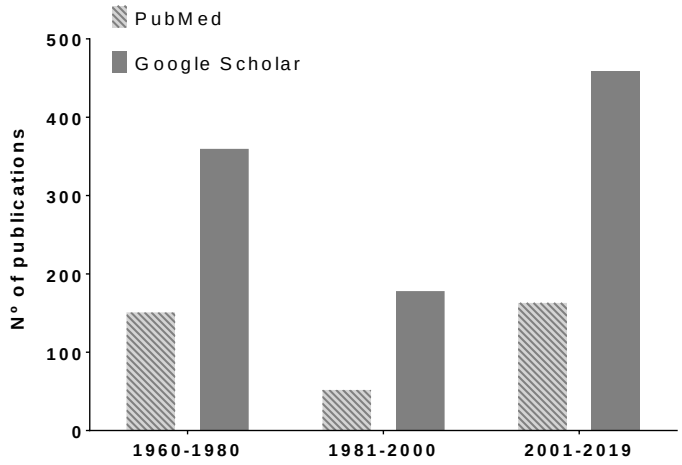

Figure 4. Number of publications on BALOs since 1960. Medline and Google Scholar were searched for the term "*Bdellovibrio*" in the titles of the publications. All languages are included.

The extraordinary repertoire of species susceptible to predation by BALOs enables a wide range of potential applications based on their predatory capabilities, such as biocontrol agents in medicine, utilization in agriculture, aquaculture and water treatment (Atterbury et al., 2011; Lin et al., 2007; Loozen et al., 2015; Scherff, 2AD). Furthermore, it has been proposed as an excellent source of valuable biotechnological enzymes and as a biological lytic tool for intracellular product release, due to its hydrolytic arsenal (Martínez et al., 2013, 2012). In view of its unique lifestyle, it represents a sound model for evolution studies. Penetration into other cells constitutes a new adaptation that could be subject to studies focusing on the origin of the above mentioned eukaryotic cells (Davidov and Jurkevitch, 2009; Margulis, 1996).

4. *BDELLOVIBRIO BACTERIOVORUS* HD100

Bdellovibrio bacteriovorus HD100 is a small (0.5 x 1.0 µm), monoflagellate, gram-negative bacterium belonging to the class of δ-proteobacteria. It possesses a large genome (~3.8 Mb), containing a wide-ranging hydrolytic arsenal which is crucial during the penetration of the prey cell. It is also vital during the lysis of the ghost prey cells, when the progeny is released (150 genes coding for proteases, 10 glycanases, 20 DNases, 9 RNases and 15 lipases) (Rendulic et al.,

2004). This predator exhibits a biphasic growth cycle (Figure 5), including a free-swimming attack phase (AP) and an intraperiplasmic growth phase (GP) inside the prey´s periplasm, forming the so-called bdelloplast structure.

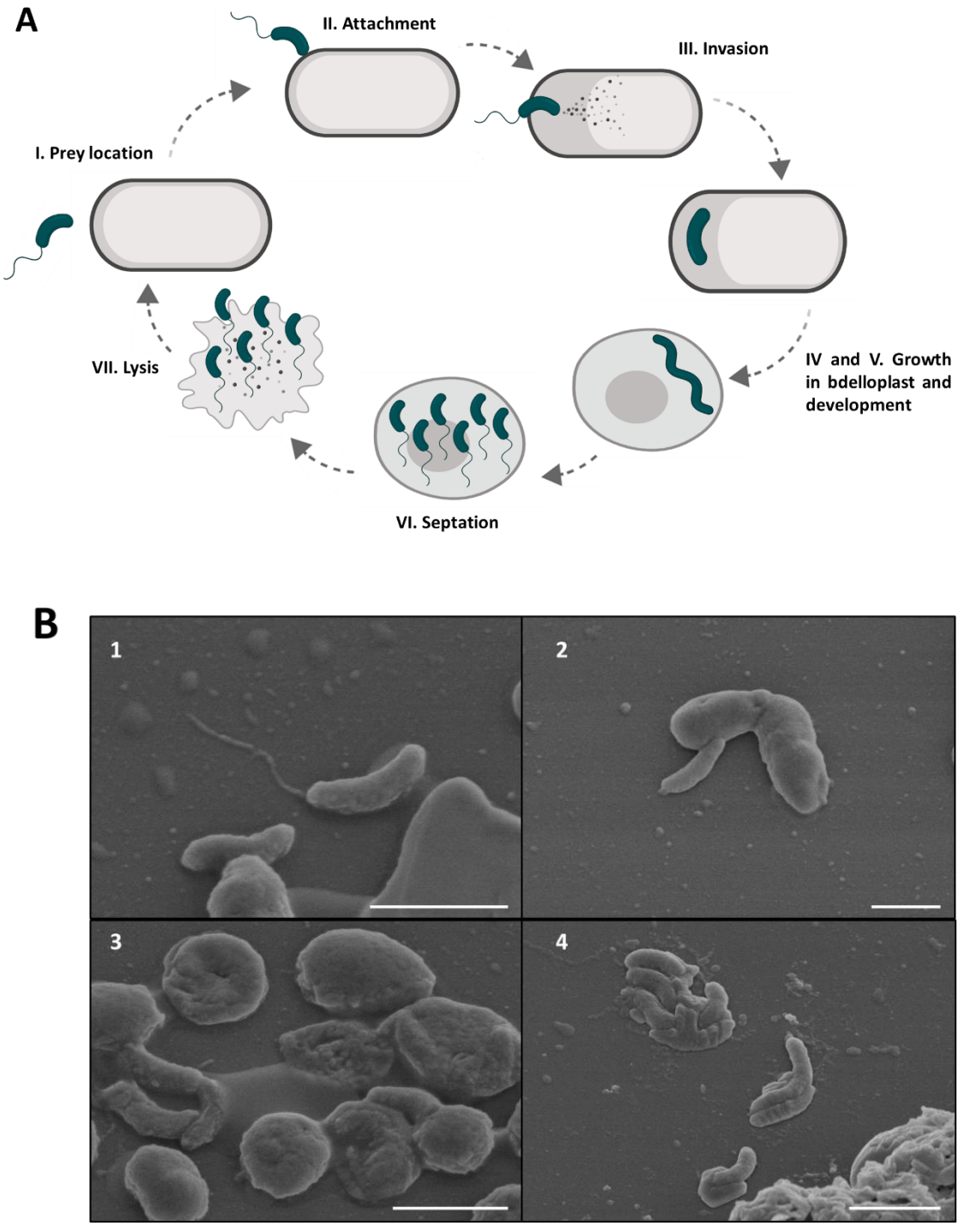

Figure 5. A) The predatory cycle of *B. bacteriovorus* HD100. I) Prey location: *B. bacteriovorus* moves towards prey-rich regions. II) Attachment: the predator anchors to the host cell, which leads to the infection. III) Invasion: *B. bacteriovorus* enters the periplasm of the prey cell. IV and V) Growth in bdelloplast and development: the prey has a rounded appearance due to cell wall

modification and *B. bacteriovorus* grows in the periplasm and replicates its DNA. *B. bacteriovorus* uses the prey cytoplasm as a source of nutrients. VI) Septation: the predator septs when resources become limited and it matures into individual attack phase cells. VII) Lysis: mature attack-phase cells lyse the cell wall of the bdelloplast, initiating the search for fresh prey. The complete cycle takes about 4 h. **B) Electronic microphotographies of the growth cycle of *B. bacteriovorus* HD100 preying on a *Pseudomonas putida* KT2440.** 1) Attack phase cell of *B. bacteriovorus*. 2) Attachment of the predator to the surface membrane of the prey cell. 3) Bdelloplast structure containing the predator inside. 4) Lysis of the ghost prey cell using the hydrolytic arsenal of the progeny. White lines in the bottom of the micrographies represent a scale bar of 1 µm.

During AP, free-living cells from the extracellular environment actively seek new prey. There has been previous research on chemotaxis as a mechanism for prey location; however, the role of chemical detection in driving movement towards prey cells remains uncertain. In this sense, strain HD100 has 20 methyl-accepting chemotaxis proteins (MCP) encoded in its genome (Rendulic et al., 2004), but no evidence of specific movement towards any chemicals or prey bacteria was found. Nonetheless, a positive attraction of BALOs to ecological niches rich in prey organisms has been proposed (LaMarre et al., 1977; Straley et al., 1979; Straley and Conti, 1974).

After attachment, and once the predator-prey interaction is stable and irreversible, the predator enters into the prey`s periplasm, where it grows and replicates the DNA during the GP using the cytoplasm of the prey cell as a source of nutrients and biomass building blocks. When the nutrients of the prey are exhausted, the *B. bacteriovorus* cells grow as a filament and sept into several daughter cells. Then, by means of a large array of hydrolytic enzymes, the ghost-prey outer cell membrane is lysed and the daughter cells are released into the medium (Lambert et al., 2006b).

4.1 Prey range and predatory efficiency

Predatory bacteria attack and digest other bacteria and may therefore play a role in shaping microbial communities. In order to further understand bacterial predation and to develop predatory bacteria as biocontrol agents, it is important to characterize the variation in predation phenotypes, such as prey range, and to examine the evolution of predatory bacteria lineages at different scales. Prey range depends upon the predator´s ecosystem and the available food web, as well as on the predation strategy (Jurkevitch and Davidov, 2006; Pernthaler, 2005).

Thus, the manner in which BALOs shape microbial communities depends in part on which bacterial species are susceptible to predation and how efficient the latter is. In the case of members growing exclusively in extreme environments, where constraints are strict (e.g. Saltwater BALOs; (Piñeiro et al., 2008)), the number of susceptible prey cells is lower compared with that of the BALOs present in several biological niches, such as *B. bacteriovorus*, which possesses a wide repertoire of prey cells. Annex 1 shows a compilation of the prey range of *Bdellovibrio* and other BALOs studied in recent years. Traditionally, the most common prey used to isolate and characterize BALOs were almost exclusively from the phylum Proteobacteria: *Escherichia coli*, *Pseudomonas* spp. and *Erwinia* spp. for terrestrial habitats and *Vibrio parahaemolyticus* for marine ecosystems (Jurkevitch and Davidov, 2006). Importantly, however, an increasing number of clinical and environmental pathogens is being assessed in an attempt to validate BALOs as a biocontrol agent.

Despite the wide range of susceptible prey for BALOs, predatory efficiency is strain-dependent. Indeed, *Bdellovibrio* spp. has been reported to be able to distinguish between different prey species in heterogenic co-cultures (Rogosky et al., 2006).

Finally, oxygen has a crucial effect both on the survival and the predation ability of BALOs (Schoeffield, 1996). *Bdellovibrio* strains are unable to grow under anoxic conditions, but are capable of surviving for a limited period of time. In contrast, under microaerobic conditions, the predator cells are able to prey, albeit more slowly than in the optimal oxygen conditions. This ability equips the predator to prey upon anaerobic species such as oral pathogenic bacteria (Van Essche et al., 2009).

4.2 Epibiotic predation by *B. bacteriovorus*

Despite the fact that *B. bacteriovorus* HD100 is known to employ an intraperiplasmic strategy to capture its prey, a recent report has demonstrated the possibility of reducing *Staphylococcus aureus* population by means of epibiosis (Iebba et al., 2014a). Thus, epibiotic predation provides an alternative to intraperiplasmic predation. Epibiosis is an individual extracellular method of predation and requires cell-to-cell contact between predator and prey (Figure 3B). During this attachment, the predator secretes enzymes directly into its prey and then assimilates the hydrolyzed molecules released from the interior of the prey cell (Pasternak et al., 2013). Importantly, in other strains of epibiotic predators, the division occurs by binary fission in contrast to the multiple fission associated with intraperiplasmic predation (Koval et al., 2013). It is unknown whether or not the HD100 strain divides during epibiotic predation. The members of the group of BALOS employing epibiotic predation are the δ-BALO *B. exovorus*

(formerly *Bdellovibrio* sp. strain JSS) and the α-proteobacterium (α-BALO) *Micavibrio aeruginosavorus*.

Although much less is known about the physiology, ecology and molecular mechanism of epibiotic predation, it could constitute an effective strategy in relation to gram-positive pathogens lacking the proper scaffolding to support the classical intraperiplasmic predation by *B. bacteriovorus* HD100.

4.3 Resistance to *B. bacteriovorus*

Several reported cases describe how *B. bacteriovorus* is unable to prey upon gram-negative bacteria. One example involves the presence of an extracellular proteinaceous layer (S-layer) that can block attachment between predator cells and the lipopolysaccharide (LPS) layer in *Caulobacter* sp. (Koval and Hynes, 1991). Another example refers to predation by *B. bacteriovorus* on α-proteobacteria, such as *Rhodobacter,* which possess an LPS that differs significantly from that of other gram-negative bacteria (Strittmatter et al., 1983), and predation on these strains is therefore generally slower.

In addition, although *B. bacteriovorus* can reduce the prey population in predatory culture by over 90%, some surviving prey cells remain in the co-culture. This prey cell population presents a temporarily resistant phenotype, and when it is grown again in rich medium it can be fed upon with the same predatory efficiency (Shemesh and Jurkevitch, 2004). This appears to be a suitable resistance strategy, as complete eradication of the food source would be devastating for a bacterial predator that can only replicate inside a prey cell. In this way, the prey avails of sufficient time to regrow.

5. HOST-INDEPENDENT *B. BACTERIOVORUS*

The life cycle described above involving the prey is termed Host/prey Dependent (HD) growth. However, some mutants of *B. bacteriovorus* can also grow as a Host/prey Independent (HI) microorganism, in rich medium, where it grows as a filamentous cell that can subsequently replicate and septs by multiple fission as the wild type strain (Figure 6).

Since the isolation of *B. bacteriovorus* in 1962, it has been noted that it can also form saprophytic colonies on hard agar plates in the presence of heat-treated prey bacteria. The successful isolation of HI variants requires a much higher number of predatory cells compared to that needed for plating on prey lawns (Stolp and Starr, 1963). This is due to the low frequency of development of these saprophytic predators (one in 10^6-10^7 cells) in rich medium (Shilo et al.,

1965). This rate is quite similar to the mutational rate of bacteria (Schaaper, 1993). It was not until the 1990´s that the HI phenotype was attributed to mutations in the predator´s genome. The region containing these mutations is called the "*hit*" locus (host-interaction locus) and no function has heretofore been assigned to it (Cotter and Thomashow, 1992; Roschansky et al., 2011). In addition, some HI isolates lack mutations at the *hit* locus, and other genes may therefore be involved in the switching pathway from HD to HI (Capeness et al., 2013; Wurtzel et al., 2010). The genomic alteration of the *hit* locus was analyzed by means of next-generation sequencing (NGS) and the gene *bd0108* was identified as being related with the HI phenotype. This gene encodes a 101 amino acid protein and has no homologs outside the *Bdellovibrionaceae* family. The gene *Bd0108*, those in the surroundings (*bd0109-bd0113*, *bd0118*, *bd0119*) and other ones associated with the HI phenotype (*bd3461*, *bd3464* or *bd3852*) are related with the formation of the Type IV pili, which is involved in the prey invasion process (Chanyi and Koval, 2014). Mutant strains in some of these genes are unable to recognize and to attach to the prey cell in liquid co-cultures.

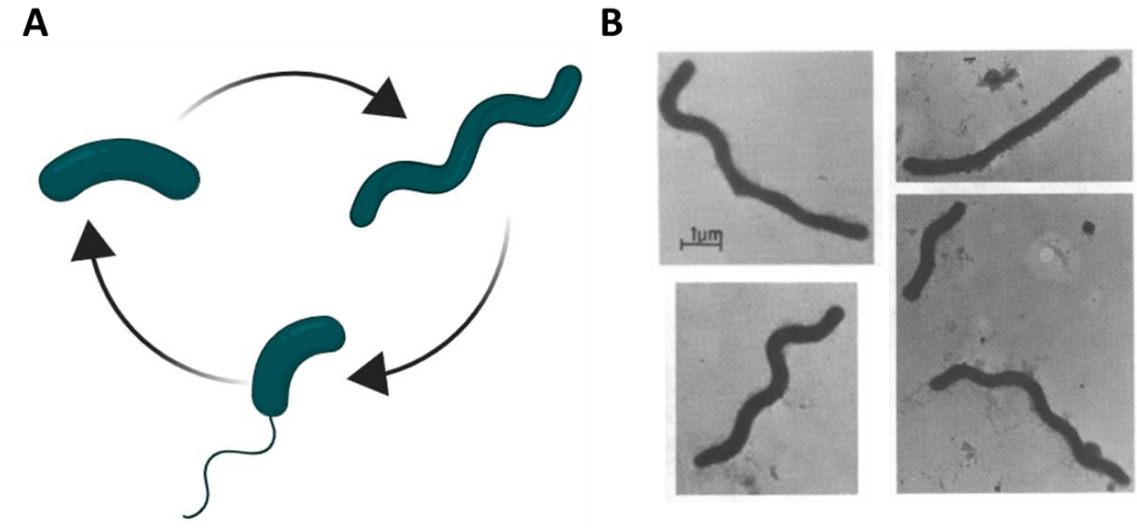

Figure 6. A) Life cycle of HI *Bdellovibrio* variants. One in 10^6-10^7 AP predator cells undergoes a genetic mutation that means it can grow free of prey and rely on acquiring nutrients from the medium. Cells grow as filaments emulating the GP state (stage 6 in the predatory growth cycle Figure 5A). After growth and cell elongation, the division of the predator filament forms AP-size cells. This cell is able to enter the predatory cycle or, as it still retains the prey-independent mutation, can undergo filamentous growth once again in the absence of prey cells. **B) Phase contrast photomicrographs of elongated spiral forms of *B. bacteriovorus* 101.** Cells were stained with 0.5% uranyl acetate and the photographs belongs to the report of Seidler and Starr (R. J. Seidler and Starr, 1969).

6. *BDELLOVIBRIO* AS A TOOL FOR BIOTECHNOLOGICAL APPLICATIONS

The ecological role of bdellovibrios in nature has not been fully elucidated (Martin, 2002); however, there are indications that these bacteria play a role in microbial ecosystems, controlling the population size of bacteria in natural environments. Consequently, their intrinsic ability to lyse prey cells, as well their capability to disperse biofilms, suggests they play an important role as biocatalysts or therapeutic and biocontrol agents. Data from the genome annotation of *B. bacteriovorus* HD100 (Rendulic et al., 2004) revealed the absence of a Type III secretion system, strongly associated with pathogenic infection of eukaryotic cells (Coburn et al., 2007). This implies an advantageous use of predatory bacteria for medical application, because therapy rejection is avoided. Furthermore, the utilization of *B. bacteriovorus* provides a new platform enabling a reduction of the antibiotic therapies responsible for the current widespread drug resistance among microbial pathogens.

6.1 *B. bacteriovorus* as a source of biocatalysts

Taking into account the interesting lifecycle of BALOs and the crucial role played by their hydrolytic arsenal, it is unsurprising that they are considered to constitute a rich source of hydrolytic enzymes of great interest for industry. Lipases, nucleases, hydrolases or glucanases are some of the potential candidates contained within their genomes (Rendulic et al., 2004). For example, *B. bacteriovorus* HD100 possesses two depolymerases of polyhydroxyalkanoates (PHA) as part of its hydrolytic repertoire, encoded by the genes *bd2637* and *bd3709*. These enzymes are able to specifically degrade short- or medium-chain-length PHA, respectively, in an efficient manner (Martínez et al., 2012).

With respect to these enzymes, and taking into account the lytic ability of *B. bacteriovorus*, this predator could be used as a biological lytic tool for extracting value-added intracellular bio-products such as PHA. This would entail employing a PHA-producing bacterium, such as *P. putida*, as prey (Martínez et al., 2016). This application was developed during the present thesis and will be described and discussed in Chapter 3.

6.2 *Bdellovibrio* strains as a living antibiotics

Since Atterbury et al. (Atterbury et al., 2011) conducted the first successful test of *B. bacteriovorus*, eliminating *Salmonella enterica* in young chicks, several trials with BALOS have been conducted, aimed at eradicating pathogenic bacteria. These studies involved the use of different animal models (*Galleria mellonella*, *Caenorhabditis elegans* or Zebrafish) and cell lines (human keratocytes or epithelial cells). Annex 2 presents a complete review of the model

organism or cell lines, pathogenic bacteria and species of BALOs used focused on future therapeutic applications.

One of the most alarming global problems refers to nosocomial infections by the ESKAPE pathogens group (*Enterococcus faecium*, *Staphylococcus aureus*, *Klebsiella pneumoniae*, *Acinetobacter baumannii*, *Pseudomonas aeruginosa*, and *Enterobacter* species). Most of them are multidrug-resistant isolates and eradication thereof poses a great challenge in clinical practice (Santajit and Indrawattana, 2016). The susceptibility of different strains of this group to predation by *B. bacteriovorus* HD100 will be evaluated in Chapter 4.

An interesting case involves *P. aeruginosa*, a common environmental gram-negative bacillus which acts as an opportunistic pathogen under certain circumstances, due to its ability to colonize different niches and to utilize many compounds as carbon sources (Green et al., 1974; Williams and Worsey, 1976). Almost all cases of *P. aeruginosa* infection can be associated with the alteration of the host defense. In this respect, three of the most concurrent human diseases caused by *P. aeruginosa* are: 1) bacteremia; 2) chronic lung infection in cystic fibrosis (CF) patients; and 3) acute ulcerative keratitis in users of extended-wear soft contact lenses (Lyczak et al., 2000). In recent years, treatment of infections caused by *P. aeruginosa* poses a challenge because of the intrinsic resistance of this bacterium to many antipseudomonal agents, and due to its ability to easily acquire antibiotic resistance determinants (Feng et al., 2017).

CF is a lethal genetic disease that causes lung colonization by *P. aeruginosa* biofilms (Lyczak et al., 2002). The course of the disease is characterized by mucoid colonies and/or multidrug-resistant isolates (Winstanley et al., 2016). Patients are susceptible to chronic, persistent, and recurring respiratory tract infections, with an acute inflammatory response resulting from progressive respiratory deficiency.

The predatory ability of *B. bacteriovorus* against the prey cells of clinical isolates has previously been tested and it might represent an effective alternative treatment for CF patients (Iebba et al., 2014b). With this aim in mind, during this thesis we make use of the characterization of 75 *P. aeruginosa* isolates collected from the aforementioned first Spanish multi-center study (López-Causapé et al., 2017). An evaluation of the predatory ability of *B. bacteriovorus* HD100 against these *P. aeruginosa* strains is given in Chapter 4.

6.3 *Bdellovibrio* strains as a biocontrol agents

Apart from the clinical use of BALOs, there are other important applications with very extensive economic and ecological implications, such as agriculture, aquaculture, and food

safety. Prior to the use of *Bdellovibrio* spp. in infected chickens, in 1972 Scherff (Scherff, 2AD) described the first instance of BALOs as a biocontrol agent. A predator isolated from the rhizosphere (*B. bacteriovorus* isolate Bd-17) exhibited protective behavior against the systemic symptoms of bacterial blight in soybean caused by *Pseudomonas glycinea*. Additionally, aquatic diseases are causing big economic losses to fish farms, thus reducing the quality of the final product. For instance, *Aeromonas salmonicida*, one of the opportunistic and pathogenic bacteria responsible for the most serious diseases in aquaculture, has been reported to be susceptible to predation by BALOs (Cao et al., 2012; Li et al., 2014a). Likewise, *Bdellovibrio* spp. has been found in several bacterial communities in bioreactors for wastewater treatment, playing a significant role in sludge control (Chen et al., 2014; Li et al., 2014a; Wan et al., 2014; Weissbrodt et al., 2014).

Interestingly, a recent report has addressed the potential use of *B. bacteriovorus* as an adjuvant in the bioremediation process of phenanthrene (Otto et al., 2017). The prey cells have the ability to "escape" from the predator using their motility machinery (flagellum and cilium). With the use of this escape velocity and of a degrader bacterium such as *Pseudomonas fluorescens* as prey, the prey-predator interaction would enhance dispersal of the bioremediation agent.

6.4 Genetic tools for *B. bacteriovorus*

A wide range of different genetic techniques is available to predatory bacteria. Cotter and Thomashow (Cotter and Thomashow, 1992) originally cloned fragments of the 109J genome by complementation of the "HI phenotypes" to restore the plaque-forming ability of HI isolates on *E. coli* plates. This mutagenesis technique enabled identification of genes involved in a predator-prey interaction; these mutations were related with motility, penetration, and chemotaxis (Lambert et al., 2006a, 2003; Medina and Kadouri, 2009; Tudor et al., 2008). The genome sequence of the HD100 strain (Rendulic et al., 2004) represented a big step forward, and provided a greater understanding of the genes found in *B. bacteriovorus*, thus helping to better comprehend physiological processes at gene level. Table 1 shows the plasmids used to date for the genetic manipulation of different strains of *Bdellovibrio*. The genetic techniques, together with omics methods, such as genomic, transcriptomic and proteomic analyses, have enabled more in-depth study of *Bdellovibrio* spp. (Dori-Bachash et al., 2008; Wurtzel et al., 2010). On designing genetic tools, it ought to be noted that *B. bacteriovorus* HD100 divides by multiple fission, a fact that could influence the stability of the inserted plasmids over generations.

Currently, the availability of high-throughput experimental tools and quantitative analysis techniques allows for the design of more robust metabolic engineering strategies aimed at providing a better understanding the behavior of predatory bacteria. Furthermore, integration of the information and omics data at system level constitutes a useful platform in order for *B. bacteriovorus* HD100 to be developed as a biotechnological chassis for different purposes.

Table 1. Plasmids used for genetic modification of *Bdellovibrio*.

Plasmid	Replication Origin	Reference
pSET151	oripMB1	Lambert et al., 2003
pSSK10	oriR6K	Steyert and Pineiro, 2007
pMMB206	oriRSF1010	Steyert and Pineiro, 2007
pRL27	oriR6K	Tudor et al., 2008
pSUP202	oriRSF1010	Roschanski and Strauch, 2010
pK18*mob*sacB	oriColE1	Schafer et al., 1994; Roschanski et al., 2011
pSUP404.2		Roschanski et al., 2011
pMQ414	RSF1010	Mukherjee et al., 2017

V. MOTIVATIONS AND AIMS

Recent studies have proposed the use of microbial predators, such as *B. bacteriovorus* HD100, in clinical and biotechnological applications as agents to control or eradicate pathogenic bacteria. As the available knowledge regarding predator physiology is limited, some crucial issues remain to be explored. For example, methods for improving predatory ability as an alternative to antibiotics, a better understanding of the complex predatory lifestyle, and defining prey range and predatory efficiency, are all worth investigating. It is hoped that by investigating these issues concerning this predatory bacterium that it would lead to the development of highly specialized predators with improved capability to prey upon and kill specific target species.

To this end, the present thesis is divided into the following objectives:

1. Understand the metabolism of *B. bacteriovorus* during its biphasic life cycle at the systems biology level by the construction of a metabolic model.

2. Study the feasibility of prey-independent growth of *B. bacteriovorus* HD100 through the elucidation of preferential carbon sources.

3. Development of *B. bacteriovorus* HD100 as a biological lytic tool for the recovery of intracellular bioproducts.

4. Determine the prey range of *B. bacteriovorus* HD100 against different pathogenic prey species.

VI. COMMON MATERIALS AND METHODS

In this section, only the materials and methods that are applicable in the four chapters of the result sections are included. The particular methodology of each issue is included in the corresponding chapter.

1. GROWTH CONDITIONS OF *B. BACTERIOVORUS* HD100

B. bacteriovorus HD100 was routinely grown on two-membered cultures (co-cultures) in Hepes buffer (25 mM Hepes amended with 2 mM $CaCl_2 \cdot 2H_2O$ and 3 mM $MgCl_2 \cdot 3H_2O$, pH 7.8) or DNB liquid medium (consisting of 0.8 g l^{-1} NB (Difco™, Dickinson and Company, France) supplemented with 2 mM $CaCl_2$ and 3 mM $MgCl_2$, pH 7.2-7.6), in the presence of *P. putida* KT2440 as prey (Herencias et al., 2017) (Figure 7A and B). *P. putida* KT2440 prey was prepared from 16 h culture cells grown in NB and diluted to OD_{600} 1 in Hepes buffer at pH 7.8. To remove the prey after predation, co-cultures were filtered twice through a 0.45 µm filter (Sartorius, Germany) and predator cells were used in the following assays. Kanamycin (Km) (50 µg ml^{-1}) was added when needed (Bd3709 mutant strain and *P. putida* KT2442Z). Co-cultures were developed in 100-ml flasks in a final volume of 10 ml. Glycerol stocks of *B. bacteriovorus* HD100 were prepared by adding 300 µl of glycerol 85% to 1 ml of the coculture (HD100 cells /*P. putida* KT2440).

2. *B. BACTERIOVORUS* HD100 AND PREY VIABILITY CALCULATION

Predator and prey strain viabilities were calculated from a co-culture containing both strains. *B. bacteriovorus* strains viabilities, counted as plate forming units per milliliter (pfu ml^{-1}), were calculated from a culture performing serial dilution from 10^{-1} to 10^{-7} in Hepes buffer at pH 7.8 and developing on the lawn of prey after 48-72 h of incubation at 30 °C by using the double layer method (Figure 7C and D) (Herencias et al., 2017; Lambert and Socket, 2008). Briefly, 0.1 ml of the appropriate dilution was mixed with additional 0.5 ml of prey cell suspension of *P. putida* KT2440 pre-grown in NB and prepared in Hepes buffer at pH 7.8 at OD_{600} 10, vortexed and plated on DNB solid medium. To calculate prey strain viability, 10 µl of each dilution was placed on LB solid medium (or the specific growth medium, see Chapter 3 and 4 for details) and colony-forming units per milliliter (cfu ml^{-1}) were counted.

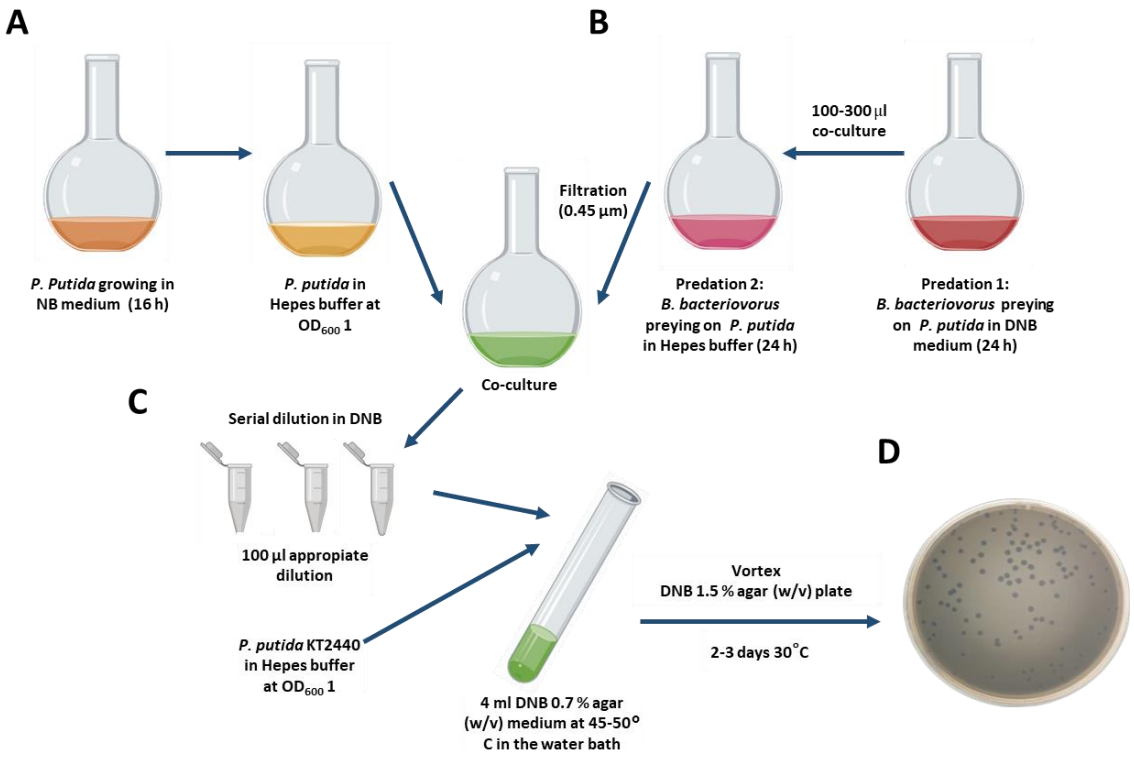

Figure 7. Workflow to set up *B. bacteriovorus* co-cultures and quantification of the viability of the predator. **A)** Preparation of the prey cell suspension (here, *P. putida* KT2440). **B)** Preparation of *B. bacteriovorus* cells. Two-steps cultivation of the predator is needed to obtain the predatory cells ready for the experiment. The HD100 cells in the first step comes to the glycerol stock. **C)** Double layer method to quantify the cell number of *B. bacteriovorus* HD100. **D)** Development of *B. bacteriovorus* HD100 on a lawn of prey on DNB agar plates after 2-3 days of incubation at 30 °C. *Bdellovibrio* cell number can be quantified as plaque-forming-units (pfu ml^{-1}).

3. BIOMASS CALCULATION

Cellular biomass, expressed in grams of the cell dry weight (g CDW) per liter, was determined gravimetrically as previously reported (Martínez et al., 2013). Briefly, ten milliliters of culture medium were centrifuged for 15 min at 13000 x *g* at 4 °C. Cell pellets and the supernatants were separated and subsequently freeze-dried for 24 h and finally weighted. The biomass calculation was obtained from the pellet weight.

4. PHASE CONTRAST AND FLUORESCENCE MICROSCOPIC TECHNIQUES

Cultures were routinely visualized with a 100X phase-contrast objective and images were taken with a connected camera Leica DFC345 FX. Staining for nucleoids was performed by incubation with 2 µg ml^{-1} (4´,6-diamidino-2-phenylindole, DAPI) and visualized by fluorescence

microscopy using a Light transmitted and epifluorescence Axioplan Universal Microscope Zeiss and a digital camera Leica DFC 350 FX.

5. SCANNING ELECTRON AND TRANSMISSION ELECTRON MICROSCOPIC TECHNIQUES

For scanning electron microscopy (SEM), co-cultures of *B. bacteriovorus* HD100 growing on *P. putida* KT2440 were harvested, washed twice with distilled sterile water, fixed with 2% (w/v) paraformaldehyde for 2 h at room temperature and washed three times with distilled sterile water. The dried samples were mounted on aluminum stumps and sputter-coated with chromium before examination under an ESEM apparatus (Philips XL 30) at an accelerating voltage of 15 kV.

6. STATISTICAL ANALYSES

Data sets were analyzed using Prism 6 software (GraphPad Software Inc., USA). Comparisons between two groups were made using Student's-test. Comparisons among multiple groups were made using one-way or two-way analyses of variance (ANOVA) test, depending on whether one or two different variables were considered, respectively. The relation between the microbial counting and the genome number were analyzed by Kendall analyses.

RESULTS

VII. COMPREHENSIVE ANALYSIS OF THE PREDATORY BACTERIA *BDELLOVIBRIO BACTERIOVORUS* THROUGH A GENOME SCALE METABOLIC MODEL

COMPREHENSIVE ANALYSIS OF THE PREDATORY BACTERIA *B. BACTERIOVORUS* THROUGH A GENOME SCALE METABOLIC MODEL

1. INTRODUCTION

As described in *General Introduction*, the growth cycle of this predator consists of two phases (Figure 5): a free attack phase (AP), where *B. bacteriovorus* is in the environmental niche searching for preys, and an intraperiplasmic growth phase (GP), where the predator is consuming the prey as a source of carbon and energy to reproduce into several daughter cells (Sockett, 2009b). Although numerous studies have examined the predation of *B. bacteriovorus* using different gram-negative species as prey and under different experimental condition, it is still unclear what is the precise force which drives this interaction; the key factor responsible for the transition between the different phases and whether some prey species are more susceptible to predation than others. In fact, most of its physiological and metabolic capabilities are still unknown due to the complex lifestyle, the difficulty of cultivability under laboratory conditions and the requirement of two member cultures.

Interestingly, host-independent (HI) mutant strains of *B. bacteriovorus* have been developed under laboratory conditions. These HI predators are able to grow axenically (without prey) in a rich-nutrient medium mimicking the dimorphic pattern of elongated growth, division and differentiation (Figure 6) (Eksztejn and Varon, 1977). It is worth to notice that the axenic growth of these mutant strains is given by a mutation in the host interaction (*hit*) locus, which has been described as a putative regulatory element. This argues in favor that this mutation has not any metabolic (enzymatic) impact and the main metabolism of these HI derivatives should not have suffered changes with respect to that of the wild type strains.

To develop a predictive mechanistic framework for identifying key features of the extended metabolic network of predatory growth, in this chapter, we have constructed a genome-scale metabolic model (GEMs) that captures the metabolism of the predatory bacterium *B. bacteriovorus* HD100 driving the rational understanding of its characteristics. GEMs are created based on the combination of genome sequence data and detailed biochemical evidence. These models are constrained in order to predict the behavior of complex biological

systems, such as predators and predator-prey interactions, and their responses to the environments (Thiele and Palsson, 2010).

Constraint-based metabolic models are created sustaining three fundamental types of limitations (Bordbar et al., 2014): i) a steady-state mass balance constraint, which establishes the total production and consumption rates of each metabolite to be equal, ensuring there is no accumulation of intracellular metabolites. ii) The reaction reversibility, to ensure the operation in the proper direction within the metabolic network. iii) The upper and lower bounds of each reaction, which limit a small number of reactions such as growth rate and uptake and production rate. Although these constraints reduce the solution space of the metabolic network, there are multiple solutions for the intracellular flux distribution, but this kind of models can be used to obtain the optimal solution for a given objective.

A number of constraint-based tools have been developed in order to predict metabolic fluxes in response to genetic or environmental changes (O 'Brien et al., 2015). These methods have been used to predict central metabolic fluxes and growth rates for a variety of gene mutants and growth conditions, to design rationally mutant strains and also to produce different value-added products, such as polymers or commodity chemicals.

The comprehension of the complex metabolism of bacterial predators with biphasic growth cycles such as *B. bacteriovorus* supposes a great challenge and it remains elusive to date. Moreover, the potential of this predator to be used as biotechnological chassis depends on the quantity and quality of the available metabolic knowledge. This chapter provides a first step in the understanding at system level this predatory bacterium by the integration of different platforms: metabolic reconstruction combined with transcriptomic data set to construct two specific condition models.

2. MATERIALS AND METHODS

2.1 General concepts in the metabolic reconstruction

The advent of genomic age and the subsequent large amount of derived high-throughput data have largely contributed to a deeper understanding of microbial behavior, at system level (Bordbar et al., 2014). Specifically, GEMs are being used for analyzing bacterial metabolism under different environmental conditions (Monk et al., 2014; O 'Brien et al., 2015). GEMs are structured representations of the metabolic capabilities of a target organism based on existing biochemical, genetic and phenotypic knowledge which can be used to predict phenotype from genotype (Nielsen, 2017).

The COBRA Toolbox for Matlab is a leading software package for genome-scale analysis of metabolism. The application of Constraint-Based Reconstruction and Analysis (COBRA) approaches (Heirendt et al., 2007) together with specific GEMs have been successfully applied for a better understanding of interspecies interactions such as mutualism, competition, and parasitism providing important insights into genotype-phenotype relationship (Lewis et al., 2012).

2.1.1 Metabolic network reconstruction

Metabolic reconstruction is a procedure through which the components of the metabolic network of a biological system (genes, proteins, reactions, and metabolites) that are involved in metabolic activity are identified, categorized and connected to form a network.

The metabolic network reconstruction process carried out herein consists of four major stages (Figure 8) (Thiele and Palsson, 2010): 1) generation of a draft reconstruction based on the genome annotation of the target organism and biochemical databases. 2) Manual reconstruction refinement, where the entire draft reconstruction will be re-evaluated and refined in order to identify and resolve errors, gaps, and inconsistencies in the network. During this step, the reconstruction is converted to a mathematical format. 3) Define the external metabolites and the biomass equation. 4) Validation of the model with additional experiments or available experimental data.

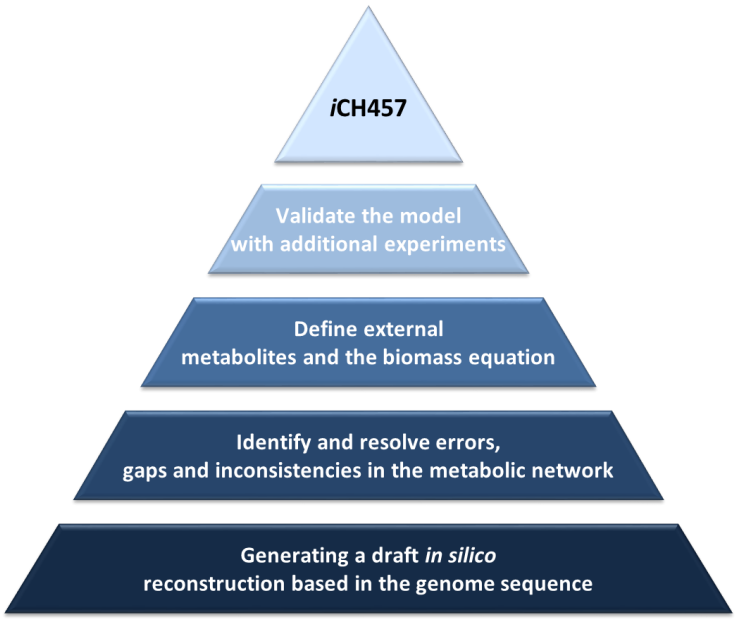

Figure 8. Metabolic network reconstruction process. An initial model draft is constructed from genome annotations and from preexisting biochemical and physiological knowledge of the species. All this information needs to be manual revised. For instance, mass-and charge-balancing of the network reactions are crucial to guarantee comparable properties of the model and the cell or organism. A standard test for most metabolic reconstructions is performed in order to verify that each biomass precursor, which makes up a new cell, can be produced by the model in different growth conditions. The final step is the validation of the network using experimental data available in the literature.

2.1.2 Flux balance analysis (FBA)

FBA is by far the most popular constraint-based modeling technique and it is used in many applications of GEMs. FBA uses optimization of an objective function to find a subset of optimal states in the large solution space of possible states that is shaped by the mass balance and capacity constraints. The applications of FBA for metabolic systems include prediction of the growth rates, uptake rates, knockout lethality, and product secretion. In FBA, the solution space is constrained by the statement of a steady-state, under which each internal metabolite is consumed at the same rate as it is produced (Orth, 2010).

The conversion into a mathematical format can be done automatically by parsing the stoichiometric coefficients from the network reaction list (e.g. using the COBRA toolbox (Schellenberger et al., 2011). The stoichiometric matrix, *S*, has the dimensions *m* by *n* where *m* is the number of the metabolites in the reaction network and *n* is the number of reactions. Therefore, each column represents a reaction and each row represents the stoichiometric

participation of a specific metabolite in each of the reactions (Figure 9). FBA was used to predict growth and flux distributions. FBA is based on solving a linear optimization problem by maximizing or minimizing a given objective function to a set of constraints. The fundamentals of FBA have been reviewed elsewhere (Bonarius et al., 1997; Varma and Palsson, 1994). A particular flux distribution of the network, *v*, indicates the flux levels through each of the reactions. Based in principles of conservation of mass and the assumption of a steady state, the flux distribution through a reaction network can be characterized by the following equation: $S \times v = 0$ (Orth, 2010; Varma and Palsson, 1993). Constraints are placed on individual reactions that state the upper and lower bounds on the range of flux values that each of the reactions can have. This constraint is described in the following form: $\alpha_1 \leq v_1 \leq \beta_1$, where α_1 is the lower bound on flux v_1, and β_1 is the upper bound. If no information about flux levels is available, the value of α_1 is set to zero for irreversible fluxes, and in all other cases, α_1 and β_1 are left unconstrained, allowing the flux to take on any value, positive or negative.

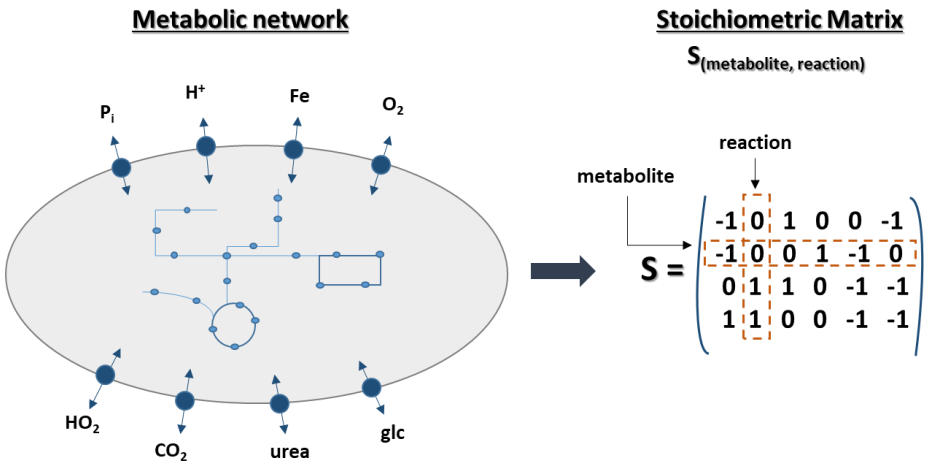

Figure 9. Mathematical representation of metabolic models. The first step in the metabolic reconstruction involves the mathematical representation by a stoichiometric matrix, *S*, of the network reaction list. The columns of *S* correspond to the network reactions, while the rows represent the network metabolites. The substrates in a reaction are defined to have a negative coefficient, while products have a positive value. The metabolites participating in a reaction have non-zero entry in the *S* matrix. Figure adapted from (Thiele and Palsson, 2010).

2.1.3 Condition-specific models

Since GEMs provide a "context for content" for metabolic information, besides of the genomic information used for the reconstruction, the integration of other omic information into the network will contribute increasing the applicability and reliability of the system. The inclusion of transcriptomic, proteomic or metabolomic data into the GEMs constrains the

possibilities of the solution space and gives a more realistic meaning to the *in silico* results. This contextualization becomes crucial in the case of *B. bacteriovorus*, that present a biphasic and it has been reiteratively demonstrated a differential behavior between AP and GP.

In this context, GIM^{3}E (Gene Inactivation Moderated by Metabolism, Metabolomics and Expression) is an algorithm that enables the development of condition-specific models based on an objective function, transcriptomics, and cellular metabolomics data. This platform has been successfully used to accurate the solution space of *Salmonella typhimurium* metabolism during growth and virulence states (Schmidt et al., 2013).

2.2 Genome-scale metabolic network reconstruction: *i*CH457

The genome-scale metabolic model of *B. bacterivorous* HD100 (*i*CH457) was constructed using standardized protocols for metabolic reconstruction (Monk et al., 2014; Thiele and Palsson, 2010), which is briefly detailed in Figure 10A. An initial and automatic draft model was generated from the annotated genome of *B. bacteriovorus* HD100 (GenBank number: BX842601.2) through Model Seed server (Aziz et al., 2012). Additionally, the metabolic content of *B. bacteriovorus* was mapped with those from two broadly used and high-quality GEMs belonging to *E. coli* (*i*JO1366; (Feist et al., 2007)) and *P. putida* (*i*JN1411; (Nogales et al., 2017)) generating additional drafts by using MrBac Server (Liao et al., 2011). Once these models were unified into a final reconstruction, we proceeded to a thoroughly manual curation step of the available metabolic information collected. During this iterative manual curation process, the final inclusion of each individual biochemical reaction, was evaluated by consulting genomic (Rendulic et al., 2004), metabolic, transporter and GEMs databases, including: Kyoto Encyclopedia of Genes and Genomes (KEGG,(Ogata et al., 1999)), BRENDA (Placzek et al., 2017), BIGG (King et al., 2016). Transport reactions were also added by using the TransportDB (Elbourne et al., 2017) database. Relevant reactions added during this procces were listed in Annex 3. Finally, we performed manual gap filling step in order to connect the network as possible and to remove inconsistencies. *Bdellovibrio* legacy literature has been thoroughly consulted ensuring high confidence in the metabolic content included. When specific data of HD100 strain were not available, information from phylogenetically related organisms was used as previously suggested (Thiele and Palsson, 2010).

2.3 Biomass Function

It is commonly assumed that the objective of living organisms is to divide and proliferate. Thus, many metabolic network reconstructions have a so-called biomass function, in which all known metabolic precursors of cellular biomass are grouped (e.g. amino acids, nucleotides,

phospholipids, vitamins, cofactors, energetic requirements, etc.). Since no detailed studies about *B. bacteriovorus* biomass composition are available, the biomass composition from *E. coli* and *P. putida* (Nogales et al., 2017) were used as a template for the biomass function of *i*CH457. However, data from *B. bacteriovorus* were added (e.g. nucleotide composition (from genome sequence)) when available. The detailed calculation of the biomass composition is provided in Table 2.

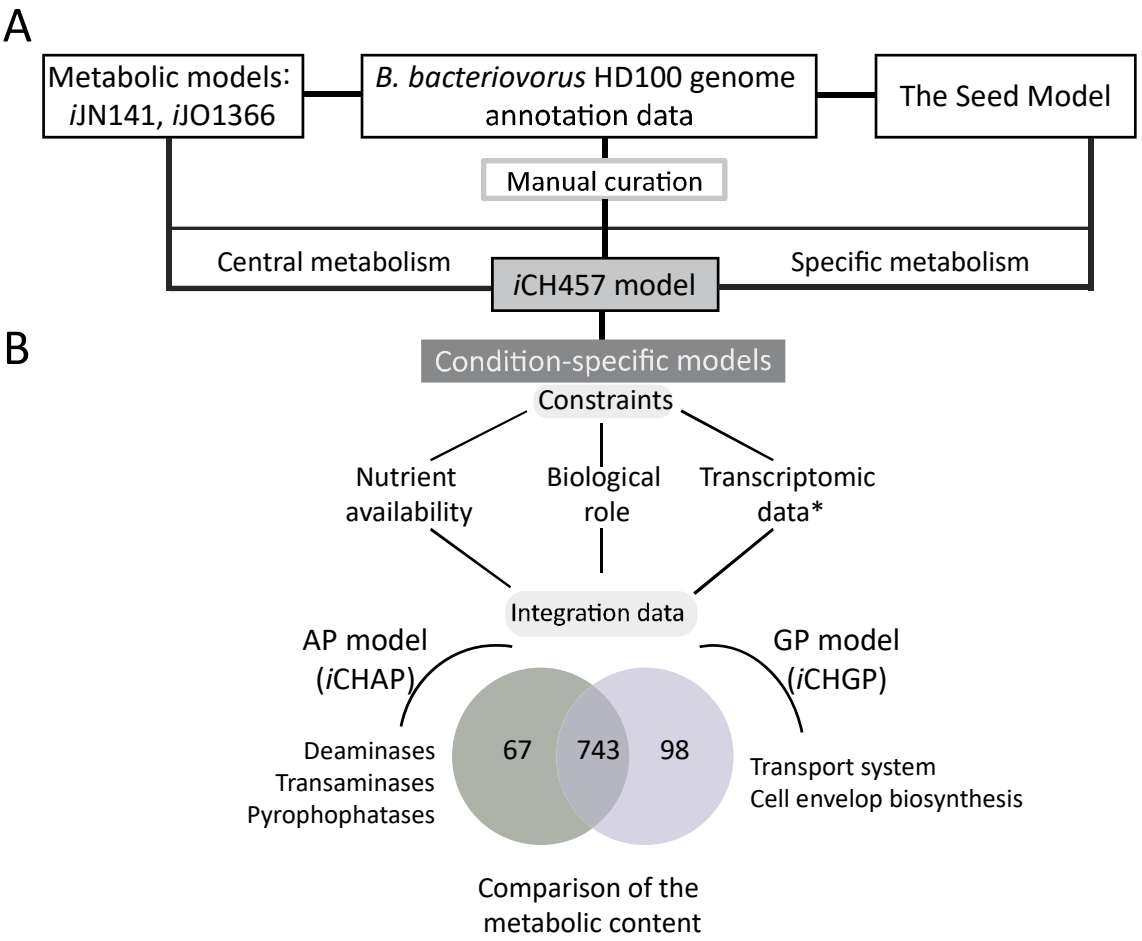

Figure 10. *i*CH457 metabolic model pipeline. A) The draft of metabolic reconstruction was based on available metabolic models (*i*JN1411 and *i*JO1366), the genome sequence of *B. bacteriovorus* HD100 and the automatic model Seed. Manual curation is required to accurate the information contained into the metabolic model and several steps of network validation and analysis are required to finally obtain the metabolic model *i*CH457. **B)** Generation of condition-specific models: *i*CHAP and *i*CHGP. The general model *i*CH457 was constrained based on nutrient availability (minimal and rich *in silico* media), biological role (ATP production or biomass generation) and transcriptomic available data (Karunker et al., 2013)*. GIM^{3}E algorithm was used to construct the condition-specific models. These two models share 743 reactions, while

67 reactions are only active in *i*CHAP, 98 are only expressed in *i*CHGP. This reaction profile defines the solution space of each metabolic model.

Table 2. List of biomass components. The abbreviations used during this thesis are the standard used in the platform BIGG (http://bigg.ucsd.edu/; (King et al., 2016)).

Abbreviation	mmol/gDW	Abbreviation	mmol/gDW	Abbreviation	mmol/gDW
h2o	45.5608	**asp_L**	0.1642	**phe_L**	0.2634
nadph	0.0004	**ala_L**	0.3038	**tyr_L**	0.0746
nadp	0.00013	**his_L**	0.1288	**val_L**	0.2906
nadh	0.00005	**leu_L**	0.42	**arg_L**	0.4732
nad	0.00215	**thr_L**	0.2397	**pro_L**	0.2732
accoa	0.00005	**trp_L**	0.1189	**succoa**	0.000003
fad	0.00001	**asn_L**	0.1399	**pg160**	0.0824
coa	0.000006	**glu_L**	0.1824	**pg161**	0.0296
atp	45.7318	**gln_L**	0.197	**pg180**	0.0005
amp	0.001	**met_L**	0.0896	**pg181**	0.025
adp	45.5608	**cys_L**	0.1502	**murein5p5p**	0.0054
gtp	0.1345	**ser_L**	0.4361	**murein5p5p5p**	0.0055
utp	0.1301	**lys_L**	0.2558	**hemeO**	0.0005
ctp	0.133	**gly**	0.2811	**udpg**	0.003
dttp	0.0882	**ile_L**	0.2131	**btamp**	0.000002
dgtp	0.0909	**clpn160**	0.0207	**pe161**	0.0007
dctp	0.0902	**clpn161**	0.268	**pe180**	0.0031
datp	0.0884	**clpn180**	0.0036	**pe181**	0.0058
ppi	0.7302	**clpn181**	0.0542	**mlthf**	0.05
pi	45.5628	**pe160**	0.0957	**lipopb**	0.000003
h	45.5604				

2.4 Reaction essentiality analysis

In order to determine the effect of a single reaction deletion, all the reactions associated with each gene in *i*CH457 were individually suppressed from the matrix *S.* FBA was used to predict the mutation growth phenotype. The *singleReactionDeletion* function in the COBRA Toolbox (Schellenberger et al., 2011) was used to simulate knockouts. A lethal deletion was defined as that yielding 10% of growth rate values of the original model. The simulations for reaction essentially were performed using the rich *in silico* medium for *i*CH457 (Annex 4). In addition, *i*LB rich medium was used with *P. putida* model.

2.5 Generation of condition-specific models: *i*CHAP and *i*CHGP

To construct specific-condition metabolic models, the constraints were incorporated in the model by a stepwise procedure (Figure 10B). Firstly, the objective function was adjusted to the biological role of AP and GP. ATP maintenance or biomass equations were selected as

objective functions for AP and GP, respectively. In addition, different *in silico* media were designed for each phase simulating the availability of nutrients, rich or minimal media (Annex 4). Finally, the gene expression datasets (mRNA levels) collected for each phase (AP and GP) were obtained from Karunker et al. (Karunker et al., 2013). These data were incorporated to constrain even further the solution space using the GIM^{3}E algorithm as described previously (Nogales and Agudo, 2015). As input, GIM^{3}E builds reduced models by removing those reactions not available in the expression dataset while preserving model functionality. It should be noted that GIM^{3}E considers which genes are expressed or not, but not the modifications in mRNA levels under different experimental conditions. A given gene was considered expressed when its RNA levels in the RNA-seq analysis were ≥ 10 RPKM.

The distribution of possible fluxes in the condition-specific models was calculated using Markov chain Monte Carlo sampling (Schellenberger et al., 2011). The median value from the distribution was used as the most probable flux value.

2.6 Software

All computational simulations were performed using the Matlab-based COBRA toolbox (Schellenberger et al., 2011).

3. RESULTS

3.1 Characteristics of *B. bacteriovorus* metabolic reconstruction

Firstly, a genome-scale metabolic model (*i*CH457) including the metabolic content derived from genome annotation and available biochemical information was created for *B. bacteriovorus* HD100. *i*CH457 does not differentiate AP and GP, but it supposes a powerful tool for determining and analyzing the potential metabolic capabilities of the system from a global perspective. All the gene-protein-reaction associations (GPRs) included in the model were subject to a rigorous manual curation process in order to ensure the quality of the final model. Several open reading frames (ORFs) were annotated and/or re-annotated during the reconstruction process. As an example of this careful process, from the initial 75 ORFs included in the model draft belonging to amino acid metabolism based on bioinformatics evidence, only 65 (87%) were finally included. Among others, the confirmation of several genes related to amino acids metabolism, and hydrolytic enzymes were included (Annex 3).

*i*CH457 includes 457 ORF which represent the 13 % of the coding genes, whose gene products account for 705 metabolic and transport reactions (represented the 70.5 % of the total reaction of the model). The model was completed with the inclusion of 296 non-gene associated reactions (29.5 %) based on physiological and/or biochemical evidence supporting their presence in *B. bacteriovorus*. For instance, genes related to the ACP acyltransferase (*Bd0438* or *Bd1667*) needed for glycerophospholipid biosynthesis were included based on the physiological evidence provide by Nguyen and col. and Muller and col. (Müller et al., 2011; Nguyen et al., 2008). Overall, *i*CH457 accounts for a total of 1001 reactions and 955 metabolites distributed in three different compartments: cytoplasm, periplasm and extracellular space.

Reactions from *i*CH457 fall up into 12 main functional categories (Figure 11). Noteworthy, cell envelope metabolism seems to be the most represented group with a total of 222 reactions, including peptidoglycan metabolism, lipopolysaccharide metabolism, glycerophospholipid metabolism, and murein metabolism. Catabolic reactions represent up to 37%, such as the degradation of the peptidoglycan by specific carboxypeptidases which have an important role in the degradation of the prey cell wall to penetrate into the periplasm, complete the growth cycle and also recycle the envelop components (Lerner et al., 2012).

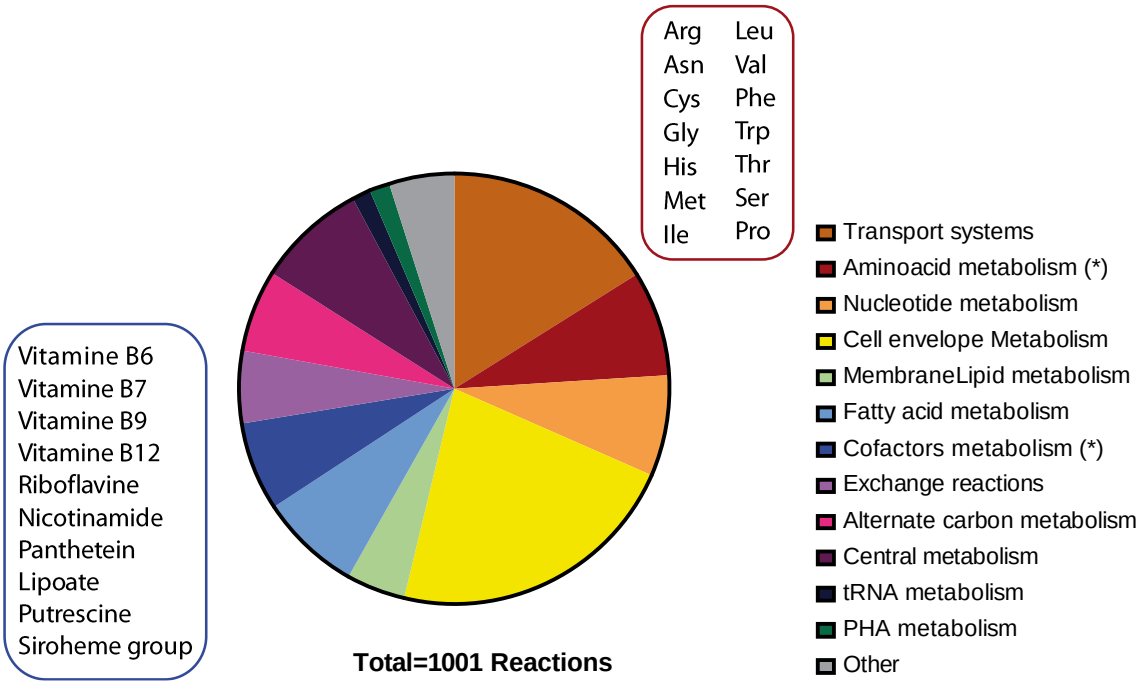

Figure 11. Distribution of the reactions of the system in 12 global functional categories. The metabolites inside the rectangles correspond with the auxotrophies in the cofactor metabolism (dark blue fraction) and the amino acid metabolism (brown fraction), respectively. Asterisks (*) mean the metabolite group that contains auxotrophies.

In the past 15 years, GEMs have garnered considerable research attention and numerous metabolic reconstructions have been generated for several organisms (Oberhardt et al., 2009). The metabolic models within the δ-proteobacteria group are underrepresented among this phylum and only a few of them have been constructed, for instance for *Geobacter* spp. and *Desulfovibrio vulgaris* (Sun et al., 2009; Stolyar et al., 2007; Flowers et al., 2018). Thus, the model of *B. bacteriovorus* HD100, *i*CH457, represents a new model within this group, that as depicted in Table 3 it provides a complete reconstruction of this important bacterial group in terms of metabolites and reactions included. Moreover, although another microbial interaction has been modeled, such as mutualism, this is the first metabolic model of a predatory bacterium (Stolyar et al., 2007).

Table 3. Comparison of the metabolic properties of *i*CH457 compared with other δ-proteobacteria (*Geobacter* species and *Desulfovibrio vulgaris*) metabolic models and with the well-establish metabolic reconstruction of *P. putida* (*i*JN1411) and *E. coli* (*i*JO1366).

	***i*JN1411**	***i*JO1366**	***Geobacter metallirre-ducens***	***Geobacter sulfirreducens***	***Desulfovibrio vulgaris* Hildenborough**	***i*CH457**
Protein-coding Genes	5350	4405	3532	3530	1016	3584
Genes (%)	1411 (26%)	1366 (31%)	747 (21%)	588 (17%)	744	457 (13%)
Metabolites	2057	1136	769	541	1016	956
Reactions	2754	2251	697	523	951	1001
Reference	(Nogales et al., 2017)	(Orth et al., 2011)	(Sun et al., 2009)	(Mahadevan et al., 2006)	(Flowers et al., 2018)	This work

3.2 Model-driven assessment of auxotrophies and biomass building block transport systems highlight the predatory lifestyle of *B. bacteriovorus*

During the reconstruction process, we identified several incomplete biosynthetic pathways (amino acids, cofactors, and vitamins) which agree with the numerous auxotrophies previously reported in HD100 (Rendulic et al., 2004). In fact, model-based analyses identify up to 24 auxotrophies. Overall, the presence of folic acid, pantothenate, pyridoxal phosphate, biotin and lipoate in the *in silico* culture medium will be required for growth. These auxotrophies have been detected not only with the functional genomic but during the gap filling step in the reconstruction process of the metabolic model *i*CH457.

Concerning nucleosides monophosphate, we found that *B. bacteriovorus* accounts for the complete biosynthetic pathways for these key biomass building blocks. Interestingly, it was suggested that prey nucleosides monophosphate produced from the hydrolysis of the nucleic acids represent an efficient source of nucleic acids for the predatory bacterium (RNA and DNA) (Hespell et al., 1975). In fact, radiotracer studies showed that 109J strain mainly utilized host nucleosides monophosphate during intraperiplasmic growth, but it also has the capacity to synthesize its own pool of nucleotides (Matin and Rittenberg, 1972; Ruby et al., 1985). This

"saving energy" mechanism has also been reported for phospholipid assimilation and the recycling of some unaltered or altered fatty acids from the prey (Kuenen and Rittenberg, 1975; Nguyen et al., 2008) which supposed a more efficient incorporation of the cellular components of the prey.

Due to their lifestyle and the obligate requirement of essential biomass building block from prey, the transport subsystem became an important key for the survival of *B. bacteriovorus*. In fact, this category was found to be one of the most representative in terms of number of reactions (161), highlighting their importance in cellular interchange. Although a comprehensive analysis of the transport systems in the predator has been previously reported (Barabote et al., 2007), the predicted substrate specificity needs more experimental support. *i*CH457 model accounts for 67 % of the annotated transport system reported in the genome.

It is worth to remark the case of peptide transporters; despite that amino acids from the proteins breakage have been suggested as major energy sources during the intraperiplasmic growth of *B. bacteriovorus* (Hespell et al., 1973), we notice a significant lack of specific amino acid transporters annotated during the reconstruction process. Instead, we found a large number of di- and tripeptides transporters, suggesting that small peptides might be taking up from the prey by the predator.

3.3 *i*CH457 exhibits high accuracy by predicting physiological states of *B. bacteriovorus* under different nutrients scenarios

Agreements with experimental data often indicate a balanced and accurated reconstruction while ensuring a correct energy generation in the model. In order to address this validation process, we use the model to estimate cell-biomass production by using five different carbon and energy sources, and the *in silico* predictions were subsequently compared with those experimental data already available in the literature. FBA was used to make growth rate predictions, the biomass generation and to determine the initial flux distribution.

Previously to be used as accurate hypothesis generation tools, GEMs need to be properly validated by assessing their ability to compute already known physiological states of the target organisms. This process provides information about model including its connectivity and completeness. Moreover, the predictability of any GEM is a key attribute ensuring the quality of the metabolic reconstruction. GEMs are often validated predicting known growth rates, secretion rates, and nutrients supporting growth in well-defined conditions, e.g., minimal media using a single carbon and energy source. However, the obligate predatory lifestyle of *B. bacteriovorus*, and the complex environment provided by the prey, in terms of nutrients, make

challenging classical validation workflows. Therefore, for *i*CH457 validation, we took advantage of spontaneous HI *Bdellovibrio* strains developed under laboratory conditions. Such HI strains exhibit similar lifecycle when growing in a rich medium than the wild type strain growing inside the intraperiplasmic space of the prey (Figure 6) (Seidler and Starr, 1969). Even more, these HI strains are supposed to possess identical metabolic capabilities than the parental strains, because the HI phenotype has been attributed to putative regulatory mechanisms rather than to metabolic genes (enzymes) (See *General Introduction)* (Cotter and Thomashow, 1992; Roschanski et al., 2011). Thus, for GEMs validation process, including potential carbon sources and biomass generation rates, we decided to use data from HI- *Bdellovibrio* strains.

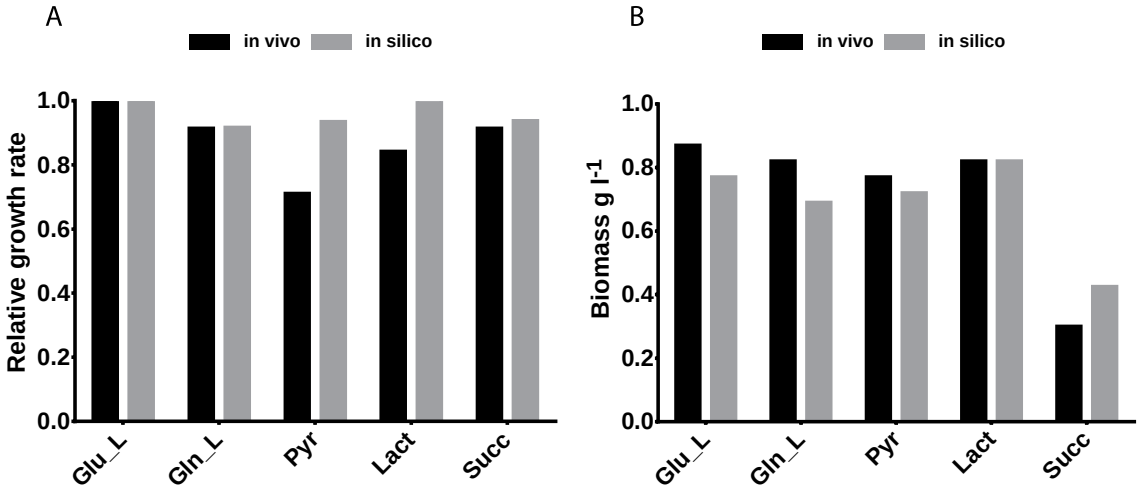

Figure 12. Evaluation of the metabolic capabilities of *i*CH457. A) Comparison of the growth performance of the *in silico i*CH457 strain and a derivative strain of *B. bacteriovorus* 109 Davis on different carbon sources. Experimental values of growth rate were calculated using the mass doubling time previously compiled in Ishiguro et al. (Ishiguro, 1974). The *in silico* growth rate was calculated with the minimal medium defined in Annex 4 supplemented with the tested carbon source. **B)** Comparison of the biomass production predicted *in silico* with the available experimental data performed with the prey-independent *B. bacteriovorus* 109 Davis (Ishiguro, 1974). *In vivo* and *in silico* biomass data were expressed as Kendall's rank correlation coefficient (τ = 0,88) for *i*CH457. Glu_L: glutamate, Gln_L: glutamine, Pyr: pyruvate, Lact: lactate, Succ: succinate.

Specifically, we validate the predictive capabilities of the *i*CH457 by comparing *in silico* results with experimentally determined biomass production and growth rates of the HI strain *B. bacteriovorus* 109 Davis (Ishiguro, 1974). The *in silico* growth rates were calculated with the minimal medium defined in Annex 4 supplemented with the tested carbon source. *i*CH457 was very precise predicting growth rate on five different carbon sources obtaining an accuracy close

to 100% in the case of glutamate, glutamine and succinate, and 70% for pyruvate and lactate (Figure 12A). The discrepancies found between *in silico* predictions and *in vivo* results might be explained by an incomplete formulation of biomass function or higher energy maintenance requirements under the simulated conditions not accounted for in the current reconstruction. In fact, higher *in silico* growth rates are often found due to the intrinsic nature and limitation of FBA. Firstly, because FBA supposes a final evolution state in stark contrast with the scenario *in vivo* which could lack the proper adaptation to these metabolites as a primary carbon source (Fong et al., 2005). Secondly, because it only predicts steady-state fluxes and does not account for any regulatory constraints, which should play an important role in the uptake of substrates from the extracellular medium (Orth, 2010). In any case, the model predictions showed a significant accuracy comparable with other high-quality genome-scale models already available (Nogales et al., 2017).

Beyond the availability to predict growth rates, it is valuable to assess the ability of the model predicting the maximum amount of biomass produced from known concentrations of given carbon and energy sources. Similar high accuracy was found regarding the predictability of biomass production between *in silico* and experimental data (Kendall`s coefficient $\tau = 0.88$) (Figure 12B). Overall, the high accuracy exhibited by *i*CH457 aims us to use the model to characterize the metabolic states that underline the biphasic growth cycle of *B. bacteriovorus*. Noteworthy, the *in silico* analysis provided in these evaluations largely confirmed the prey independent metabolic states shedding light on the potential autonomous metabolism of the predator. These results are in good agreement with the large amount of HI derivative strains isolated previously (Seidler et al., 1969) and the recent description of the metabolic response of AP cells in NB medium to synthesize and secrete proteases (Dwidar et al., 2017). Therefore, the obligate predatory lifestyle of *B. bacteriovorus* could be questioned, at least from a metabolic point of view.

3.4 Reaction essentiality towards understanding the predator´s lifestyle

It is well-known that the environmental conditions and natural habitat of a given bacterium largely influence its evolutionary traits, including processes of genome expansion/reduction. In this thesis, we address from a computational perspective whether the genome content of the predator has been influenced by its complex lifestyle. We proceed to perform a genome-scale analysis of essential reactions in *i*CH457. No large-scale experimental reaction essentiality data are available for *Bdellovibrio* strains and the information can only be deduced for the literature. The network reaction(s) associated with each gene was individually

"deleted" by setting the flux to 0 and optimizing for the biomass function. To properly contextualize the reaction essentiality analysis, we decided to compare the predator results with those from a free-living organisms such as *P. putida* KT2440 (Nogales et al., 2017).

The graphics presented in Figure 13, showed that 335 of 1005 (~33 %) reactions in the FBA models for *i*CH457 are essential for growth (the growth rate becomes 0 when the reaction is removed from the metabolic network), compared to 221 of 2826 (~8 %) for *i*JN1411. The comparison of the essential reaction of *B. bacteriovorus* HD100 (*i*CH457) and *P. putida* KT2440 (*i*JN1411) provided three main groups of essential reactions (Figure 14): i) the common essential reactions between a free-living microorganism and a predatory bacterium, ii) essential reactions exclusively from free-living organism species, iii) essential reactions exclusively from the predator. Potentially the 126 common reactions would be part of that hypothetical essential metabolic network.

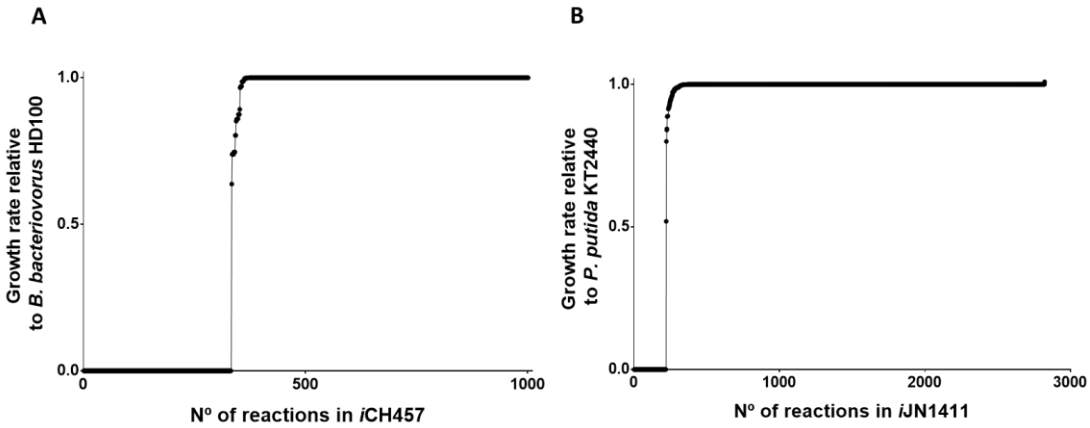

Figure 13. **Metabolic robustness of A) the *i*CH457 metabolic network of *B. bacteriovorus* HD100 and B) the *i*JN1411 metabolic network for *P. putida* KT2440**. These graphs represent the growth rate of each reaction mutant normalized to the wild type, being 1 for deletion in the reaction without any effect and 0 for the lethal deletion.

Overall, the reactions found in the common essentiality group are related with cell envelope, nucleotide, and cofactors. Among the essential reactions found exclusively in *P. putida* (95 reactions), only 17 reactions are present in *i*CH457 metabolic model and they are related mostly with the cofactor and prosthetic group biosynthesis. From this result together with the auxotrophies the predator possesses, it is possible to deduce the adaptation of *B. bacteriovorus* towards non-free-living microorganism, where the uptake of the metabolites become crucial to survive.

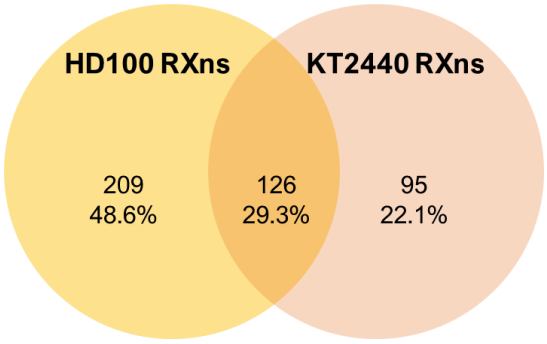

Figure 14. Reaction essentiality analysis. Prediction of the essential reaction of *B. bacteriovorus* HD100 (orange circle) and *P. putida* KT2440 (red circle) using *in silico* rich medium (Annex 4) and *i*LB medium (Nogales et al., 2017), respectively.

3.5 Analysis of the predator´s lifestyle using condition-specific models: Attack Phase (*i*CHAP) and Growth Phase (*i*CHGP) models

B. bacteriovorus possesses a biphasic growth cycle, leading by an extracellular attack phase (AP) and an intraperiplasmic growth phase (GP). It has been previously reported that these two stages are clearly differentiated in terms of gene expression (Karunker et al., 2013) and also in the biological role (Lambert et al., 2009), changes that must be strongly determined by the microenvironment.

B. bacteriovorus AP cells are exposed to extracellular environment with highly diluted concentration of nutrients, but during GP the predator finds a very rich environment inside of the prey. Thereof the predator could hardly find nutrients during AP which determines the search, attaching and invasion of new preys as main biological objective under this scenario. It could be envisaged that, during this period, the predator metabolism is rerouted to obtaining energy, in terms of ATP, allowing the flagellum movement and facilitating the collision with prey cells thanks to its high velocity (Kuru et al., 2017). Once the predator enters the prey periplasm it uses the cytoplasm as a source of nutrients initiating GP. Bacterial cytoplasm is a very crowded compartment where most of the components of a microorganism are localized (30-40% of macromolecules and over 70% of proteins; (Zimmerman and Trach, 1991). Thus, the cytoplasm is an extremely rich environment supporting growth and the completion of *B. bacteriovorus* life cycle (Vendeville et al., 2011; Zhang, 2011). In consequence, it is reasonable to hypothesize that the main aim of this phase is to grow, which implies a highly active metabolism (catabolism and anabolism) supporting fast biomass generation. In fact, recent transcriptomic analyses have shown a highly activated anabolism in this phase (Karunker et al., 2013).

To obtain a deeper understanding of this predatory bacterium in each phase of the life cycle, we proceed to construct two different condition-specific models. Based on the environmental conditions, we have defined two different *in silico* media: minimal and rich medium for AP or GP, respectively (Annex 4). It is worth to notice that they are composed by the same metabolites but in different concentrations. Secondly, focusing on the biological role, we used different biological objective for simulating AP and GP phases. Thus, under AP and GP, ATP production and biomass production were selected as objective functions, respectively. Finally, in order to constrain, even more, the solution space in each growth phase, data from RNA-seq analyses during AP and GP (Karunker et al., 2013) were integrated into the metabolic model using GIMME (Becker and Palsson, 2008). GIM^{3}E is an algorithm which minimized the use of the reactions whose encoding gene expression levels are under a certain threshold, and find a flux distribution consistent with the objective function (biomass generation for GP or ATP production for AP). Overall, in order to construct GP and AP-condition models, *i*CH457 was constrained in terms of i) nutrient availability, ii) biological objective, and iii) gene expression profile, resulting in two new models *i*CHAP and *i*CHGP, mimicking AP and GP growth phases, respectively (Figure 10B).

As previously described, the number of reactions of each specific model was significantly reduced (from 1001 to 810 and 841 for AP and GP, respectively), which means reduced solution spaces, thus promoting more accurate predictions. As could be expected because of the different biological objective in each phase, the condition-specific models were significantly different regarding the metabolic content (Figure 10B). For instance, we found several reactions only present during AP (67 reactions), such as glycerophospholipid degradation enzymes, β-oxidation pathway enzymes, and other different reactions during GP (98 reactions) i.e. enzymes responsible of the cell envelope biosynthesis (Annex 5). In other words, the unique enzymes present during AP should be involved in energy production and guarantee the survival of the cell. In contrast, during GP the unique reactions were involved mainly in the biosynthesis of biomass building blocks. These reaction profiles allowed the optimal pipeline for the estimation of the carbon flux distribution within the metabolic network (Markov chain Monte Carlo sampling; (Schellenberger et al., 2011). These predictions were used for establishing significant differences in the metabolic content between AP and GP. Thus, the prediction of the carbon flux distribution between the two condition-specific models revealed integrated information about the metabolism of the predator (Figure 15). The behavior during AP seems to follow a balanced oxidative metabolism aimed at energy production including intense flux across TCA and oxidative phosphorylation. On the contrary, no significant fluxes were predicted across

anaplerotic and biosynthetic pathways including gluconeogenesis, pentose phosphate, and lipid biosynthesis, suggesting negligible participation of these metabolic hubs during AP. Interestingly, a completely inverse metabolic scenario was predicted under GP. First, this specific model predicted key energetic metabolic pathways being partially inactive during GP. For example, it is important to remark an incomplete performance of TCA cycle when several stages including citrate synthase (CS), aconitase (ACONT), isocitrate dehydrogenase (ICDH), and malate dehydrogenase (MDH) were predicted carrying no flux at all. Instead, acetyl-CoA derived from amino acid catabolism was mainly funneled to the lipid biosynthesis. Reduction equivalents powering oxidative phosphorylation were produced, almost exclusively, from glutamate metabolism via α-ketoglutarate dehydrogenase and succinate dehydrogenase, thus ensuring ATP production. Finally, a very high flux through gluconeogenesis from pyruvate was predicted enabling the required building blocks, for nucleotides and cell envelope biosynthesis in this phase (Figure 15).

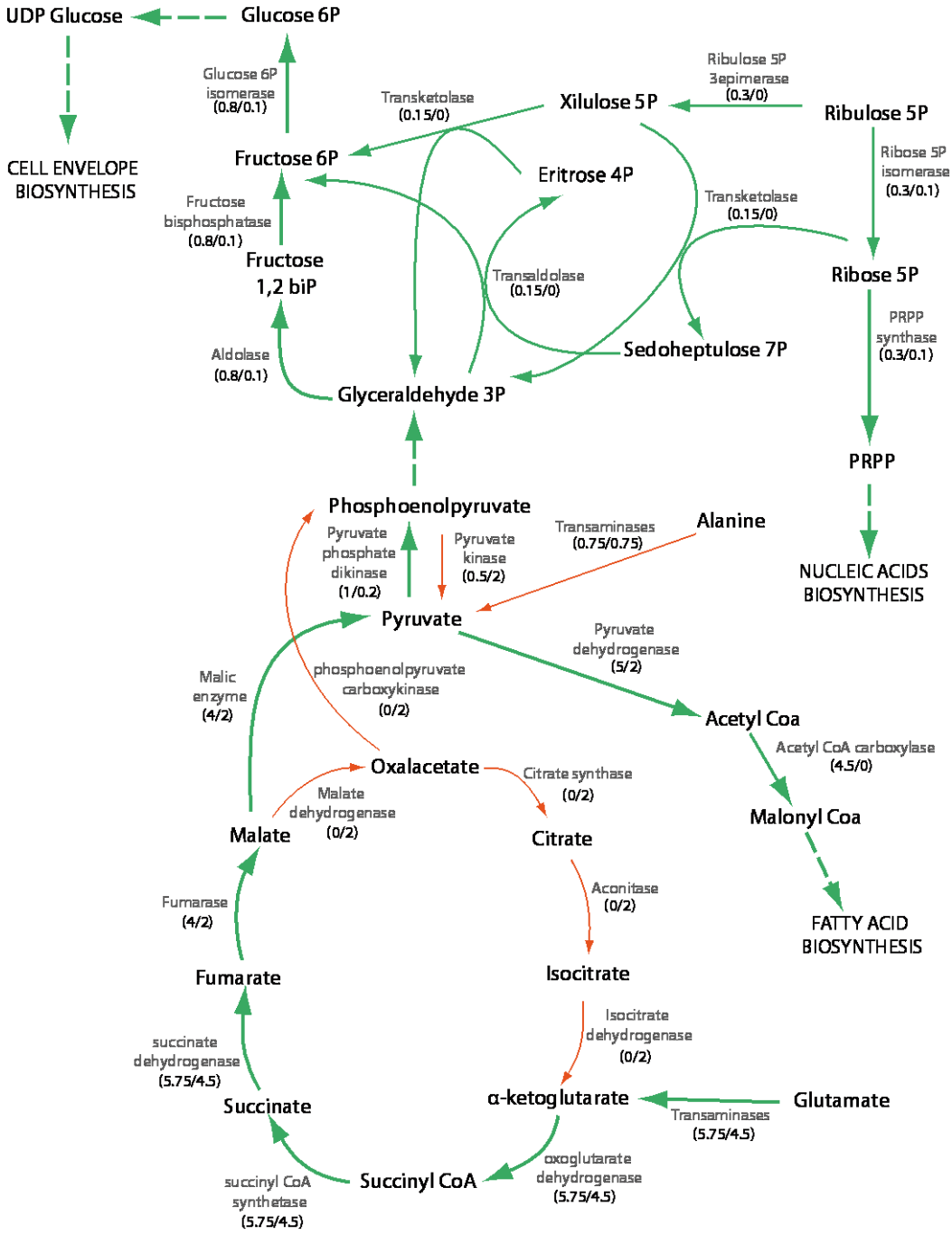

Figure 15. Prediction of the carbon flux distribution in *i*CH457 metabolic network. Graphical representation of the metabolic carbon fluxes during the lifestyle of *B. bacteriovorus* HD100. The numbers above the name of the reactions represent the more probable flux in each phase (GP flux/AP flux) as determined by Monte Carlo sampling analysis. The thick dark green arrows were represented to highlight the carbon flux distribution in GP compared with AP. The thin orange arrows were represented to highlight the reactions that are active in AP compared with GP. As the major carbon sources are amino acids, alanine and glutamate come directly from the breakdown of the dipeptides or from the single amino acids. Eritrose 4 phosphate and glyceraldehyde 3 phosphate come from the degradation pathways of serine and threonine.

VIII. DEVELOPMENT OF AN ACTIVE AND FUNCTIONAL AXENIC CULTURE OF *B. BACTERIOVORUS* HD100

DEVELOPMENT OF AN ACTIVE AND FUNCTIONAL AXENIC CULTURE OF *B. BACTERIOVORUS* HD100

1. INTRODUCTION

B. bacteriovorus HD100 is a predatory bacterium, which lives by invading the periplasm of other gram-negative bacteria. This predator uses the nutrients available in the cytoplasm of its prey as carbon and energy sources to grow and septate into the progeny to finally lyse the prey and begin another attack round. During its growth cycle, there are two different phases strongly differentiated, the attack phase (AP), where the predator is searched for prey, and the growth phase (GP), where the predator elongates as a filament to finally divide into the daughter´s cells (Figure 5). The model *i*CH457, as it was described in Chapter 1, has been used to characterize and predict the metabolic potential and behavior of the biphasic lifestyle of *B. bacteriovorus. i*CH457 provides an extraordinary platform to understand the metabolism of the predator, including hidden metabolic capabilities, such as the deactivation of some key metabolic step during the GP (decarboxylative phase of the TCA). Overall, Chapter 1 describes the different metabolic pathways used by the predator in AP or GP. This also allowed to deeply understand the use of amino acids as a carbon source. Interestingly, the model simulations also postulate reiteratively that the predator should be able to grow axenically taking into account its metabolic capabilities, despite its obligate predatory condition. In other words, *in silico* simulations suggest that other physiological factors, different from the metabolic requirements, would be behind of the obligate predatory lifestyle of *B. bacteriovorus*.

Although *B. bacteriovorus* exhibits an obligatory parasitic life cycle, it is possible to isolate different mutants that no longer require prey cells for growing. These HI variants can be routinely cultivated on standard complex media (Figure 6) (Seidler and Starr, 1969). In terms of growth cycle, HI cells differ from the host-dependent (HD) strains in the growth phase, which is intraperiplasmic in the HD strains and extracellular in the HI mutants. In fact, it has been described that this HI phenotype derives from some mutations in the *hit* (host interaction) locus (Cotter and Thomashow, 1992) (See *General Introduction*).

It has been postulated that the transition to HI behavior can be a consequence of the stimuli of some growth initiation factors (GIF) present in the bacterial cellular extract or in the

supernatant of bacterial cultures. The behavior of these variants seem to be indistinguishable from the wild type strains in terms of metabolic capabilities and predatory ability since the described *hit* locus are not disturbing any catabolic function (Roschanski et al., 2011). It has been described that the *hit* locus codes for some proteins related to the Type IV pili, responsible for the recognition and attachment to the prey cell membrane (Chanyi and Koval, 2014).

A recent report has demonstrated the impact of exposing the obligate predatory *B. bacteriovorus* HD100 to rich medium (Dwidar et al., 2017). The authors observed an increment in size of the predator cells at optical microscopy, suggesting that the obligate predatory bacterium, *B. bacteriovorus*, could increase its biomass in the absence of prey. During this chapter the metabolic growth and capabilities of *B. bacteriovorus* HD100 culturing in a rich medium in terms of biomass production, ATP intracellular levels and replication will be evaluated. The concept of "growth" hereafter is considered as nucleotide, ATP and biomass production. Aside from characterizing the physiological behavior of the predator without the prey interference, we have applied chromatographic techniques to analyze the uptake of metabolites responsible for the activation of the metabolism. This approach would provide key information to define nutritional requirements to allow the transition between AP and GP. The axenic cultivation of *B. bacteriovorus* HD100 would suppose a step further towards the rational control of the predator in order to be used for biotechnological or clinical applications.

2. MATERIALS AND METHODS

2.1 Strain media and axenic growth conditions

B. bacteriovorus HD100 was routinely grown in Hepes buffer at pH 7.8 or DNB liquid medium, in the presence of *P. putida* KT2440 as prey, as it is described in the *Common Materials and methods section*. The HI mutants *B. bacteriovorus* HI18 and HI24 (E. Jurkevitch laboratory collection) were grown in PYE medium (10 g l^{-1} peptone and 3 g l^{-1} yeast extract) (Schwudke et al., 2003). The axenic growth of *Bdellovibrio* cells was carried out in PYE (BdQ cells) or PYE10 (10 g l^{-1} peptone and 10 g l^{-1} yeast extract) media (BdQ10 cells). CAV medium is composed of 200 µM of each amino acid: phenylalanine, glutamate, glutamine, aspartate, asparagine, arginine, threonine, serine, cysteine, histidine, lysine, glycine, proline, isoleucine, leucine, valine, methionine, tyrosine, triptophan and alanine. This medium was supplemented with a solution of trace elements (composition of stock solution 1000 × 2.78 g $FeSO_4 \cdot 7H_2O$ l^{-1}, 1.98 g $MnCl_2 \cdot 4H_2O$ l^{-1}, 2.81 g $CoSO_4 \cdot 7H_2O$ l^{-1}, 1.47 g $CaCl_2 \cdot 2H_2O$ l^{-1}, 0.17 g $CuCl_2 \cdot 2H_2O$ l^{-1}, 0.29 g $ZnSO_4 \cdot 7H_2O$ l^{-1}), 5 µM of KH_2PO_4, 5 µM of K_2HPO_4 and 5 µM of $NHCO_3$. All these compounds are suspended in Hepes buffer 25 mM at pH 7.8.

2.2 Quantification of the genome number of *B. bacteriovorus*

The number of genomes of the predator was estimated by quantitative PCR (qPCR). A DNA fragment of 121 bp located in the coding region of the housekeeping gene *bd2400* (Dori-Bachash et al., 2009) was amplified using the oligonucleotides Bd2400-1 (5´-GCGACTCCAGAACAGCAGATT) and Bd2400-2 (5´- GAATCCGCGGACTGCATTGTA). qPCR was performed using the SYBR Green (LightCycler® 480 SYBR Green I Master) technology in a LightCycler 480 Real-Time PCR system (Roche Applied Science, Germany). Samples were directly analyzed from the culture (containing either prey and predator or predator alone), without DNA extraction. For the calibration curve, genomic DNA was purified from a filtered co-culture of *B. bacteriovorus* HD100 using the IllustraTM bacteria genomicPrep Mini Spin Kit (GE Healthcare, USA) following the instructions of the manufactures. For the measurements, 200 µl of each sample were collected and stored at -20 °C until analysis. Samples were initially denatured by heating at 95 °C for 5 min, followed by 45 cycles of amplification (95 °C, 10 s; test annealing temperature, 60 °C, 10 s; elongation and signal acquisition, 72 °C, 10 s). For quantification of the fluorescence values, a calibration curve was made using serial dilution from 5 to $5 \cdot 10^{-7}$ ng of *B. bacteriovorus* HD100 genomic DNA sample. qPCR was performed with triplicate samples from three independent biological experiments. The negative control was achieved with genomic

DNA from *P. putida* KT2440 as a template. The results were analyzed using the $2^{-\Delta\Delta Ct}$ method (Livak and Schmittgen, 2001).

The genome number of *B. bacteriovorus* HD100 per milliliter can be calculated as follows (Zheng et al., 2008):

n° of genomes of Bd = (ng of DNA in the sample by qPCR)/(weight of the amplicon)

being the weight of the amplicon of $1.24 \cdot 10^{-10}$ ng. The calculations of concentration (genome ml^{-1}) consider that the genome of the predator contains one copy of the *bd2400* gene.

During the replication process, it is possible the formation of several replication forks that can interference the quantification of the genomes. Thus, the homogeneous replication across the predator chromosome was evaluated by qPCR quantification system using different genes distributed along the genome of *B. bacteriovorus* HD100. The selected genes and their features are listed in Table 4.

Table 4. Parameters of the selected genes used to quantify the genome number of *B. bacteriovorus* HD100 by qPCR. Locus on the genome: *bd2478* (293927-292831), *bd0562* (170745-171884), *bd1803* (339602- 337938) and *bd3230* (22311-23105).

Gene	Protein	Gene Length (pb)	Mw of the amplicon (g mol $^{-1}$)	Oligonucleotide 5´-> 3´
Bd2478	Alanine dehydrogenase	1107	$1.51 \cdot 10^5$	F: CAGCTTCGCTTCTGCAGCCAAGTG R: GCGTGCGTCAGTATGTGAGCGAAG
Bd0562	Citrate synthase	1140	$1.04 \cdot 10^5$	F: GCTGGCGGATTCTCCACTCAAC R:GCTTCAGCGCCGTTGTCGTTGG
Bd1803	Fatty acid CoA ligase	1665	$8.22 \cdot 10^4$	F: GGTTGCAGCACACAACTGGAGAAGC R: CGTGTGAAAGTCAGCGTGGCAGG
Bd3230	Thymidilate synthase	785	$1.17 \cdot 10^5$	F: GGCCGCACCATCGATCAGATCAC R: CCAGCTGTATCAGCGCAGTGCTG

2.3 Amplification of DNA and *hit* locus sequencing

PCR amplifications were performed in the buffer recommended by the manufacturer adding 0.05 µg of template DNA, 1 U of Phusion DNA polymerase and 0.4 µg of each deoxynucleotide triphosphate. Conditions for amplification were chosen according to the GC content of the oligonucleotides used, provided by the manufacturer (Sigma- Aldrich, USA). DNA fragments were purified by standard procedures using the Gene Clean Turbo Kit (MP Biomedicals, USA). PCR products were purified using the High Pure Purification Kit (Roche Applied Science, Germany). The oligonucleotides used to amplify and sequence the different *hit*-

related genes are listed in Table 5. All oligonucleotides used in this work have been designed by Geneious (https://www.geneious.com).

Table 6. Oligonucleotides sequences used to amplify the *hit* locus genes to corroborate the wild type phenotype of the predator cells grown in rich medium.

Target gene	Oligonucleotide	Sequence 5´-> 3´
Bd0108	Bd9	CTAGCTAGCAGAAGGTGATTATATGAAAA
	Bd32	AGGAAGCTTTACTGTCTTCCAGTCCCGGCTTTC
	BdRa	AGTGTATTGCCTACCGTACCG
	BdFa	GCCTCATTAGGGTCTTCGCC
Bd3461	3461Ra	GACAAGAGGGTGGTCCGAAG
	3461Fa	CTCTGTCACCACCACGTCC
	3461Fb	CCAGCACGTTCATGTCGTTTTC
	3461Fc	TTGTCGTAACCTGTACCGCC
Bd2400	Bd2400Ra	CGACTTGCAAACATGGACGT
	Bd2400Fe	TTCAACTGTTCTGGCGTTGC
	Bd2400Fd	CGAGACACTTCCACCCAGTT
	Bd2400Fc	GTTTCACTTGGTCCGCACAG
	Bd2400Fb	TTCACCATCCAGTCGTAGCG
	Bd2400fa	ATCAAACCCACACCCAGGAC

2.4 Analysis of extracellular metabolites by GC-TOF-MS

Gas chromatography Time of Flight coupled with Mass Spectrometry (GC-TOF-MS) was used to determine the composition and concentration of the extracellular medium along the time. The supernatants of the cultures were collected, frozen at -80 °C and lyophilized. All GC identifications were based on retentions times and/or comparisons with commercially available standards. Moreover, the National Institute of Standards and Technology (NIST) (Neto et al., 2016) Mass Spectra Library based on a pre-defined matching criteria (similarity index ≥ 70%, (Scheubert et al., 2017)) against mass spectral libraries were used too. Two different analyses were performed during this chapter. An untargeted analysis to determine the global composition of the supernatants and a targeted analysis focused on amino acids to quantify the concentration.

2.4.1 Untargeted analysis of the supernatant of B. bacteriovorus HD100

Previous to the analyses, the samples were derivatized to increase the volatility of polar metabolites. To this aim, 5-10 mg of the supernatant, 300 µl of pyridine and 200 µl of BSTFA (with 1% TMCS) were added to each sample and heated with stirring at 70 °C for 1 h. Subsequently, the reaction mixture was transferred to the GC autosampler vials for subsequent GC-TOF-MS analyses (Chang and Ho, 2014).

Agilent 7890A Gas Chromatography (Agilent Technologies, USA) coupled to Waters Micromass GCT Premier Mass Spectrometer (coupled to COMBI-PAL-GC (EI)) (Waters Corporation, Milford, MA) was used for separation and detection in the GC-TOF-MS setup. A GC column (ZB-5MSplus, Phenomenex, USA) of 30.0 m x 250 µm x 0.25 µm was used. Helium was used as the carrier gas at a flow rate of 1.0 ml min^{-1}. The split ratio for injector was set to 1:10, with a total injection volume of 2 µl. Front inlet and ion source temperatures were both kept at 270 °C. Oven temperature was set to equilibrate at 60 °C for 1 min, before initiation of sample injection and GC run. After sample injection, the oven temperature was increased at a rate of 6 °C min^{-1} to 325 °C and held at 325 °C for 3 min. The MS detection was operated in EI mode (70 eV) with detector voltage of 1900 V. Full scan mode with a mass range of m/z 50–800 was used as data acquisition method. The metabolite identities will be confirmed by targeted analysis.

2.4.2 Targeted analysis in the supernatant of B. bacteriovorus cultures: Amino acids

Silylation was used as derivatization technique to obtain volatile compounds. To this aim, 5-10 mg of the supernatant of *B. bacteriovorus* culture were weight and 500 µl of acetonitrile, 300 µl of pyridine following by 200 µl of BSTFA (with 1% TMCS) were added to each sample. Norvaline was used as internal standard (0.5 mM in each sample) for amino acid quantification. The mixtures were heated at 100 °C for 1 h (Molnár-Perl and Katona, 2000). Samples were subjected to GC-MS analysis on a 30 m x 0.25 mm I.D. x 250 µm Agilent J&W HP-5ms ((5%-Phenyl) methyl- polysiloxane) capillary column.

The reaction mixtures were analyzed in an Agilent series 7890A apparatus coupled to a 5975C MS detector (EI, 70 eV) and a split-splitless injector from Agilent (Agilent Technologies, USA). An aliquot (1 µl) of the organic phase was injected into the gas chromatograph at a split ratio of 1:20. Helium was used as the carrier gas at a flow rate of 1 ml min^{-1}. The injector and transfer line temperatures were set at 250 °C and 280 °C, respectively. The oven temperature program was: initial temperature 80 °C for 0.5 min, then from 80 °C to 290 °C at a rate of 35 °C min^{-1}, at which temperature it was held for 3 min, then from 290 °C to 320 °C at a rate of 40 °C. The mass spectra were recorded in full scan mode (m/z 73- 800). A mix of L-amino acids

(analytical standard AAS18-5ml from Sigma-Aldrich, USA) was used as a standard for identifications.

2.5 Intracellular ATP measurements of *B. bacteriovorus* cells growing in rich medium

Intracellular ATP levels were determined by an ATP bioluminescence assay kit (ATP Biomass Kit HS, BioThema, Sweden) according to the manufacturer instructions. To measure the intracellular ATP, 1 ml of *B. bacteriovorus* cells was centrifuged for 15 min at 13000 x *g* and 4 °C and the pellet was suspended in 1 ml of saline solution (0.85% NaCl), to remove the extracellular ATP. For each condition, four different experiments were carried out and two technical replicates were measured. To normalize the ATP intracellular values, the number of the viable predator cells was also measured by the double layer method (See *Common Material and Methods* for details).

2.6 Consumption, production rate and growth rate calculations in BdQ10 cells

The uptake and/or secretion rate (qs) for each metabolite were obtained for steady-state BdQ10 culture. BdQ10 cells are cells of *B. bacteriovorus* HD100 exposed to PYE10 medium. Steady-state means that the flux of each reaction remains unchanged over time. The calculations were carried out as follow for consumption (or production) rate: $qs_i = (C_{i72}-C_{i0})/72$, where C represents the concentration of each metabolite, i, obtained from the GC-MS analysis. The specific growth rate, μ, in BdQ10 cultures was calculated (in units of g CDW·l $^{-1}$·h^{-1}) as the variation of biomass during the 72 h of growth. The biomass calculations are detailed in *Common Materials and Methods*.

3. RESULTS

3.1 Feasibility of developing axenic cultures of *B. bacteriovorus* HD100: Quantification of the number of genomes of the predator in PYE medium

A recent report has described that HD100 strain seems to activate the metabolism when it is incubated in rich nutrient conditions (Dwidar et al., 2017). This result, together with the interesting predictions of *i*CH457 model of its potential growth in the absence of prey, prompted us to check the feasibility of growing HD100 strain in a rich medium. Specifically, we addressed the ability of the predator to activate its metabolic network by monitoring the ATP intracellular levels, the nucleotide biosynthesis (replication ability) and the biomass production.

To fulfill this objective, *B. bacteriovorus* was grown in PYE medium. The strain HD100 exposed to rich-nutrient-growth conditions in the absence of the prey will be named from now on as BdQ (*Bdellovibrio* quiescent cell) and the HD100 cells incubated in Hepes buffer (control culture) will be named AP cells.

In PYE medium, BdQ cells were able to develop as elongated cells, mimicking the GP phenotype of HD100 in the bdelloplast as it was predicted by the model (Figure 16A). The AP cells kept their short morphology along the experiment (Figure 16B). Since an increment of cell size did not categorically suppose an increment of all macromolecular cellular components, the biosynthesis of nucleic acids was evaluated. To analyze the capability of BdQ cells for DNA synthesis, cell viability and DNA replication (number of genomes in the culture) were measured. BdQ or AP cells were prepared with an initial concentration of $2{\cdot}10^8$ or $5{\cdot}10^8$ pfu ml^{-1}, respectively, and samples were collected each 24 h during 5 days. After the first 48h of incubation, BdQ kept constant in terms of cell viability and number of genomes. However, a significant difference was appreciated after 72 h. The viability decreased drastically up to $5{\cdot}10^5$ pfu ml^{-1} at the end of the experiment (120 h), while the number of genomes duplicated ($5{\cdot}10^8$ genomes ml^{-1}). A decrease of 4-log in the viable number of the predator was detected in the control AP cells along 72 h as well as in the number of genomes, that could be related with the degradation of the nucleotides once released into the extracellular medium from the dead cells (Figure 16E). These results might suggest that BdQ cells were able to generate biomass (increment of size cell) and to replicate their genome owing different replication nucleus, a fact that was validated by dyeing with DAPI the BdQ elongated cells. In Figure 16D it is possible to appreciate an elongated BdQ cell about 25 µm containing around 5-6 genomes (potential daughter cells).

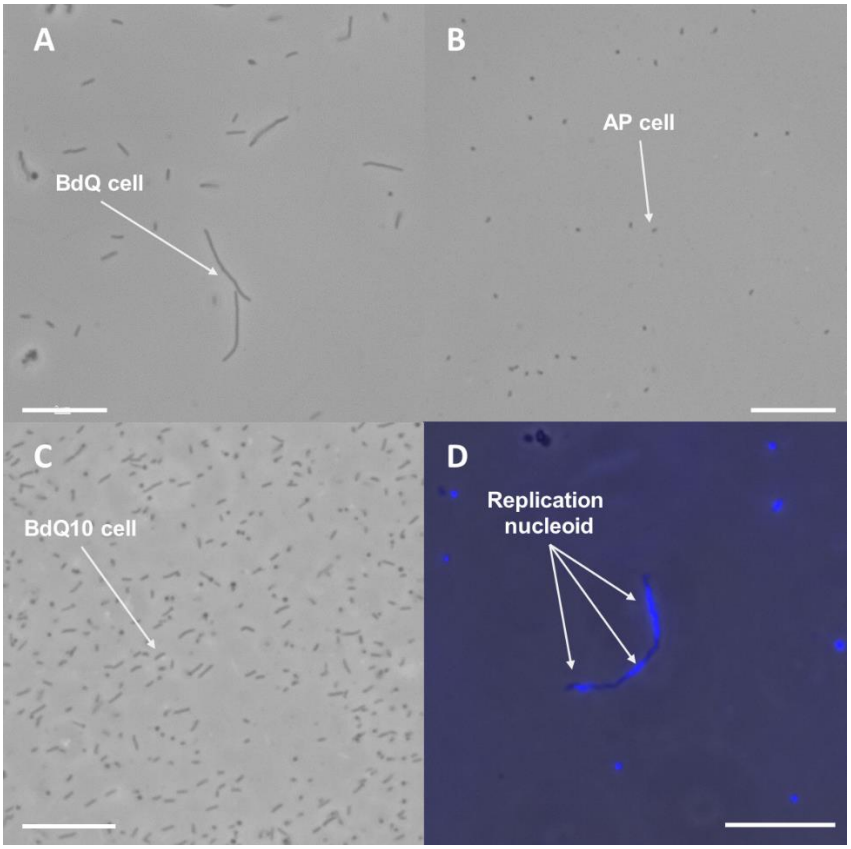

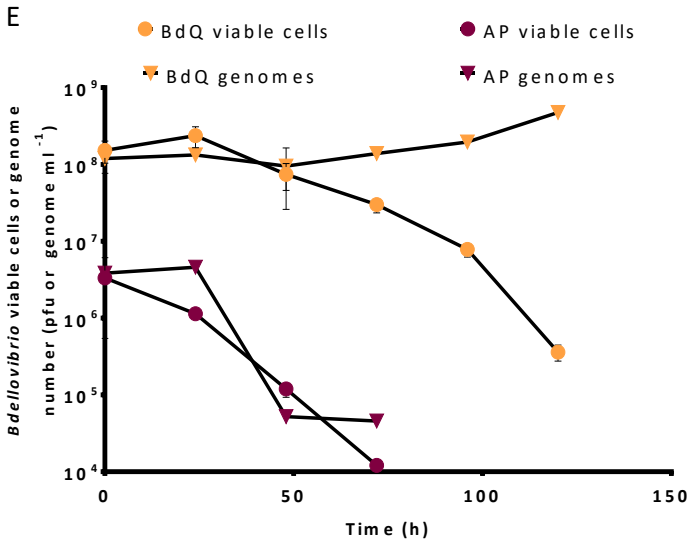

Figure 16. Development of BdQ cells. A) *B. bacteriovorus* cell grown in PYE medium for 24 h (GP). **B)** Morphology of *B. bacteriovorus* AP cells in Hepes buffer at 24 h (AP). **C)** Global view of a culture of BdQ10 cells in PYE10 medium. **D)** Merged fluorescent images of DAPI-stained BdQ cell. The images were obtained after 24 h of incubation at 30 °C in PYE medium. **E)** Viable cell number (circles) or genome number (triangles) of *B. bacteriovorus* grown in Hepes buffer (purple figures) or PYE (orange figures). White lines in the bottom of the micrographies represent a scale bar of 10 µm.

These results allow to establish a growing model for *B. bacteriovorus* that would provide a great system to understand the physiology of this bacterium in an axenic culture for physiological and morphological studies by avoiding the interference with prey cells during the growth phase.

3.2 Analysis of the DNA replication in the genome of *B. bacteriovorus* HD100

Replication is characterized by the formation of replication forks along the chromosome. In order to confirm the homogeneous replication of the genome of the predator and to validate the qPCR system as a reliable and accurate method, we monitored the genome number of *B. bacteriovorus* HD100 using different genes distributed along the chromosome (See Materials and Methods). Table 6 showed the quantification of the genome number by measuring the selected genes. It is important to remark that there are no significant differences between the values of genome number across the chromosome. This result highlights the constant replication of the predatory machinery and certifies this method to be used to calculate predator replication.

Table 6. Analysis of the genome number calculated using different genes along the chromosome of *B. bacteriovorus* HD100. No significant differences are described by statistical analysis. Data are representative of 3 independent experiments. The location of the genes along the genome is described in Materials and Methods.

Gene	Sample	Genome number (genome ml^{-1})
Bd2400	0 h	$(1.04 \pm 0.29) \cdot 10^{11}$
	24 h	$(4.26 \pm 0.04) \cdot 10^{13}$
Bd0562	0 h	$(2.22 \pm 0.32) \cdot 10^{11}$
	24 h	$(4.94 \pm 0.05) \cdot 10^{13}$
Bd2478	0 h	$(3.04 \pm 0.59) \cdot 10^{11}$
	24 h	$(5.17 \pm 0.03) \cdot 10^{13}$
Bd1803	0 h	$(1.53 \pm 0.31) \cdot 10^{11}$
	24 h	$(3.77 \pm 0.02) \cdot 10^{13}$
Bd3230	0 h	$(1.79 \pm 0.03) \cdot 10^{11}$
	24 h	$(2.45 \pm 0.04) \cdot 10^{13}$

3.3 Development of a homogeneous population of BdQ cells

As previously showed, PYE medium provided a heterogeneous size population of BdQ cells (Figure 16A). In order to monitor BdQ cell growth, it was necessary to solve this restriction obtaining a homogeneous BdQ population. The average BdQ size was 1.684 ± 2.301 µm, which reflects a distribution highly disperse. Consequently, the cells were expected to be in different physiological state, which could lead to errors in the quantification of physiological parameters, such as ATP and biomass. Conversely, the average cell size in the AP cells was very homogeneous 0.6883 ± 0.0156 µm (Figure 17A and B). In order to promote the elongation of the BdQ cells, the medium was optimized increasing the concentration of YE from 3 to 10 g l^{-1}. YE contains some biosynthetic building blocks, key intermediate metabolites, vitamins and cofactors that should improve the axenic growth of *B. bacteriovorus* (Ames and MacLeod, 1985). In agreement with this premise, a more homogeneous population of BdQ (average size of 1.310 ± 0.0391 µm) was observed under these conditions (Figure 16C). Hereafter, this modified medium will be named PYE10 and the predator cultured under this condition BdQ10.

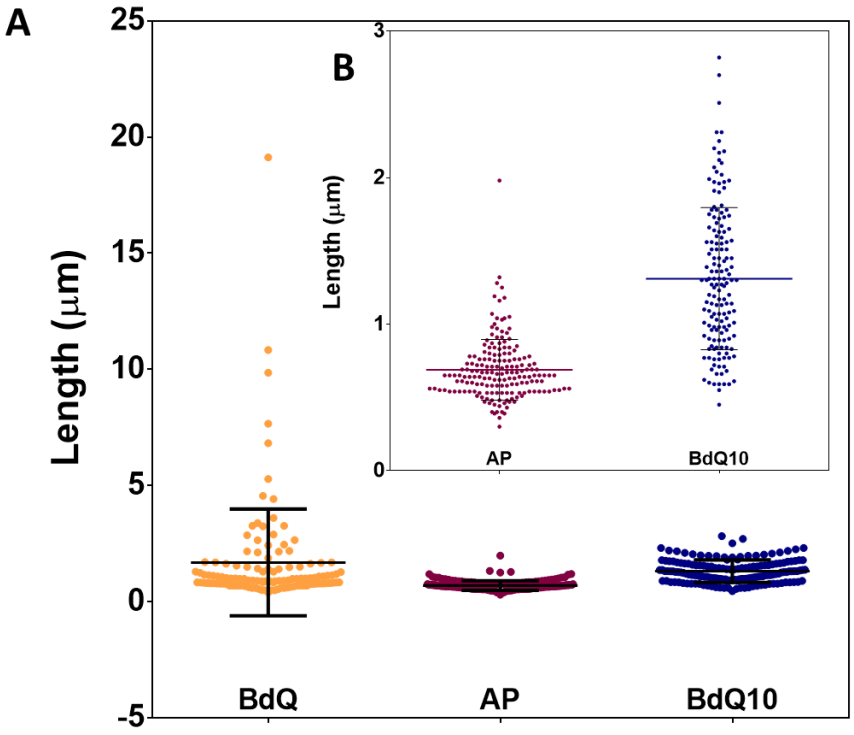

Figure 17. Scatter plot showed the cell size distribution of *B. bacteriovorus* incubated in different medium after 24 h of incubation. A) Distribution of BdQ cells (yellow), AP cells (purple) and BdQ10 cells (blue). The solid line indicates the median and the standard deviation. **B)** Zoom of the distribution of AP and BdQ10 cells. N=300-500 cells from four different biological replicates in each condition were measured using ImageJ software.

3.4 Analysis of the *hit* locus of *B. bacteriovorus*

As previously described, HI phenotype emerges when HD predators are exposed to rich medium. Most common HI mutations have been reported in different regions of the genes *bd0108* and *bd3461*. To ensure the absence of spontaneous mutations in BdQ10 cells yielding HI prey independent mutants, different genes of the *hit* locus described in the literature (Roschanski et al., 2011) were sequenced and compared with the wild type strain HD100 grown in a co-culture with prey. Two different HI mutants, HI18 and HI24, (from E. Jurkevich laboratory collection) were used as controls, containing mutations in the genes *bd0810* and *bd3461* as shown in Figure 18. The alignments of the *bd2400* housekeeping gene (Dori-Bachash et al., 2009), confirmed that all the predator cell cultures belonged to *B. bacteriovorus* species. The alignments of the *hit*-related locus (*bd0810* and *bd3461*: (Roschanski et al., 2011)) revealed that the elongated BdQ cells preserved the wild type genotype (Figure 18). BdQ cells do not contain any of the mutations presented in these regions. The gene *bd3464* was also described as responsible to HI phenotype, but the sequencing and alignment of these regions did not reveal any mutation in AP or BdQ10 (GP) cells (data not shown). Overall, althought the complete genome of the BdQ10 cells will be sequenced to fully confirm these results, our findings suggest that BdQ10 cells are not HI.

3.5 Monitorization of the ATP metabolism and biomass production

To further confirm the active metabolism of the BdQ10 cells, the biomass production and the ATP intracellular levels were also tested. In order to analyze these parameters, BdQ10 and AP cells were prepared with an initial concentration of $5.08 \cdot 10^{9}$ pfu ml^{-1}. 10 ml of these samples were additionally collected to measure biomass production. We found a 2-fold increase in biomass in BdQ10 cells compared with the control culture after 24 h (Figure 19A). The intracellular ATP levels of BdQ10 during 24 h increased almost 5-fold when compared with time 0 h (Figure 19B). In contrast, the biomass and ATP levels of AP cells far from increasing decreased significantly. Taking into account the previous data, it was possible to calculate some physiological parameters of BdQ10 cells, such as the growth rate (μ = 0.0158 h^{-1}) and the intracellular ATP production ($Y_{ATP} = 5 \cdot 10^{-7}$ mmol g^{-1}CDW h^{-1}).

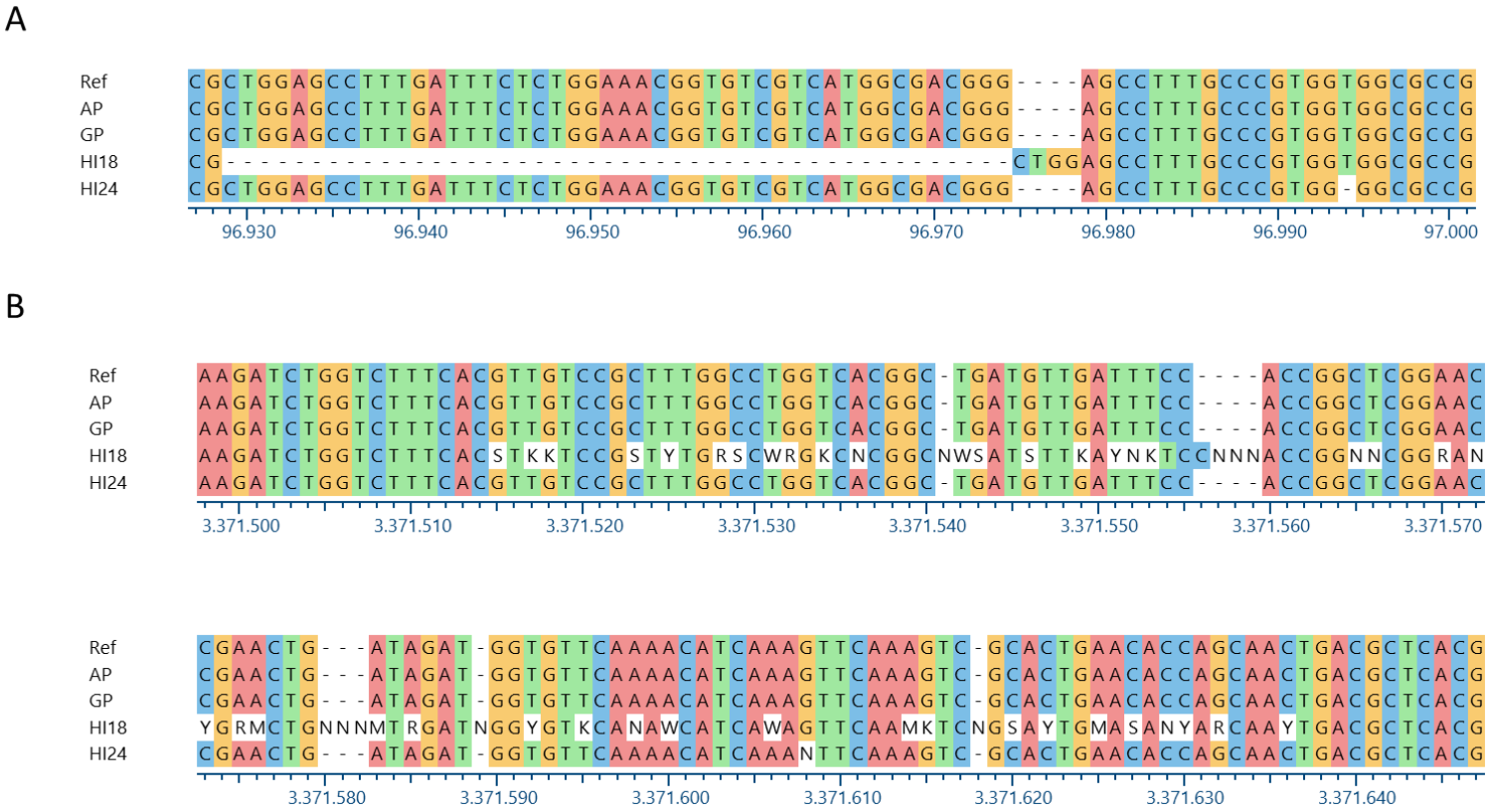

Figure 18. Alignment of *hit* locus in BdQ10 and AP cells and HI18 and HI24 mutant strains. A) *bd0108* gene and B) *bd3461* gene. These sequences were aligned with CLUSTALX (Thompson et al., 1997) and processed in Geneious (Geneious 10.2.2 (https://www.geneious.com)) to identify conserved regions. Sequences are presented in the 5'→3' orientation. Ref: Reference sequence of *B. bacteriovorus* HD100 available in NCBI database. AP: Sequence of AP cells (control cells). GP: Sequence of BdQ10 cells growing in the form of a filament. HI18: Sequence of HI18 mutant strain. HI24: Sequence of HI24 mutant strain. Colors mean different nucleotides.

These data strongly suggested an efficient ATP production as well as an intense synthesis of biomass in rich medium. In fact, after 5 days of incubation in this medium, despite the viability was comprised (orange dots in Figure 16), the remained BdQ10 cells were able to return to the previous predatory state and prey upon *P. putida* KT2440. *P. putida* population was reduced as efficient as fresh predator cells did in 24 h (Figure 19C).

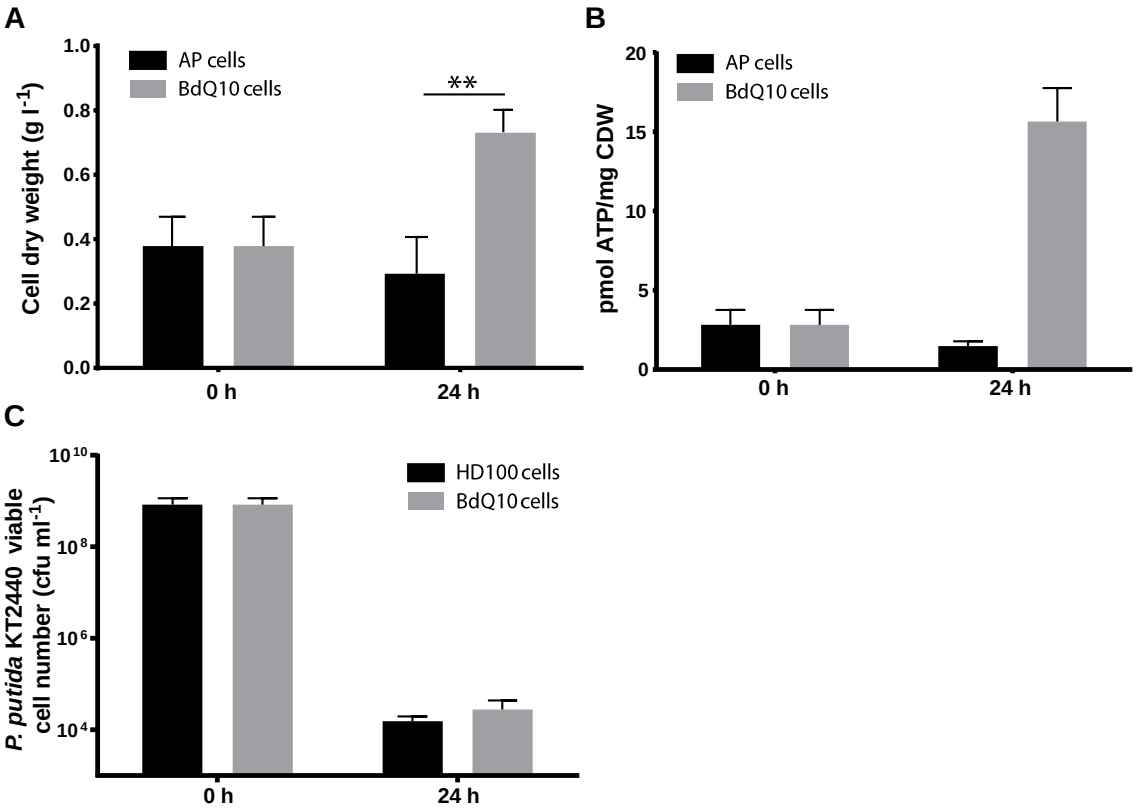

Figure 19. Monitorization of the anabolism of BdQ10 versus AP cells. A) Measurement of ATP intracellular levels of AP cells (black bars) or BdQ10 cells (grey bars). **B)** Total biomass of the culture of AP cells (black bars) or BdQ10 cells (grey bars). Asterisks represent $P< 0.001$. **C)** Number of viable cells of *P. putida* KT2440 at time zero and after 24 h of predation with fresh HD100 cells (black bars) or BdQ10 (grey bars). 0 h represents the BdQ10 cells grown on PYE10 for 5 days.

3.6 GC-MS analysis of the culture supernatant of BdQ10 cells

According to the above results, the wild type strain *B. bacteriovorus* HD100 characterized as an obligate predatory bacterium, was able to grow axenically taking up the metabolites present in PYE10 medium. This axenic elongation (BdQ10 cells are not able to sept) was monitored in terms of DNA replication (genome number per cell), biomass production and ATP generation. To examine the metabolites that *B. bacteriovorus* was able to metabolize and to shed light into the preferred carbon sources, we analyzed the supernatant of the culture

medium by a non-targeted GC-TOF-MS analysis. This technique allows the identification of a wide range of trace amounts of GC-amenable compounds in a single sample in complex matrices (McClenathan et al., 2016). To this aim, BdQ10 was grown for 48 h. The supernatants of the culture were collected and analyzed at 0 and 48 h in order to follow the uptake of different PYE10 components along the time as well as the potential secretion of metabolites.

Table 7 and Annex 6 give a comprehensive overview of the metabolic composition of the supernatant of different samples (semi-quantitative data). The analyses of the chromatograms allowed the identification of numerous compounds and created *a priori* knowledge necessary for further targeted analyses. Table 7 shows a heat map visualization of the metabolites identified by GC-QTOF-MS analysis in each of the samples. The estimated concentration of these untargeted analyses is performed separately in each condition, where one metabolite can be related only with the rest of the metabolites detected in the same condition (column). Then, the results of each column are not comparable among the different columns. It is worth to notice that the relative concentration of the PYE10 components (used as a control) at 0 and 24 h varies over the time (AMES et al., 1985). However, the amino acidic composition of PYE10 medium does not seem to change after 48 h in this non-targeted analysis. In contrast, the composition of the supernatant collected from the BdQ10 (PYE10 + Bd 24 h) culture changed drastically. Different compounds derived from the metabolism of the predator direct or indirectly were identified. Interestingly, in this sample the area of the peaks of each metabolite is quite similar, resulting in comparable concentrations (colors).

Since the prevalent presence of amino acids as major components in PYE10, we further focused on the quantification of all these metabolites in order to analyze the evolution and the preference of carbon sources for *B. bacteriovorus* over time. With this aim, we performed a direct analysis of GC-MS targeted to the amino acids, which were previously described as major carbon sources and taking into account the results obtained during our non-target analysis.

Table 7. Heat map visualization of the compounds identified in the GC-QTOF-MS analysis. Chromatographic analyses were performed in three different silylated samples: PYE10 at time 0, PYE10 at 48h and supernatant of PYE10 with BdQ10 cells after 48h. Color bars indicate relative signal intensity. Bd: *B. bacteriovorus* HD100.

Metabolite	PYE10 0 h	PYE10 24 h	PYE10 + Bd 24 h
acetic acid			
L-valine			
alanine			
glycine			
L-norvaline			
serine			
phosphate			
glycine			
butanedioic acid			
propanoic acid			
fumaric acid			
L-threonine			
L-methionine			
malic acid			
L-proline			
L-glutamic acid			
rythronic acid			
phenylalanine			
1-H-indole-2-acetic acid			
10-hydroxybenzoflavine			
glutamine			
arabinofuranose			
phosphoric acid			
D-altrose			
ornithine			
arabinohexanoic acid			
tyrosine			
D-glucose			
D-galactose			
D-mannitol			
alpha-D-mannopyranoside			
D-gluconic acid			
hexadecanoic acid			
inositol			

The concentration of each amino acid was quantified along the time (0 and 48 h) and the differences between the control culture at the beginning of the experiment and culture of BdQ10 were calculated as consumption rate. PYE10 was also incubated without bacteria to control the spontaneous degradation of the components.

Figure 20 shows the uptake and secretion profile of each amino acid detected in the analyses as well as the initial concentration. These analyses have revealed that almost all of the amino acids are susceptible to be consumed by *B. bacteriovorus* HD100. Positive and negatives values mean secretion or absorption of the metabolites, respectively. The consumption of each amino acid was normalized to its initial concentration. The metabolites with higher values are serine, threonine, proline, and valine. Thus, these metabolites were the preferred to be consumed.

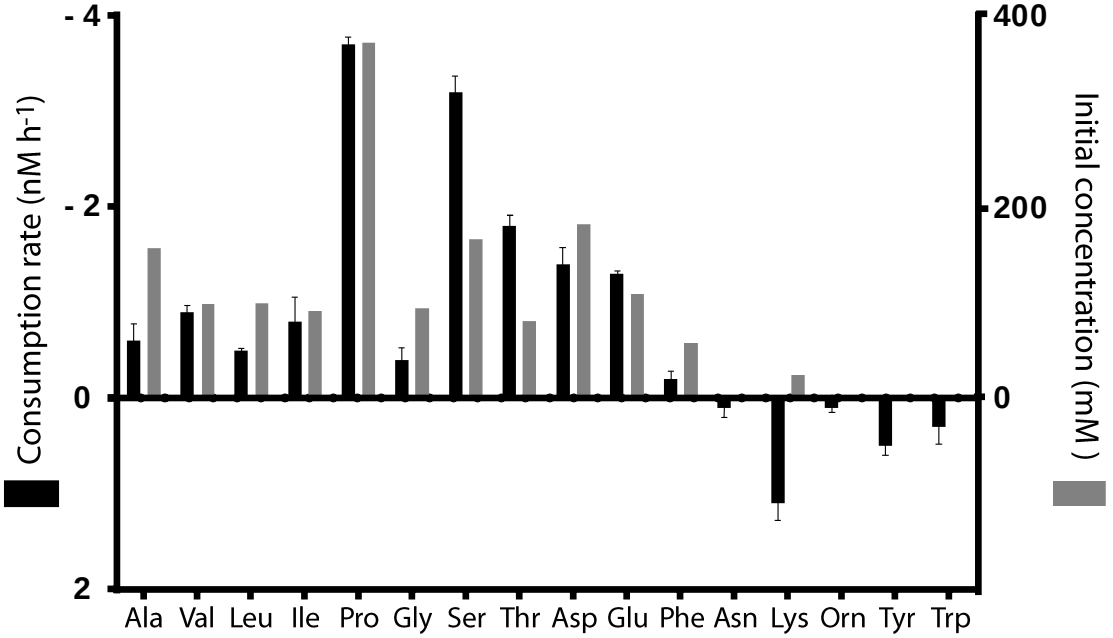

Figure 15. Consumption and production rates of amino acids. Uptake and secretion rates of BdQ10 cells measured experimentally by GC-MS (black bars) and the initial concentration of each metabolite (grey bars). The error bars are standard deviations calculated from 3 replicates. The uptake of metabolites is represented by negative values while the secretion corresponds with positive values.

3.7 Design of a minimal synthetic medium mimicking the transition phase from AP to GP

Taking into account the analysis of the metabolites taken up by *B. bacteriovorus* from PYE10, we decided to incubate the predator on a medium called CAV, only composed by amino

acids, inorganic molecules and a cocktail of vitamins to supply the auxotrophies (See *Materials and Methods*).

Figure 21A shows the evolution of the genome number of the predator along the time using CAV as carbon, nitrogen and energy sources. An increase of 2-fold during 48 h and 4-fold in 72 h was observed compared to the control culture (AP cells). From this nucleotide biosynthesis, we can infer a theoretical growth rate of 0.058 h^{-1}. The biomass of the predator cells growing under this condition did not increase in the 72 h of incubation (data not shown) and could be related to a rational use of the amino acids focusing the energy obtained on the survival and reproduction of the species. This strategy has been widely extended in the parasitic organism and viruses (Moran, 2002). Figure 21B shows that intracellular ATP levels along the time related to the biomass, kept constant compared to the control culture. These results highlighted, firstly, the evident use of the metabolites present in CAV, which are responsible for the activation of the metabolism of the predator in terms of nucleotide biosynthesis and production of minimal energy requirements. Secondly, it is important to remark the efficient ATP production system of the predator. ATP is being produced as much as it is consumed in the anabolism for cellular maintenance.

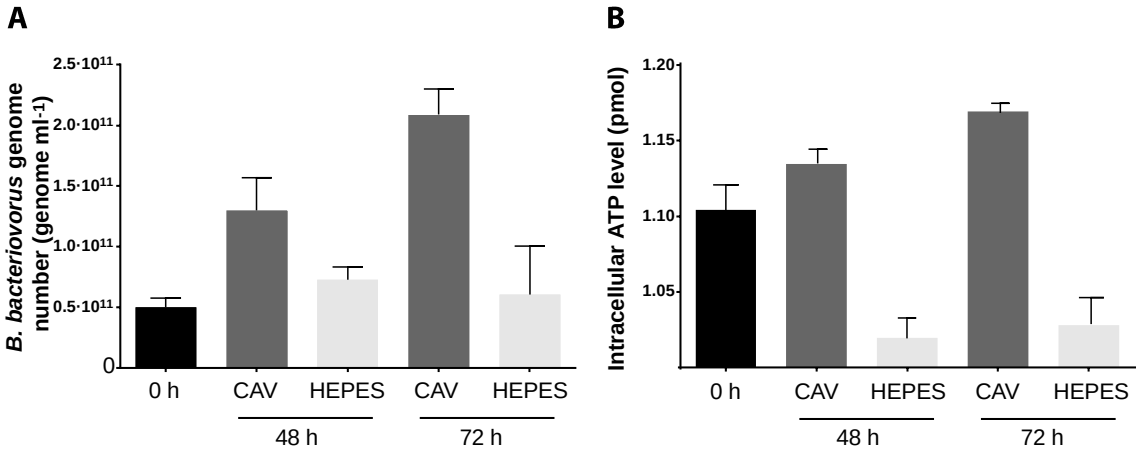

Figure 21. Monitorization of the anabolism of *B. bacteriovorus* in CAV medium. A) Genome number of the culture of *B. bacteriovorus* HD100 at the onset of the experiment (time zero) and within 48 and 72 h in CAV or Hepes buffer. **B)** Measurement of ATP intracellular levels.

To further demonstrate the uptake of the CAV components, we also performed a GC analysis of the supernatant of the cultures to follow the consumption. Table 8 shows the consumption of the metabolites found in the analysis. The concentration of each amino acid was 200 µM in the CAV medium. This corresponds with saturated concentrations avoiding biological constraints in the uptake of the metabolites. Remarkably, at 48 h of incubation, glutamate was

the only amino acid that is consumed almost completely, demonstrating that this metabolite is the most preferred under this condition. Once this amino acid was consumed, the concentration of the other components in the medium started to decrease, being aspartate, threonine, and valine the favorite metabolites.

This constitutes a confirmation of the preferred nutrients of *B. bacteriovorus* HD100 when amino acids are supplied in the medium.

Table 8. Consumption rate of the amino acids at 48 and 72 h referred to the concentration of each compound at the beginning of the measurements.

	Consumption rate at 48 h (%)	Consumption rate at 72 h (%)
Alanine	0.0	8.0
Aspartic Acid	1.6	36.0
Glutamic Acid	92.2	100.0
Glycine	0.0	15.0
Proline	0.0	11.0
Serine	0.0	17.7
Threonine	7.8	48.1
Valine	0.0	31.0

IX. DEVELOPMENT OF *BDELLOVIBRIO BACTERIOVORUS* AS BIOLOGICAL LYTIC TOOL FOR INTRACELLULAR BIOPRODUCTS RECOVERY: THE PROOF OF CONCEPT OF POLYHYDROXYALKANOATES

Part of the results included in this section and the corresponding methodology have been accepted and published in the journal Scientific Reports. Citation: Martínez, V*., Herencias, C*., Jurkevitch, E., Prieto MA., 2016. Engineering a predatory bacterium as a proficient killer agent for intracellular bio-products recovery: The case of the polyhydroxyalkanoates. Scientific Report 6: 24381 (2016) doi:10.1038/srep24381. The authors' contribution in the publication was: Martínez V. designed and performed the experiments and wrote the paper. Herencias C. designed and performed the experiment and wrote the paper. Jurkevitch E. contributed to the final version of the manuscript. Prieto MA. designed the experiments, supervised the findings of this work and the writing of the paper. *: These authors contributed equally to this work.

DEVELOPMENT OF *B. BACTERIOVORUS* AS BIOLOGICAL LYTIC TOOL FOR INTRACELLULAR BIOPRODUCTS RECOVERY: THE PROOF OF CONCEPT OF POLYHYDROXYALKANOATES

1. INTRODUCTION

Taking into account the potential application of predatory bacteria as a source of biocatalysts due to their extensive and powerful hydrolytic arsenal, in this chapter, we give an example of the use of a *B. bacteriovorus* as a killer bacterium for biotechnological purposes. Given the predatory lifestyle of BALOs and their ability to lyse other bacteria, we take advantage of HD100 predator as a novel downstream living lytic agent for the production of valuable intracellular bio-products. One of the most challenging downstream production processes is the isolation of bacterial polyesters or polyhydroxyalkanoates (PHAs) at industrial scale. These biodegradable polymers, which are produced by a wide variety of bacteria, are attractive alternatives to petroleum-based plastics (Prieto et al., 2016). They accumulate as intracellular granules in the bacterial cytoplasm and can reach up to 90% of cell dry weight. Depending on the length of the lateral chain, these polymers have different mechanical and physicochemical properties. Several short-chain-length-PHAs (scl-PHA) such as poly-3-hydroxybutyrate (PHB), are currently produced at large scale by several companies (Chanprateep, 2010) and have extensive applications in packaging, moulding, fibre production and other commodities. Medium-chain-length-PHAs (mcl-PHA, with carbon numbers ranging from 6 to 14) are also promising candidates as bioplastics given their longer-side-chain-derived properties of reduced crystallinity, elasticity, hydrophobicity, low oxygen permeability and biodegradability. Moreover, mcl-PHA are being used to resorbable materials for medical applications, and as food coatings, pressure-sensitive adhesives, paint binders and biodegradable rubbers (Sudesh et al., 2011). However, their condition as intracellular bio-products makes their recovery difficult and expensive (Jacquel et al., 2008; Madkour et al., 2013).

In the last years, a great effort has been made for isolating these biopolymers, which is the key step for process profitability in the fermentation system (Madkour et al., 2013). Different methods such as mechanical cell disruption by high-pressure homogenization, separation processes (filtration, froth flotation, continuous centrifugation), enzymatic digestion or use of

detergents and solvents have been investigated (Jacquel et al., 2008). However, the high costs of the process or the reduced quality of the recovered polymer due to the applicability of these methods supposed a considerable disadvantage.

Here, we present a robust and expandable downstream system based on the use of the predatory bacterium *B. bacteriovorus* HD100 as a cell lytic agent. It has been shown that *B. bacteriovorus* HD100 can prey upon PHA-producers such as *P. putida* KT2440 while the latter accumulates large amounts of mcl-PHA within its cells (Martínez et al., 2013). After lysing the prey, the predator hydrolyzes and consumes part of the PHA released into the extracellular environment; indeed, significant quantities of PHA granules and free hydroxyalkanoic acid (HAs) oligomers (54% and 25%, respectively, of PHA accumulated by the prey bacteria) (Martínez et al., 2013) can be recovered. This is due to the activity of an extracellular-like mcl-PHA depolymerase (PhaZBd), which forms part of the hydrolytic arsenal of *B. bacteriovorus* (Martínez et al., 2013, 2012; Rendulic et al., 2004). In this chapter, *B. bacteriovorus* HD100 was engineered in order to avoid the degradation of prey-produced PHA. Besides, we showed the ability of *B. bacteriovorus* to attack high cell density prey cultures, allowing the release of the polymer.

To further demonstrate the feasibility of the system, engineered *B. bacteriovorus* strains were tested against different gram-negative bacteria that accumulate PHA. The results provide a proof-of-principle that this system could be used for intracellular bio-products recovery.

2. MATERIALS AND METHODS

2.1 Bacterial strains, media and growth conditions

Plasmids used in this work are described in Table 9. Unless otherwise stated, *Escherichia coli*, *P. putida* KT2440, *P. putida* KT2442Z, *Cupriavidus necator* and *Rhodospirillum rubrum* strains were grown in nutrient broth (NB) medium (Difco, Dickinson and Company, France) or in lysogeny broth (LB) medium (Green and Sambrook, 2012) at 37 °C (*E. coli*) and 30 °C (*P. putida*, *C. neca*tor and *R. rubrum*) at 250 rpm. Chloramphenicol (Cm) (30 μg ml^{-1}) and kanamycin (Km) (50 μg ml^{-1}) were added when needed. Growth was monitored with a Shimadzu UV-260 spectrophotometer at 600 nm (OD_{600}). Solid media were supplemented with 1.5% (w/v) agar. For PHB production, *E. coli* ML35 (pAV1) strain was grown in LB medium supplied with 1% glucose, at 30 °C for 40 h; *C. necator* was grown in LB medium supplied with 2% glycerol for 24 h. For mcl-PHA production, *P. putida* strains were grown in 0.1 N M63, a nitrogen-limited minimal medium (13.6 g of KH_2PO_4 l^{-1}, 0.2 g of $(NH_4)_2SO_4$ l^{-1}, 0.5 mg of $FeSO_4 \cdot 7H_2O$ l^{-1}, adjusted to pH 7.0 with KOH). This medium was supplemented with 1 mM $MgSO_4$ and a solution of trace elements (composition 1,000 ×, 2.78 g of $FeSO_4 \cdot 7H2O$ l^{-1}, 1.98 g of $MnCl_2 \cdot 4H_2O$ l^{-1}, 2.81 g of $CoSO_4 \cdot 7H_2O$ l^{-1}, 1.47 g of $CaCl_2 \cdot 2H_2O$ l^{-1}, 0.17 g of $CuCl_2 \cdot 2H_2O$ l^{-1}, 0.29 g of $ZnSO_4 \cdot 7H_2O$ l^{-1}) and sodium octanoate (15 mM) was used as sole carbon source, as previously described (Moldes et al., 2004). *B. bacteriovorus* HD100 was routinely grown on two-membered cultures as described in *Common Materials and Methods* (Herencias et al., 2017).

2.2 DNA manipulations

DNA manipulations and other standard molecular biology techniques were essentially performed as described previously (Green and Sambrook, 2012). PCR amplifications were performed with 0.05 μg of DNA template. The amplification mixture also contained 2 U of AmpliTaq DNA polymerase (Perkin-Elmer Applied Biosystems, USA), 0.5 μg of each deoxynucleotide triphosphate, and 2.5 mM $MgCl_2$ in the buffer recommended by the manufacturer. Conditions for amplification were chosen according to the GC content of the corresponding oligonucleotides. DNA fragments were purified by standard procedures using Gene Clean Turbo kit (MP Biomedicals, USA). Genomic DNA was isolated with the bacteria genomicPrep Mini Spin kit (GE Healthcare, USA). PCR products were purified with the High Pure plasmid isolation kit (Roche Applied Science, Germany).

Table 9. Plasmids and oligonucleotides used in this study. [a]Engineered endonuclease sites in the oligonucleotides are shown underlined.

Plasmid or oligonucleotide	Genotype, description or sequence (5' to 3')	Reference
Plasmid		
pACYC184	p15A, Cm^R, Tet^R	
pAV1	pACYC184 derivative containing PHB biosynthetic genes (*phbABC*) from *C. necator* H16, Cm^R	Prieto Lab collection
pK18*mob*SacB	Km^R, ColE *ori*V, Mob+, *lac*Za, *sacB*; vector for allelic exchange homologous recombination mutagenesis	(Schäfer et al., 1994)
pK18*mob*SacB-2637	pK18*mob*SacB derivative used for Bd2637 deletion	This work
pK18*mob*	*ori*ColE1 Mob^+ *lacZα*$^+$, Km^R used for direct insertional disruption	(Schäfer et al., 1994)
pK18*mob*-3709	pK18*mob* derivative used for Bd3709 disruption	This work
Oligonucleotide[a]		
PHB-F	GCTCTAGAGACGTCCCAACCACCTCTTGAA	This work
PHB-IR	CGGGATCCGGTGACCTCCTGATGAAGAAATCA	This work
PHB-IF	CGGGATCCTGATTACGTCAGCAAATCCGG	This work
PHB-R	CCCAAGCTTGTTGTGAAACAGATTGCGCCC	This work
PHO-F	GCTCTAGAG GAGCTTCTTCCAGCCATTCGTGACGAGC	This work
PHO-R	CCCAAGCTTCGGGATGACCCACGGTCATTC	This work

2.3 Construction of *B. bacteriovorus* HD100 mutants

B. bacteriovorus Bd3709::pK18*mob* strain (called Bd3709 in this chapter) was constructed via disruption of the *phaZBd* gene (ORF Bd3709) by insertion of the whole pK18*mob* plasmid, which confers kanamycin resistance. Using the oligonucleotides PHO-F and PHO-R (Table 9) and *B. bacteriovorus* HD100 genome as a template, a DNA fragment of *phaZBd* gene with 582 bp was developed introducing an artificial stop codon to interrupt the mRNA translation of the transconjugants after homologous recombination. This fragment was digested with appropriate restriction enzymes (Takara Bio, Japan) and it was ligated using T4 DNA ligase (USB Corp., Affymetrix, USA), resulting in the corresponding modified version of the gene. This gene was cloned into the corresponding *Hind*III and *Xba*I sites of pK18*mob* plasmid to yield pK18*mob*-3709. The resultant plasmid was confirmed by DNA sequencing and used to deliver the mutation to the host chromosome of *B. bacteriovorus* HD100. Biparental mating was performed using *E. coli* S17-*λpir* as donor strain and *B. bacteriovorus* HD100 as recipient strain. For conjugation, 12 ml of the overnight culture of donor strain, suspended in 100 µl of DNB, and

50 ml of *B. bacteriovorus* HD100 co-culture filtered, pelleted and suspended in 100 µl of DNB, were collected on a Millipore filter, which was subsequently placed on a DNB agar plate and incubated for 30 h at 30 °C. After incubation, the cells were suspended in 2 ml of DNB medium and plated on DNB plus kanamycin using the double-agar-overlay method (See *Common Materials and Methods Section*) with a kanamycin resistant *P. putida* strain as prey (Prieto´s lab collection). Transconjugants were isolated from double-layer agar plates and the insertion was checked by PCR. To confirm the insertion stability, ten consecutive passes from plate to plate containing DNB plus kanamycin were performed, and the insertion was checked by PCR in twenty predator plaques.

The *bd2637* gene, coding for a putative scl-PHA depolymerase (Rendulic et al., 2004), was inactivated by allelic exchange homologous recombination using the mobilizable suicide plasmid pK18*mob*SacB (Table 9). The deletion of *bd2637* gene was engineered with the DNA fragments PHBA and PHBB of 745 bp and 776 bp, respectively, generated by PCR using the primer pairs PHB-F and PHB-IR for PHBA, and PHB-IF and PHB-R for PHBB (Table 9). These two fragments were digested with appropriate restriction enzymes (Takara Bio, Japan), it was ligated using T4 DNA ligase (USB Corp., Affymetrix, USA) and finally, it was cloned into the corresponding *Hind*III and *Xba*I sites of pK18*mob*sacB plasmid to yield pK18*mob*sacB-2637. The resultant plasmid was confirmed by DNA sequencing and used to deliver the mutation to the host chromosome of *B. bacteriovorus* HD100 via homologous recombination of the suicide plasmid. Biparental mating was performed during 30 h with *E. coli* S17-λpir as donor strain as described above. The strains resulted in the first recombination event were screened for the insertion of the knockout construct via PCR. Merodiploids clones were plated twice onto double-layer agar plates with a kanamycin resistant *P. putida* strain as prey. Thereafter, merodiploids were transferred onto double-layer agar plates containing 5% sucrose in the bottom layer plus an additional 5% sucrose and *P. putida* cells within the top layer. The resulting turbid plaques were isolated and the second cross-over event was confirmed by PCR, giving the resultant mutant strain *B. bacteriovorus* ΔBd2637 (called Bd2637 in this work).

2.4 Assays for predatory capabilities of *B. bacteriovorus* HD100 and its mutant strains

Predator and prey strain viabilities were calculated from a co-culture containing both strains. The detailed protocol is described in *Common Materials and Methods* section.

For predation ability experiments in cells containing PHA, *P. putida* and *E. coli* strains grown under PHA production conditions, were centrifuged, suspended in Hepes buffer (at different cell densities) and infected with HD100 strains (10^7-10^9 pfu ml^{-1}) for 24-48 h. For the

predation experiments upon *C. necator* H16 and *R. rubrum* ATCC 11170, prey cultures were prepared in Hepes buffer (OD_{600} 1) and inoculated with 10^7 pfu ml^{-1} of *B. bacteriovorus* HD100 for 24 h. To normalize the predation experiments in PHB accumulating and non-accumulating cells, *E. coli* ML35 (pACYC184) and *E. coli* ML35 (pAV1) prey suspensions were adjusted to equal residual biomass (0.3 g l^{-1}) (this is cell biomass after subtracting the PHA weight) in Hepes buffer and infected with 10^8 pfu ml^{-1} of *B. bacteriovorus* for 24 h.

2.5 GC-MS analysis for PHA content determinations

For total PHA quantification, cultures were harvested, lyophilized and analyzed by gas chromatography-mass spectrometry (GC-MS) as previously reported (de Eugenio et al., 2007; Martínez et al., 2013). Briefly, methanolysis was carried out by suspending 5–10 mg of lyophilized cells in 0.5 ml of chloroform and 2 ml of methanol containing 15% sulfuric acid and 0.5 mg ml^{-1} of 3-methylbenzoic acid (internal standard), followed by an incubation at 100 °C for 4 or 5 h, for PHB or PHA respectively. After cooling, 1 ml of demineralized water and 1 ml of chloroform were added. The organic phase containing the methyl esters was analyzed by GC-MS. A standard curve from 0.5 to 2 mg of PHB or PHA (Cat. Number of PHB: 36,350-2, Sigma-Aldrich, USA; PHA was obtained from Biopolis S.L., Spain) was used to interpolate sample data.

2.6 HPLC-MS analysis for identification of the PHA hydrolysis products

To identify the degradation products, the supernatant of the co-cultures were analyzed by high-performance liquid chromatography-mass spectrometry (HPLC-MS) as previously reported (Martínez et al., 2013). Briefly, lyophilized supernatants of the infection mixtures were resuspended on methanol at 3 mg ml^{-1} and 25 µl were injected in the chromatographic system. Separation of the hydrolysis products was carried out on a Finnigan Surveyor (Thermo Electron, USA) pump coupled with a Finnigan LXQ TM (Thermo Electron, USA) ion trap mass spectrometer.

2.7 PHA isolation and molecular characterization

10 ml of the co-cultures of *B. bacteriovorus* preying on *P. putida* KT2440 accumulating PHA were centrifuged and the resulting sediments (wet biomass) were directly suspended in 5 ml of chloroform. Solvent phase was collected and precipitated by adding 10 volumes of methanol. Finally, the polymer was dried under vacuum for 10 min and analyzed by GC-MS for determination of PHA content and purity. As a control, 10 ml of *P. putida* KT2440 accumulating PHA cultures without predator were harvested, suspended in salt solution, and disrupted by passing through a French pressure cell twice (1,000 lb in^{-2}).

The weight-average molecular weight (Mw), number-average molecular weight (Mn) and polydispersity index (PDI) of polyesters were determined by Size Exclusion Chromatography (SEC) in a Perkin-Elmer apparatus equipped with an isocratic pump serial 200 connected to a differential refractometric detector (serial 200a). Two Styragel Column, HR 5E, 5 µm, 7.8 mm X 300 mm (Waters) were conditioned at 70 °C and used to elute the samples (2 mg ml^{-1} concentration) at 0.7 ml min^{-1}. HPLC grade N, N-dimethylformamide (DMF) supplemented with 0.1% v/v LiBr was used as mobile phase. The calibration curve was realized with polystyrene standards from 580 to $1.6 \cdot 10^6$ g mol^{-1} samples in the range of $2.9 \cdot 10^3$ to $480 \cdot 10^3$ g mol^{-1} obtained from Polymer Laboratories with sample injection volumes of 100 µl.

3. RESULTS

3.1 Construction of depolymerase mutant strains of *B. bacteriovorus* to avoid the PHA hydrolysis during predation

It has been previously demonstrated that *B. bacteriovorus* HD100 preying upon PHA-accumulating *P. putida* cultures caused the release of most PHA granules and hydrolysis products (HAs, meaning a mixture of monomers and oligomers) into the culture medium (Martínez et al., 2013). To block the degradation of prey-produced PHA by the predator cells, a *phaZBd* depolymerase mutant strain - Bd3709 - was produced by disrupting *phaZBd* via the insertion of a kanamycin resistance gene (see Materials and Methods for details). After 24 h of predation, Bd3709 mutant lysed the prey cells efficiently, resulting in a 2-log increase in the predator cell number (Figure 22A and B). The Bd3709/*P. putida* KT2440 co-culture showed a PHA content similar to the control culture (*P. putida* without *B. bacteriovorus*) after 24 h of incubation [0.85 g l^{-1} (80% of the initial PHA produced by the *P. putida* KT2440 cells)]. However, in wild type HD100/*P. putida* KT2440 co-cultures only 60% of the PHA content was recovered (Figure 22C).

Remarkably, PHA granules were visible in the extracellular medium together with the predator, while no entire prey cells were appreciable. *B. bacteriovorus* HD100 released larger amounts of HAs into the extracellular medium than the Bd3709 strain, showing that *phaZBd* disruption avoided PHA degradation during predation. Indeed, with the Bd3709 mutant, nearly all the PHA granules accumulated by the prey were recovered after the predatory event. It is worth mentioning that *B. bacteriovorus* HD100 did not produce PHA, at least in the conditions assayed (see Methods for details).

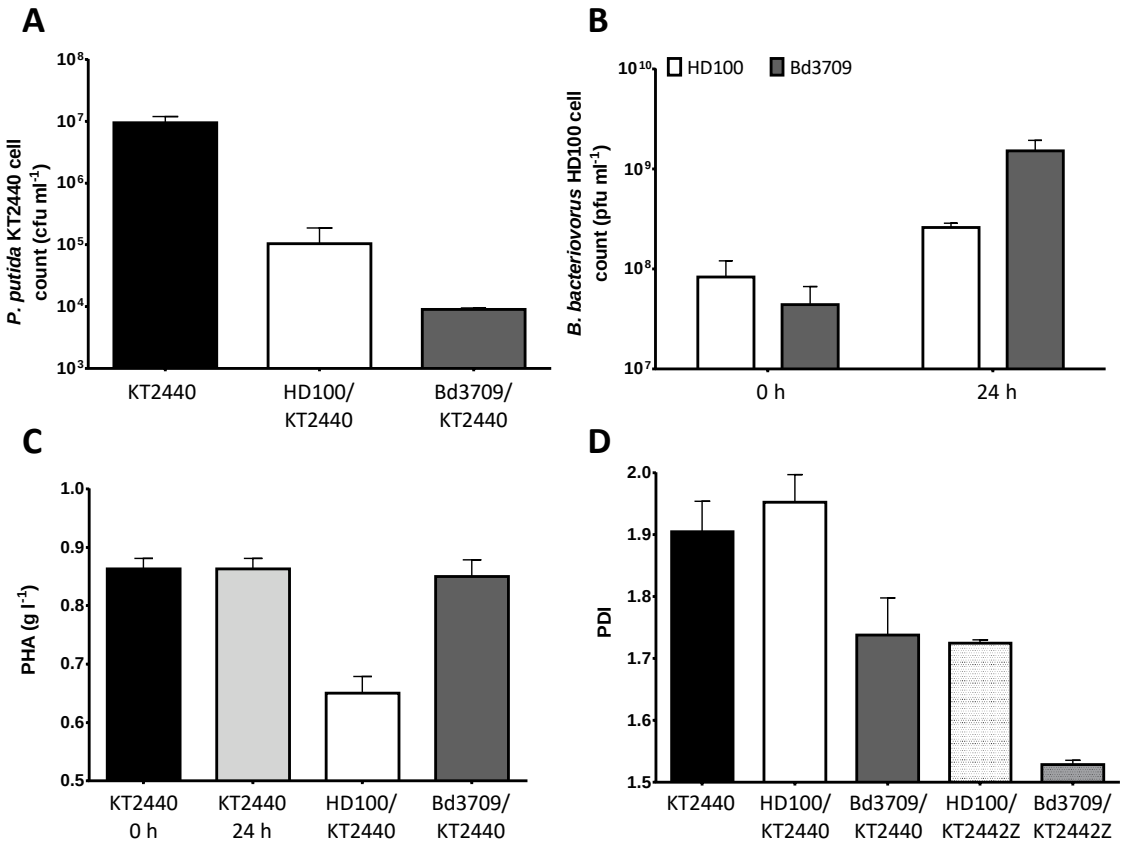

Figure 22. Monitoring predation by *B. bacteriovorus* HD100 and Bd3709 mutant strain. A) Prey cell viability assay of the co-culture at the onset of predation (black bars) and within 24 h using wild type HD100 or Bd3709 variant (white bars and grey bars, respectively). **B)** Number of viable cells of *B. bacteriovorus* HD100 and Bd3709 at time zero and after 24 h of predation upon *P. putida* KT2440 accumulating PHA. **C)** Total PHA content in the co-culture of *B. bacteriovorus* HD100 or Bd3709/*P. putida* KT2440 (white and dark grey bars, respectively) compared to the control culture (KT2440 without the predator) at the onset of predation (time zero) (black bars) and within 24 h (light grey bars). **D)** Polydispersity index (PDI) values of the PHA obtained from the co-cultures of *B. bacteriovorus* HD100 and Bd3709 strains preying on PHA-accumulating *P. putida* KT2440 or KT2442Z. Error bars mean the variation of three technical replicates.

3.2 Molecular characterization of the PHA recovered from the predation cultures

The PHA recovered from the Bd3709/*P. putida* KT2440 co-culture was compared to that recovered from the wild type HD100/*P. putida* KT2440 co-culture and that from the *P. putida* KT2440 culture (as a control experiment, using a French press). The extracted PHA from Bd3709 co-culture showed a profile with a higher weight-average molecular weight (Mw) and number-average molecular weight (Mn), and a lower polydispersity index (PDI) than the PHA recovered from the wild type HD100 co-culture (Figure 22D and Table 10). This indicates that in the latter

co-culture the biopolymer was partially degraded, increasing the heterogeneity of the polymer chains in terms of the molecular mass.

Table 10. Molecular characterization of mcl-PHA and PHB polymers. Mn: number-average molecular weight, Mw: weight-average molecular weight, PDI: polydispersity index.

Strain	Mn (kDa)	Mw (kDa)	PDI
KT2440 control	53.37 ± 7.54	100.37 ± 6.81	1.89 ± 0.13
HD100/KT2440	50.71 ± 4.48	96.41 ± 16.30	1.89 ± 0.16
Bd3709/KT2440	76.56 ± 11.30	124.80 ± 25.48	1.62 ± 0.15
HD100/KT2442Z	82.57 ± 10.56	42.78 ± 10.32	1.73 ± 0.14
Bd3709/KT2442Z	57.98 ± 6.59	88.57 ± 9.56	1.53 ± 0.13
ML35 (pAV1) control	2000 ± 300	3000 ± 200	1.8 ± 0.3
HD100/ML35 (pAV1)	600 ± 40	1060 ± 5	1.8 ± 0.1
Bd2637/ML35 (pAV1)	1000 ± 100	2000 ± 300	1.7 ± 0.1

It is well documented that *P. putida* KT2440 possesses an intracellular mcl-PHA depolymerase (PhaZKT) that plays a key role in PHA turnover (de Eugenio et al., 2010, 2007). PhaZKT degrades PHA and releases 3-hydroxycarboxylic acid monomers (HA), which can either be oxidized via the β-oxidation pathway to generate energy or be incorporated into nascent PHA polymer chains by PHA synthase, depending on the metabolic state of the cell. To evaluate the role of PhaZKT depolymerase during the predatory event, the PDI of the polymer recovered from the co-cultures of *B. bacteriovorus* HD100 and Bd3709 preying on *P. putida* KT2442Z (which lacks the PhaZKT depolymerase) was also quantified and characterized (Figure 17D). As expected, the PHA extracted from Bd3709/*P. putida* KT2442Z co-culture showed lower PDI than the PHA recovered from the wild type HD100/*P. putida* KT2442Z co-culture, highlighting the extracellular-like depolymerase of *B. bacteriovorus* as responsible for the partial degradation of mcl-PHA during predation.

3.3 Hydrolytic product profile of the PHA recovered using *B. bacteriovorus* as a lytic tool

In concordance with previous results, the profile of HAs products should differ depending on the predatory strain used for the co-culture. To check this hypothesis, prey cells of *P. putida* KT2440 cells were prepared in Hepes buffer at 5.7 g l^{-1} of biomass (corresponding to 2.4 ± 0.2·10^7 cfu ml^{-1} with a PHA content of 2.4 g l^{-1}), and subsequently, were inoculated with 5.3 ± 0.3·10^7 *B. bacteriovorus* HD100 or 3.7 ± 0.1·10^7 pfu ml^{-1} Bd3709. After 30 h of predation, the extracellular medium was analyzed by HPLC-MS. The hydrolytic product profile for

Bd3709/*P. putida* KT2440 co-culture - mainly monomers and dimers - was similar to *P. putida* KT2440 culture growing alone (Figure 23). Nevertheless, these data differed significantly to those obtained in the wild type HD100/*P. putida* KT2440 co-cultures, which showed larger proportions of dimers and trimers, similar to that obtained in *in vitro* experiments using pure PhaZBd depolymerase (Martínez et al., 2012). These differences could be attributed to the different activities of the depolymerases produced by *P. putida* KT2440 (PhaZKT, intracellular) and the predator (PhaZBd, extracellular-like) (see below). Total PHA hydrolysis products released to the extracellular medium throughout predation were quantified by HPLC-MS (Figure 23). Values of 3.3 ± 0.33 and 0.30 ± 0.05 g l^{-1} were recorded for *B. bacteriovorus* HD100/*P. putida* KT2440 and Bd3709/*P. putida* KT2440 co-cultures, respectively. To further confirm that PhaZBd degrades PHA during predation, the PHA hydrolytic product profile was also examined for the co-cultures of *B. bacteriovorus* HD100 or Bd3709 preying on *P. putida* KT2442Z (Figure 22). As expected, no HAs were found in the Bd3709/*P. putida* KT2442Z co-culture, while the hydrolytic product profile of the wild type HD100/*P. putida* KT42Z co-culture showed (mainly) dimers and trimers (Figure 23).

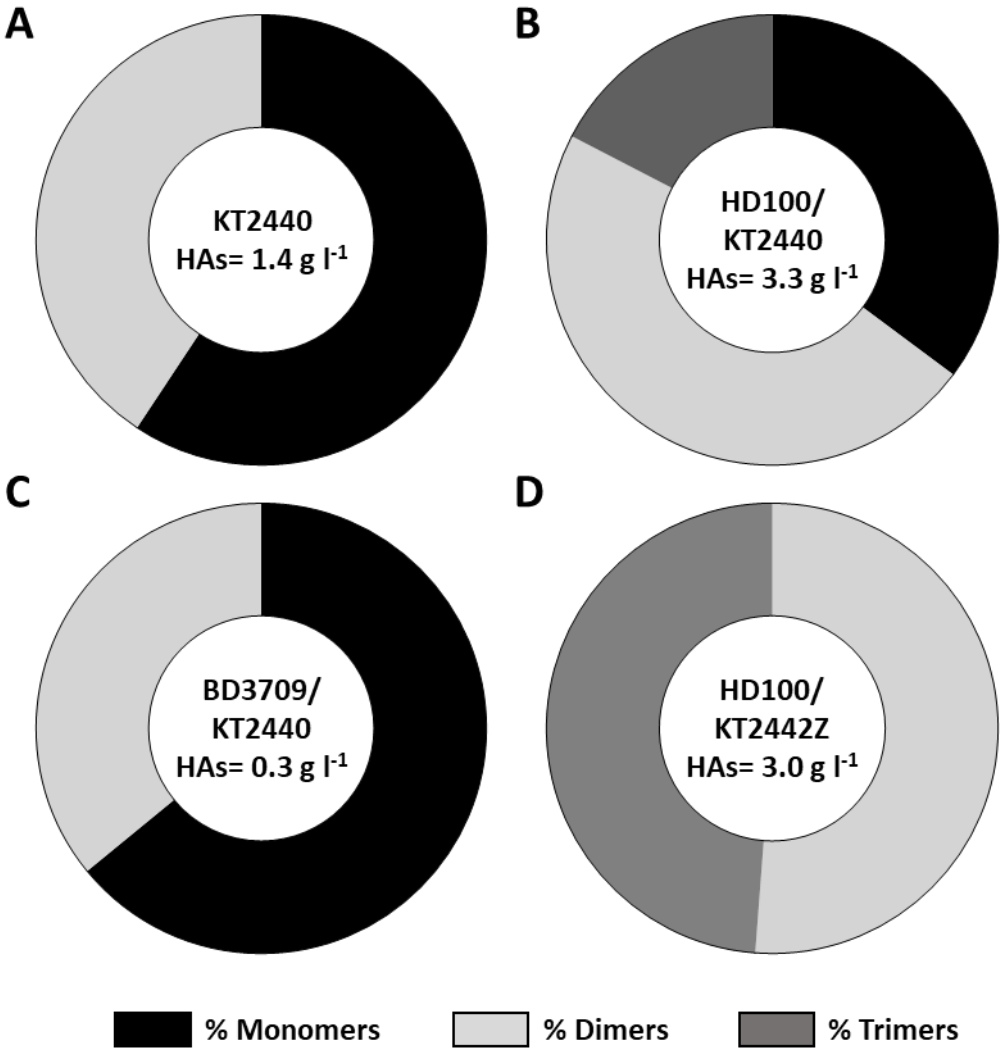

Figure 23. Mcl-PHA hydrolytic product profile identified in the co-culture supernatants of *B. bacteriovorus* strains preying on *P. putida* KT2440 and KT42Z accumulating mcl-PHA. HPLC-MS analysis after 30 h of predation by *Bdellovibrio* strains. Monomers (black fractions), dimers (light grey fractions) and trimers (dark grey fractions). **A)** Hydrolytic products in the supernatant of *P. putida* KT2440. **B)** Hydrolytic products in the supernatant of the coculture *B. bacteriovorus* HD100 and *P. putida* KT2440. **C)** Hydrolytic products in the supernatant of the coculture Bd3709 and *P. putida* KT2440. **D)** Hydrolytic products in the supernatant of the coculture *B. bacteriovorus* HD100 and *P. putida* KT2442Z. The supernatant of Bd3709/KT2442Z was also analyzed but no hydrolytic products were detected. The number inside the circles represents the total PHA hydrolysis products quantified in the culture supernatants.

3.4 Predation of *B. bacteriovorus* in high cell densities of *P. putida* KT2440 accumulating PHA

A requisite for the industrial application of the predator as a living cell-lytic system would be the capability to attack high cell density prey cultures. Therefore, the potential of *B.*

bacteriovorus HD100 to prey on high cell density cultures of *P. putida* KT2440 accumulating PHA was evaluated. Hence, prey cultures were prepared in Hepes buffer with 30.5 g l^{-1} of cell biomass (biomass production by PHA-producing pseudomonads under optimal conditions ranges between 15–55 g l^{-1}) (Elbahloul and Steinbüchel, 2009), corresponding to 8.3 ± 0.3 · 10^9 cfu ml^{-1}, with a PHA content of 15.1 g l^{-1} (Figure 24A and C). Subsequently, these cultures were inoculated with 6.3 ± 0.3·10^8 pfu ml^{-1} of *B. bacteriovorus* HD100.

After 40 h of predation, a 1-log reduction in prey cells was observed while an increase of 1-log in the viable cell number of *B. bacteriovorus* was measured (Figure 24E). This result confirms the predator's ability to prey on PHA-accumulating *P. putida* KT2440 high-density cultures. Co-cultures examination by phase-contrast microscopy clearly revealed the release of PHA granules into the extracellular medium (Figure 24B and D). However, PHA recovery optimization is required at this cell density scale since that only 65% of the PHA accumulated by the prey bacteria was recovered under our lab scale conditions (Figure 24F). Notably, the polymer was directly extractable from the wet biomass of the co-cultures. The use of the mutant strain Bd3709 turns out the same extraction values compared with the low-density co-cultures (data not shown).

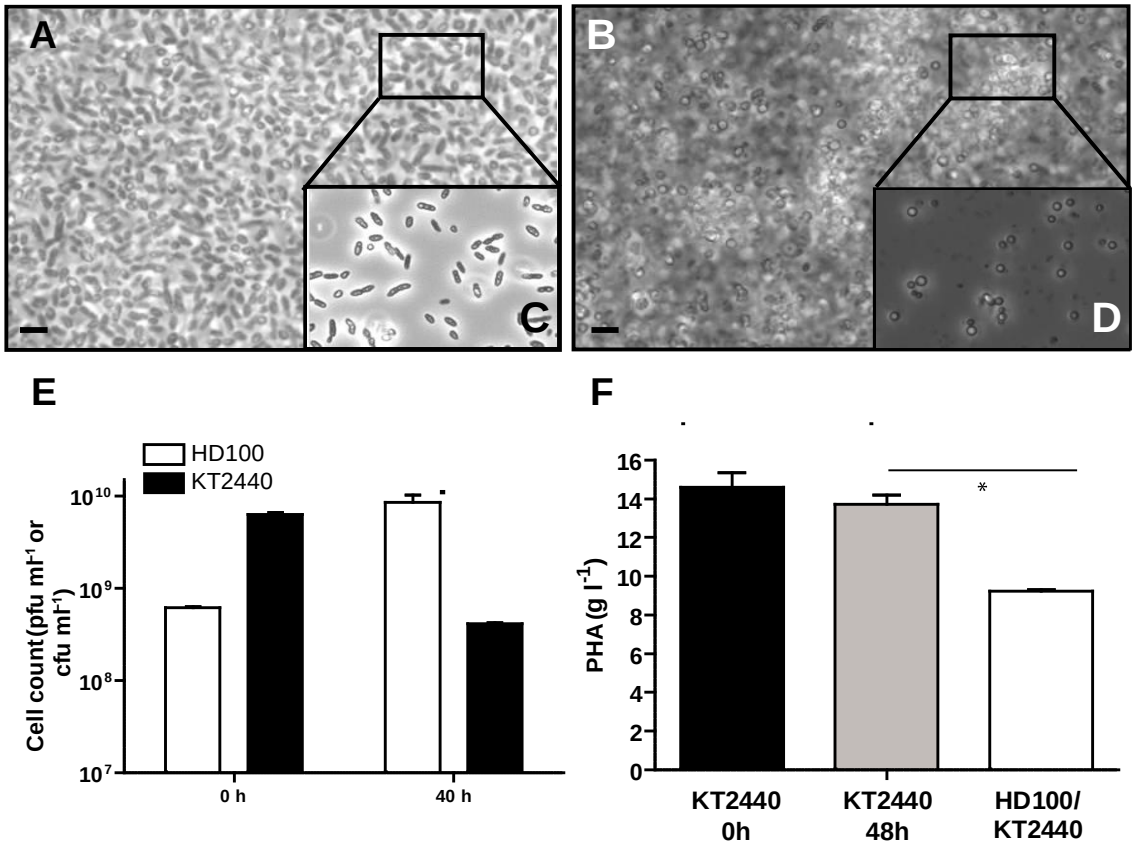

Figure 24. *B. bacteriovorus* HD100 preying on high cell densities of *P. putida* KT2440 accumulating mcl-PHA. A) Phase-contrast microscopy of a co-culture of *B. bacteriovorus* HD100 preying on *P. putida* KT2440 at the onset of predation (time zero) and **B)** after 40 h of incubation. **(C, D)** 1:100 dilution of the co-cultures from panels (A, B), respectively. Mcl-PHA granules can be observed in the extracellular medium after 40 h of predation. **E)** Cell viability assay of the co-culture of *B. bacteriovorus* HD100 and *P. putida* KT2440 (white bars and black bars, respectively) at the onset of predation (time zero) and within 40 h. **F)** Total PHA content in the co-culture of *B. bacteriovorus* HD100/*P. putida* KT2440 compared to the control culture (KT2440 without the predator, without extraction) at the onset of predation (time zero) (black bars) and within 48 h (grey bars). Asterisks (*) indicate significant differences (*$P < 0.05$). White lines in the bottom of the micrographies represent a scale bar of 3 μm.

3.5 Predation of *B. bacteriovorus* upon other PHA-producing bacteria

Since *B. bacteriovorus* attacks a wide variety of gram-negative bacteria (Jurkevitch and Davidov, 2006), the possibility of using this lytic tool in other production/extraction systems was evaluated. As a proof-of-concept, the recovery of other PHAs such as PHB was studied. *E. coli* ML35 (pAV1) producing the three main proteins for PHB synthesis in *C. necator* H16, PhaC1 (PHA synthase), PhaA (acetoacetyl-CoA reductase) and PhaB1 (ketothiolase), was used as prey bacterium. These cells were prepared in Hepes buffer at pH 7.8 at 5.25 g l^{-1} (corresponding to $2.2 \cdot 10^9$ cfu ml^{-1} and 1.3 g l^{-1} PHB) and inoculated with $1.45 \cdot 10^7$ pfu ml^{-1} of *B. bacteriovorus* HD100 (Figure 25A and B). After 24 h of predation, PHA content decreased by more than 50% of that previously accumulated by the prey, suggesting that the predator hydrolyzed the PHB. In this case, the PHB hydrolysis observed cannot be ascribed to any hydrolytic activity of the prey, since *E. coli* strains are unable to degrade PHB due to the lack of necessary depolymerases.

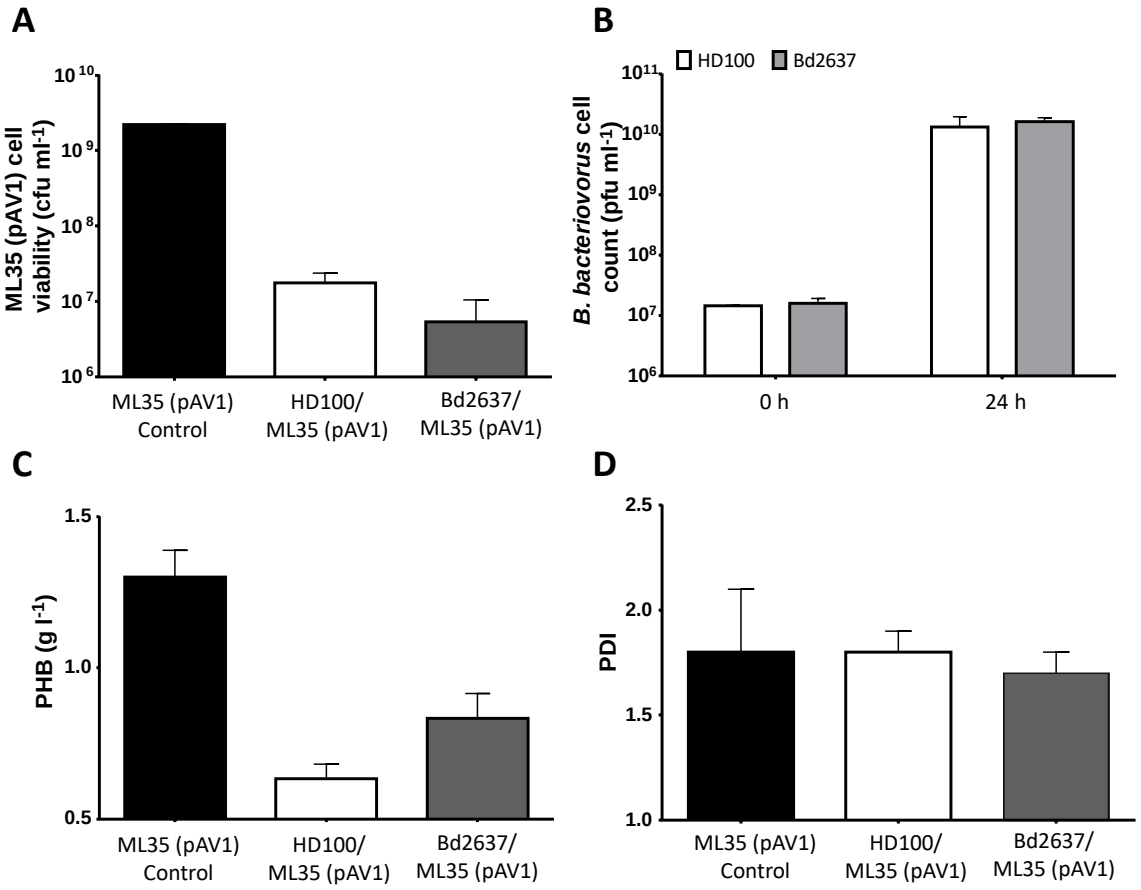

Figure 25. Monitorization of the predation by *B. bacteriovorus* HD100 and Bd2637 mutant strain. A) Prey cell viability assay of the co-culture at the onset of the predation (black bars) and within 24 h using wild type HD100 or Bd2637 variant (white bars and grey bars, respectively). **B)** Number of viable cells of *B. bacteriovorus* HD100 (white bars) and Bd2637 (grey bars) at time zero and after 24 h of predation upon *E. coli* ML35 (pAV1) accumulating PHB. **C)** Total PHB content in the co-culture of *B. bacteriovorus* HD100 or Bd2637/ML35 (pAV1) (white and dark grey bars, respectively) compared to the control culture (ML35 (pAV1) without the predator) (black bars). **D)** Polydispersity index (PDI) values of the PHB obtained from the co-cultures of *B. bacteriovorus* HD100 and Bd2637 strains preying on PHB-accumulating *E. coli* ML35 (pAV1). Error bars mean the variation of three technical replicates.

To investigate PHB degradation effect on the fitness of *B. bacteriovorus*, the wild-type strain *E. coli* ML35 (pACYC184) and the PHB-producing strain *E. coli* ML35 (pAV1), were cultured under PHB production growth conditions. Prey cultures were adjusted to equal residual (i.e., PHB-free) biomass (0.3 ± 0.05 g l^{-1}), and then inoculated with $1.9 \cdot 10^8$ pfu ml^{-1} of *B. bacteriovorus* HD100. After 24 h of predation, the predator population was 10-fold higher when preying on PHB-accumulating *E. coli* cells than on the wild-type *E. coli* cells unable to produce PHB (Figure 26A). These results suggest that predation of PHB-accumulating preys could be a benefit for *B.*

bacteriovorus in terms of biomass yield as an additional carbon source. This differs to that reported with *P. putida*; when preying on this bacterium, the number of progeny is independent of the presence of mcl-PHA (Martínez et al., 2013). The predatory ability of *B. bacteriovorus* upon ML35 (pACYC184) and *E. coli* ML35 (pAV1) was also evaluated showing efficient lysis in both strains (Figure 26B).

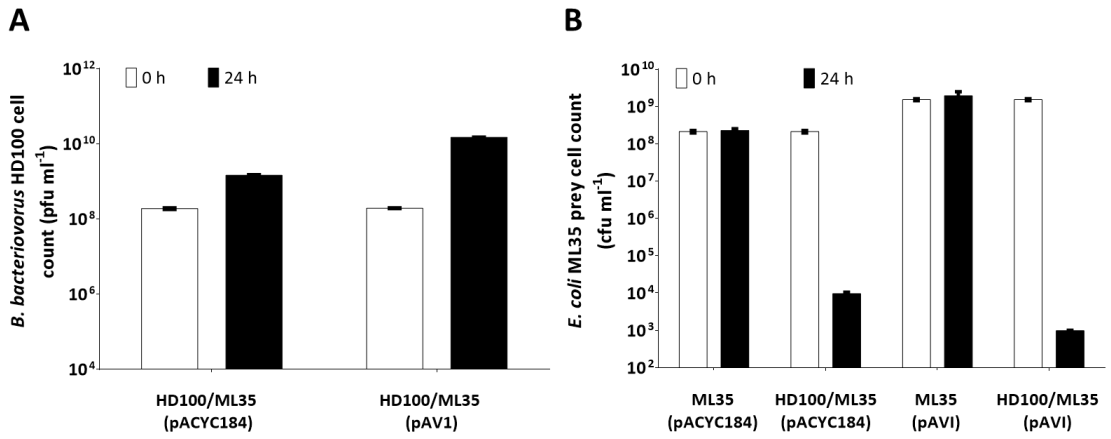

Figure 26. Influence of prey PHB content on the fitness of *B. bacteriovorus* HD100. A) Number of viable cells of *B. bacteriovorus* HD100 at the start of the experiment (time zero) and after 24 h preying upon *E. coli* ML35 cells accumulating PHB [ML35 (pAV1)] or devoid of it [ML35 (pACYC184)], previously adjusted to 0.3 g l^{-1} of residual biomass. **B)** Number of viable cells of *E. coli* ML35 accumulating PHB [ML35 (pAV1)] or devoid of it [ML35 (pACYC184)] at the start of the experiment (time zero) and after 24 h of predation with *B. bacteriovorus* HD100.

A potential extracellular scl-PHA depolymerase coding sequence was found in the genome of *B. bacteriovorus* (ORF Bd2637), as part of its hydrolytic arsenal (Martínez et al., 2013; Rendulic et al., 2004). This putative scl-PHA depolymerase might be responsible for the degradation of the prey's PHB during the predatory cycle. Therefore, the predator was engineered to avoid PHB degradation via an in-frame deletion of ORF Bd2637. Accordingly, the suicide vector pK18*mob*sacB-2637 was inserted into *B. bacteriovorus* HD100 genome via conjugation and homologous recombination, with subsequent sucrose suicide screening for gene replacement. After 24 h of predation upon *E. coli* ML35 (pAV1), Bd2637 knockout caused the release of larger amounts of PHB than did the wild type HD100 (64% and 48%, respectively) (Figure 25C). This shows that ORF Bd2637 codes for a genuine scl-PHA depolymerase confirming that Bd2637 mutant can be used as an improved lytic agent in PHB production process.

The molecular characterization of the PHB recovered from the co-cultures of the wild-type and mutant preying upon *E. coli* ML35 (pAV1) showed extremely high Mw (Kahar et al.,

2005), ranging from $3 \cdot 10^6$ to $1 \cdot 10^6$, with relatively low PDI of around 1.8–1.7 (Figure 25D and Table 10). The PDI remained nearly unchanged during the predation event, independently of the predatory strain applied in the process. These results indicated that the impact of the scl-PHA depolymerase functionality in the molecular weight and polymer PDI is not significant in our assay conditions, differing to the results obtained for *P. putida* (see above).

Predation in high-density PHB-producing *E. coli* ML35 (pAV1) cultures was also monitored. At the beginning of the experiment, host viability, cell biomass, and PHB content were $2.6 \cdot 10^9$ cfu ml^{-1}, 55 g l^{-1} and 19 g l^{-1}, respectively. After 48 h of predation, both the wild-type and Bd2637 mutant lysed prey cells efficiently, achieving 4-log reductions. Thus, the lytic system using *B. bacteriovorus* HD100 could be efficiently expanded to another system at high cell densities.

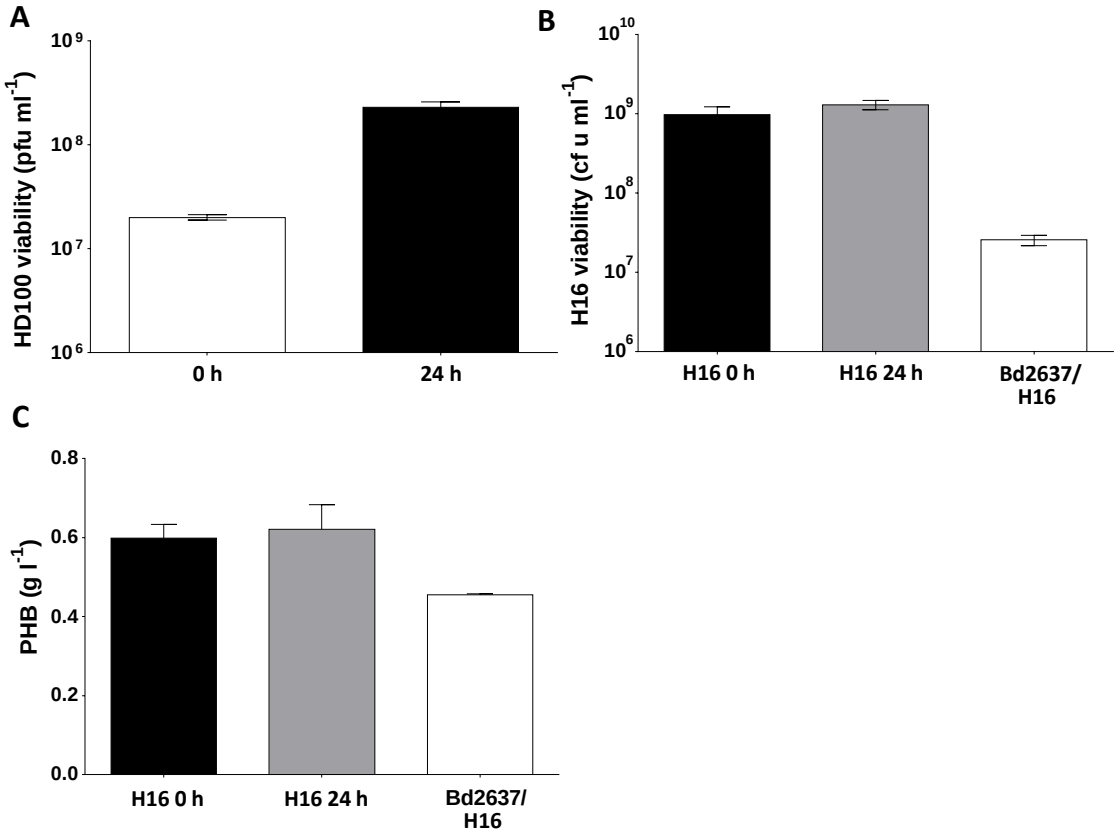

Figure 27. *B. bacteriovorus* Bd2637 preying on *C. necator* H16 accumulating PHB. A) Number of viable cells of *B. bacteriovorus* Bd2637 at time zero and after 24 h of predation upon *C. necator* H16 accumulating PHB. **B)** Number of viable cells of *C. necator* H16 accumulating PHB at time zero and after 24 h of predation without and with *B. bacteriovorus* Bd2637. **C)** Total PHB content in the co-cultures. In all graphs, error bars indicate the standard deviation of the mean (n = 3).

Finally, other PHB producers – *C. necator* H16 and the photosynthetic bacterium *R. rubrum* ATCC 11170 – were grown under PHB production conditions and infected with *B. bacteriovorus* Bd2637. Firstly, the ability of the predator to prey on PHB accumulating *C. necator* H16 was analyzed. After 24 h of infection, the progeny of *B. bacteriovorus* increase 1-log after predation (Figure 27A). At the same time, 1-log prey reduction was observed, which confirmed the susceptibility of PHB accumulating *C. necator* cells to predation (Figure 27B). Figure 27C shows the PHB content after 24 h of predation using the predator mutant strain Bd2637.

The susceptibility to prey on *R. rubrum* ATCC 11170 was also evaluated (Figure 28A and B). Figure 28C demonstrated the lytic ability of Bd2637 to prey upon *R. rubrum* cells. While 2-log reduction of the prey cells, the predator progeny increase 1.5-log (Figure 28D). These results exhibit the versatility of this lytic system showing the decrease of the prey viable cell number and the increase of the predator viability.

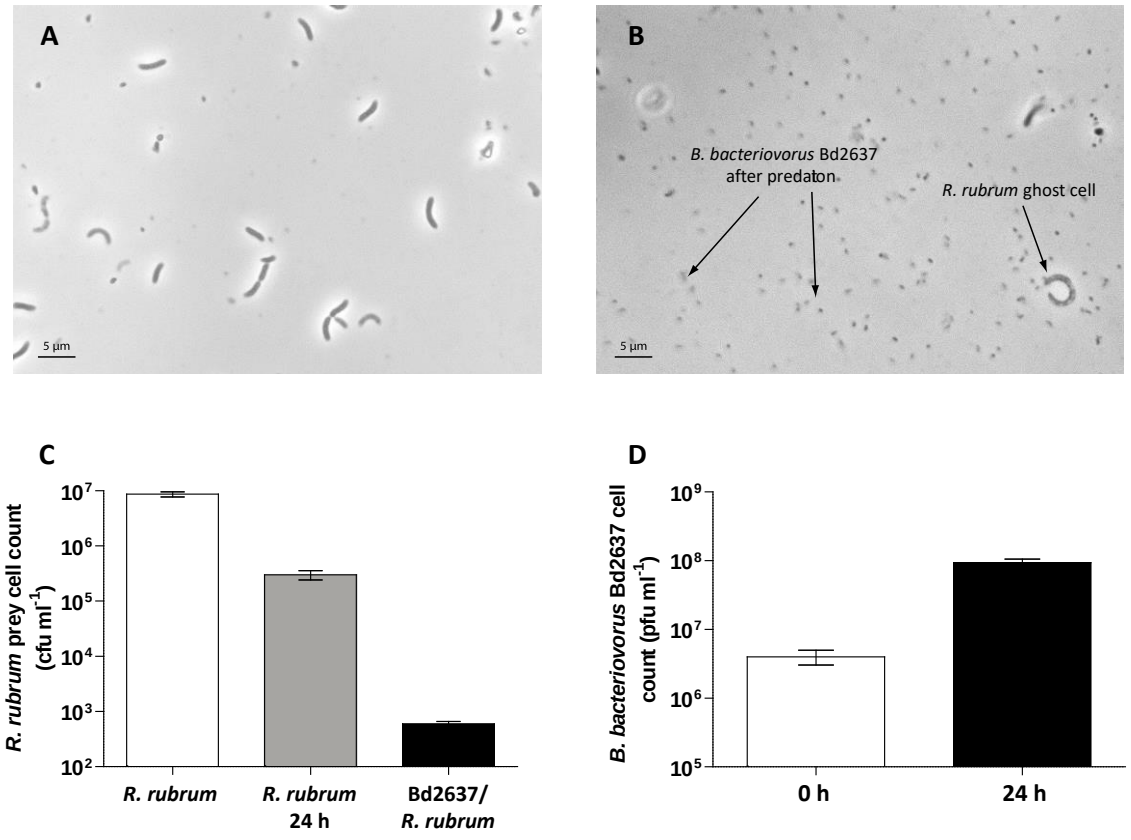

Figure 28. *B. bacteriovorus* Bd2637 preying on *R. rubrum*. (**A**) Phase-contrast microscopy of the co-culture at the onset of predation (time zero). **B**) Phase-contrast microscopy of the co-culture after 24 h of incubation with *B. bacteriovorus* Bd2637. **C)** Number of viable cells of *R. rubrum* at time zero and after 24 h of predation without and with the predator. **D)** Number of viable cells of *B. bacteriovorus* Bd2637 at time zero and after 24 h of predation. In all graphs, error bars indicate the standard deviation of the mean (n = 3).

These results demonstrated the predator's capability to prey upon other natural PHB producing bacteria, although scaling up would require optimization of PHB production and recovery conditions for each particular process.

X. *B. BACTERIOVORUS*, BIOCONTROL AGENT AGAINST PATHOGENIC BACTERIA

B. BACTERIOVORUS, BIOCONTROL AGENT AGAINST PATHOGENIC BACTERIA

1. INTRODUCTION

Recent advances highlight the potential for predators to restore ecosystems and confer resilience against globally threatening processes, including climate change and biological invasions either environmental or clinical (Roca et al., 2015). Although the impact of BALOs in the microbial network has not been elucidated (Martin, 2002), some evidence point at the control of the bacteria size population (Varon and M. Shilo, 1968). Therefore, their intrinsic ability to lyse prey cells suggests an important role as antibacterial and bioprotection agents.

The use of the predatory ability of *B. bacteriovorus* against selected pathogenic microorganisms has been widely reported from plant and fish farming to live animals (Atterbury et al., 2011; Lu and Cai, 2010; Scherff, 2AD). With the increase of antibiotic resistance in gram-negative pathogens, it becomes crucial to begin assessed experimentally the potential of *Bdellovibrio* spp. in therapy by performing *in vitro* and *in vivo* experiments using the predators to treat infected organisms (Atterbury et al., 2011; Russo et al., 2015). Several attempts are being carried out to overcome the antibiotic resistance such as new generation molecules in chemotherapy and phage therapy (Lin et al., 2017). However, most of these methods are species-specific and they could be dependent on the adaptation of the pathogens to the substance or doses, which limit the range of applicability of these methodologies. In contrast to these systems, *B. bacteriovorus* exhibits the advantage of being able to prey upon a wide repertoire of gram-negative bacteria (Annex 1), which opens new avenues for the application on different biological scenarios. Moreover, the toxicity of *Bdellovibrio* spp. on the eukaryotic cells has also been tested and, as far as has been reported, no immunologic reactions are induced (Baker et al., 2017; Monnappa et al., 2014; Shanks et al., 2013; Shatzkes et al., 2015).

The predatory capability of *B. bacteriovorus* has been traditionally evaluated by double-layer method (Herencias et al., 2017; Lambert et al., 2009), which is time-consuming and laborious to perform (*Common Materials and Methods*). During this work, several bacterial

strains have been evaluated, belonging to different pathogenic groups. With this aim, a multiwell-based system which has been developed to speed up the assessment was used. This methodology is based on the monitorization of the optical density at 630 nm of the co-cultures during 24 or 48 h.

Since it is still necessary to give insights into the predatory spectrum of *Bdellovibirio* spp., the present study aimed at evaluating the predatory activity of *B. bacteriovorus* HD100 on bacterial strains that commonly caused clinical diseases or environmental contaminations. Among them, some gram-positive bacteria related to pulmonary diseases, such as *S. aureus*, *Streptococcus pyogenes,* and *Streptococcus pneumoniae* were tested as prey. Likewise, the susceptibility to prey on some members of the ESKAPE group were evaluated (*P. aeruginosa* PAO1, *Klebsiella pneumoniae,* and *Acinetobacter baumannii*). In addition, 36 *P. aeruginosa* strains isolated from cystic fibrosis (CF) patients were also assessed, representing the first evaluation of a collection of clinical isolates as preys reported so far. Finally, to test the potential as an environmental biocontrol agent, some fish pathogens were also evaluated due to the economic impact of the losses that the infectious diseases caused in fish farms. Details of these strains and their relevance are described in the section of *General Introduction*.

2. MATERIALS AND METHODS

2.1 Bacterial strains, culture medium and growth conditions

Gram-positive bacteria *S. aureus* NCTC 8532, *S. pneumoniae* R6 (Hoskins et al., 2001) and *S. pyogenes* ATCC 12344 strains were grown in THY medium (ATCC medium 2716) at 37 °C with shaking at 250 rpm (hereafter "shaking" means 250 rpm). For counting viable cell number, blood agar was used routinely (Trypticasein soy agar (TSA; Pronadisa, Spain)) with 5% defibrinated sheep blood (Oxoid, United Kindom). *Salmonella thiphimurium* LT2 was grown in TSB medium (30 g l^{-1} Tripticasein soy broth autoclave and supplemented with 0.3% yeast extract and 0.4% glucose) at 37 °C with shaking. *K. pneumoniae*, *A. baumannii* and *P. aeruginosa* strains were grown in lysogenic broth (LB) medium (Green and Sambrook, 2012) at 37 °C with shaking. The strains *K. pneumoniae* 5214R, *K. pneumoniae* 43816R, *A. baumannii* 17978, *S. typhimurium* LT2, *P. aeruginosa* PA01 were obtained from Dr. Junkal Garmendia laboratory.

Aeromonas hydrophyla (CECT 839T) was grown in CECT 2 medium (1 g of Beef extract l^{-1}, 2 g yeast extract l^{-1}, 5 g peptone l^{-1}, 5 g NaCl l^{-1}, adjusted to pH 7.2 with NaOH) at 30 °C with shaking. *Aeromonas salmonicida* (CECT 894T) was grown in medium CECT 195 (17 g tryptone l^{-1}, 3 g soy peptone l^{-1}, 5 g NaCl l^{-1}, 2.5 g KH_2PO_4 l^{-1}, 2.5 g glucose l^{-1}) at 26 °C with shaking. *Edwarsiella ictaluri* (CECT 885T) was grown in CECT 5 medium (12.5 calf brain infusion solids l^{-1}, 5 g beef heart infusion solids l^{-1}, 10 g protease peptone l^{-1}, 2 g glucose l^{-1}, 5 g NaCl l^{-1}, 2.5 g NaH_2PO_4 l^{-1}) at 26 °C for 48h with shaking. *Edwarsiella tarda* (CECT 849T) was grown in CECT 1 medium (5 g beef extract l^{-1}, 10 g peptone l^{-1}, 5 g NaCl l^{-1}, adjusted to pH 7.2 with NaOH) at 37 °C with shaking. *Flavobacterium columnare* (CECT 7586) was grown in CECT 284 medium (5 g tryptone l^{-1}, 2 g yeast extract l^{-1}, 1.14 mg $FeSO_4 \cdot 7H_2O$ l^{-1}, 6.7 mg $CaCl_2 \cdot 2H_2O$ l^{-1}, 0.14 g KH_2PO_4 l^{-1}, 0.29 g $MgSO_4$ l^{-1}, adjusted to pH 7.2-7.4 with NaOH) at 26 °C with shaking during 24-36 h with shaking. *Yersinia ruckeri* (CECT 4319T) was grown in CECT 1 medium at 30 °C with shaking. Growth was monitored with a Shimadzu UV-260 spectrophotometer at 600 nm (OD_{600}). Solid media were supplemented with 1.5% (w/v) agar.

B. bacteriovorus HD100 was routinely grown on two-membered cultures as described in *General Materials and Methods* (Herencias et al., 2017).

2.2 Development of a multiwell system for monitoring the predatory ability of *B. bacteriovorus* HD100.

The system was set up with a coculture of *B. bacteriovorus* HD100 and *P. putida* KT2440 as control prey (Figure 29). The co-cultures were monitored in 96-microwell plates for 24 h by

measurement of OD at 630 nm every 15 min, obtaining lysis curves due to the attack of the predator. Co-cultures were prepared as previously described in *General Materials and Methods* in a final volume of 200 µl. The plates were incubated 24 h at 30 °C with orbital shaking for 20 s each 15 min using a Multiskan plate incubator (Thermo Scientific, Waltham, MA, USA). The use of this multiwell platform to monitor the lytic potential of the predatory bacteria provide an easy to use, quick and more intuitive method for evaluation compared with the traditional double-layer method used for quantification of BALOs. For the evaluation of pathogenic bacteria, prey was suspended in Hepes buffer at OD_{600} 0.5 or 1, and different concentrations of predator were used (107,10^8 and 10^9 pfu ml^{-1}). Note that the prey cells were always prepared using OD at 600 nm, but the measurements on the multiwell system weere at OD 630 nm. This differences in the wavelength are noted in all the graphs of this chapter.

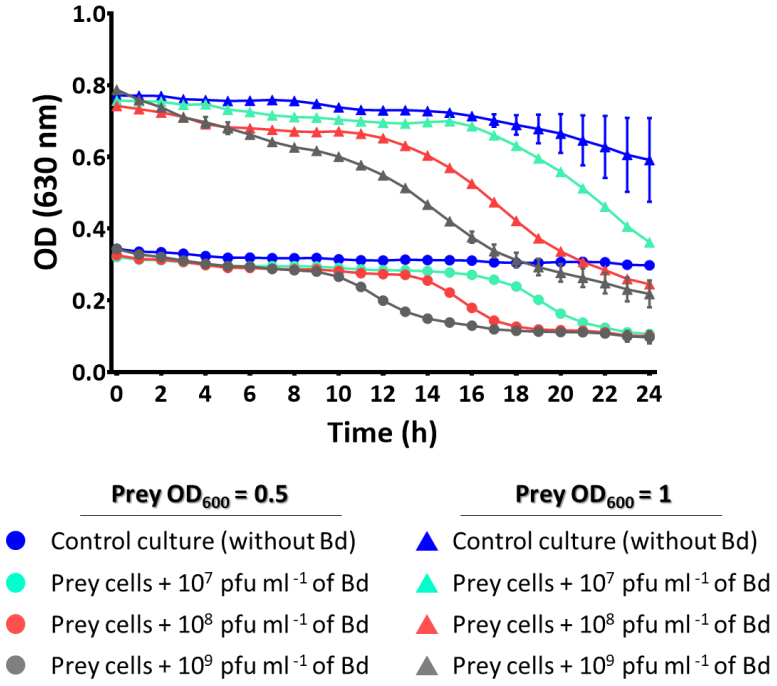

Figure 29. Set up of the monitorization of the predatory capability of *B. bacteriovorus* HD100 against *P. putida* KT2440 as prey. Prey cells were prepared at OD_{600} 0.5 (circles) and 1 (triangles). Different concentrations of predator cells were evaluated (light blue: 10^7 pfu ml^{-1}, red: 10^8 pfu ml^{-1}, grey: 10^9 pfu ml^{-1}). Dark blue represents the viability curve of the control prey culture (without predator). Bd: *B. bacteriovorus* HD100 cells.

3. RESULTS

3.1 *B. bacteriovorus* HD100 as a living antibiotic against relevant clinical pathogens

Earlier reports have proposed that *B. bacteriovorus* have the capability to rapidly diminish and kill more than 99.9% of bacterial cells grown in liquid suspension and as biofilms (Kadouri and O'Toole, 2005). This ability also takes into account of drug-resistant pathogens such as *P. aeruginosa*, *Burkholderia cepacia*, *K. pneumoniae,* and *E. coli*. With the increasing necessity of developing new and improved methods for controlling drug-resistant bacteria and biofilms, some potential advantages using predatory prokaryotes could be envisaged: i) They are highly specific for infecting exclusively bacteria (Jurkevitch and Davidov, 2006). ii) It is proved that the cell surface of *B. bacteriovorus* is only weakly immunogenic and will not induce severe immune reactions (Monnappa et al., 2014; Shanks et al., 2013; Shatzkes et al., 2015). iii) *Bdellovibrio* strains are able to prey upon human pathogens as well as drug-resistant bacteria (Kadouri et al., 2013). iv) The fast reproduction rate of the predator allows reducing the initial dose of *B. bacteriovorus* cells to be applied (Fenton et al., 2010). v) It is believed that no host cell resistance develops as a result of the predation.

In this section, we have evaluated the potential use of this predator against different clinically relevant human pathogens, such as some of the nosocomial pathogens represented in the ESKAPE group, commonly associated to antimicrobial resistance (*K. pneumoniae*, *A. baumannii, Pseudomonas aeruginosa* and *Salmonella typhimuriu m).*

We also tested the potential epibiotic predation of *B. bacteriovorus* HD100 upon the gram-positive bacteria *S. aureus*, *S. pneumoniae,* and *S. pyogenes*. This test will reveal information about the versatility of the predation strategy of *B. bacteriovorus* and could shed light about its adaptability into the ecological network.

In addition, the susceptibility of a set of clinical isolates of *P. aeruginosa* related to cystic fibrosis was evaluated for the first time representing a more realistic approach being *B. bacteriovorus* used as a living antibiotic.

3.1.1 Epibiotic predation of B. bacteriovorus HD100

Recent studies have reported the epibiotic predation of HD100 strain upon *S. aureus* (Iebba et al., 2014a). *S. aureus* is commonly found as part of the human microbiota. However, *S. aureus* is an opportunistic pathogen that can cause skin and respiratory infections. This infection triggers an inflammatory response due to the colonization of the lower respiratory tract (Harrison, 2007; Sibley and Surette, 2011). Related to this finding, and together with the trend

of increasing antimicrobial resistance of different common pathogens, we evaluated the susceptibility of other important gram-positive bacteria to predation, such as *S. pneumoniae* R6 and *S. pyogenes* ATCC 12344, both related also with respiratory tract infections (Albrich et al., 2004).

To examine the ability of *B. bacteriovorus* HD100 to prey on gram-positive bacteria commonly associated with respiratory tract diseases, bacteria were cultured until reaching the stationary phase on THY medium. After suspended in Hepes buffer at pH 7.8 at a concentration of OD_{600} 1, these prey cells were then incubated in the presence of the predator. Viability of prey and predator were counted at the onset (0 h) and at the end of the experiment (24 or 96 h).

As expected, we observed predation of *B. bacteriovorus* HD100 against *S. aureus* (Figure 30A). Predation was followed for 96 h when the reduction in the prey viable cells together with a slight increase of the predator cell number were appreciated. This result suggested that, in spite of the absence of the periplasm space, *B. bacteriovorus* is able to septate in the extracellular environment of the prey cell. Unfortunately, *B. bacteriovorus* HD100 was unable to prey upon *S. pyogenes* or *S. pneumonia* in the assayed predation conditions (Figure 30B and C).

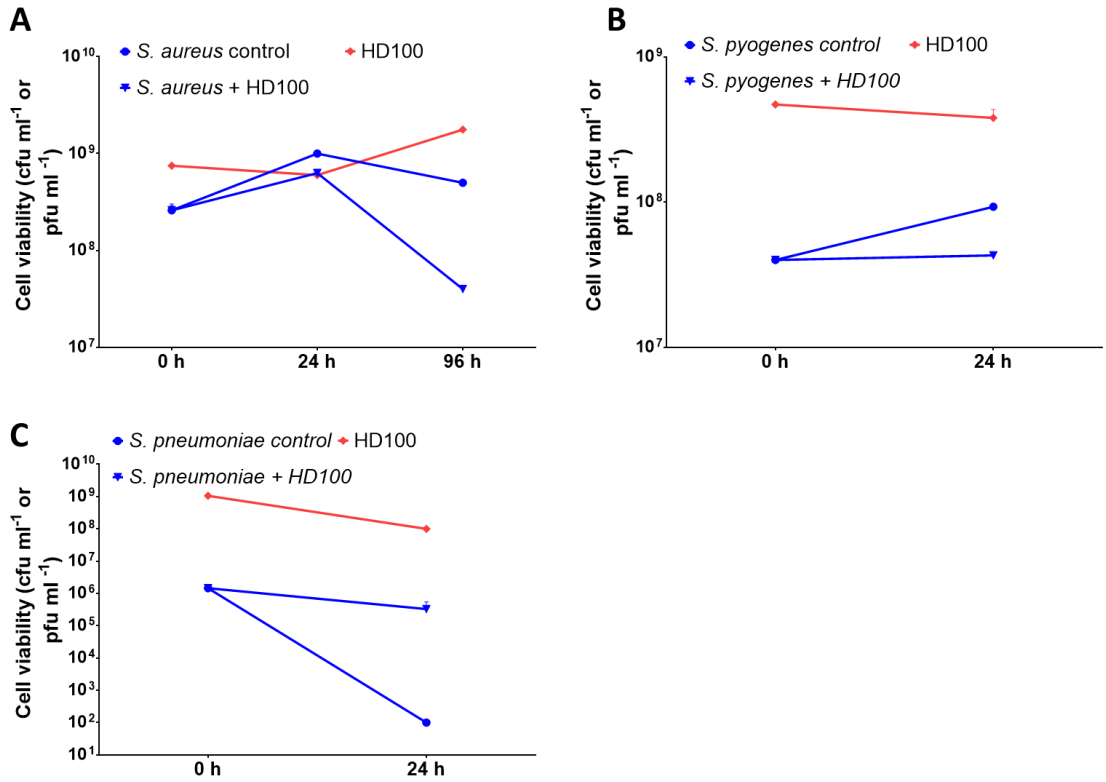

Figure 30. *B. bacteriovorus* HD100 predation on broth cultures of gram-positive bacteria used as prey. A) *S. aureus* NCTC 8532. **B)** *S. pyogenes* ATCC 12344. **C)** *S. pneumoniae* R6. The prey cells were grown up to OD_{600}=1. Blue lines represent the cfu ml^{-1} of prey cells presented in the

coculture with *B. bacteriovorus* (inverted triangle) and control culture without the predator. Red lines represent the pfu ml^{-1} of predator in the co-culture.

3.2 Potential antibiotic agent against gram-negative human pathogens

During this section, we have evaluated the antimicrobial activity of *B. bacteriovorus* against different pathogenic strains: *K. pneumoniae* 5214R, *K. pneumoniae* 43816R, *A. baumannii* 17978, *S. typhimurium* LT2, *P. aeruginosa* PA01. The lytic activity of the predator was evaluated using a multiwell system in a liquid medium, by monitoring the progressive decrease of the optical density at 630 nm due to the lysis of the prey.

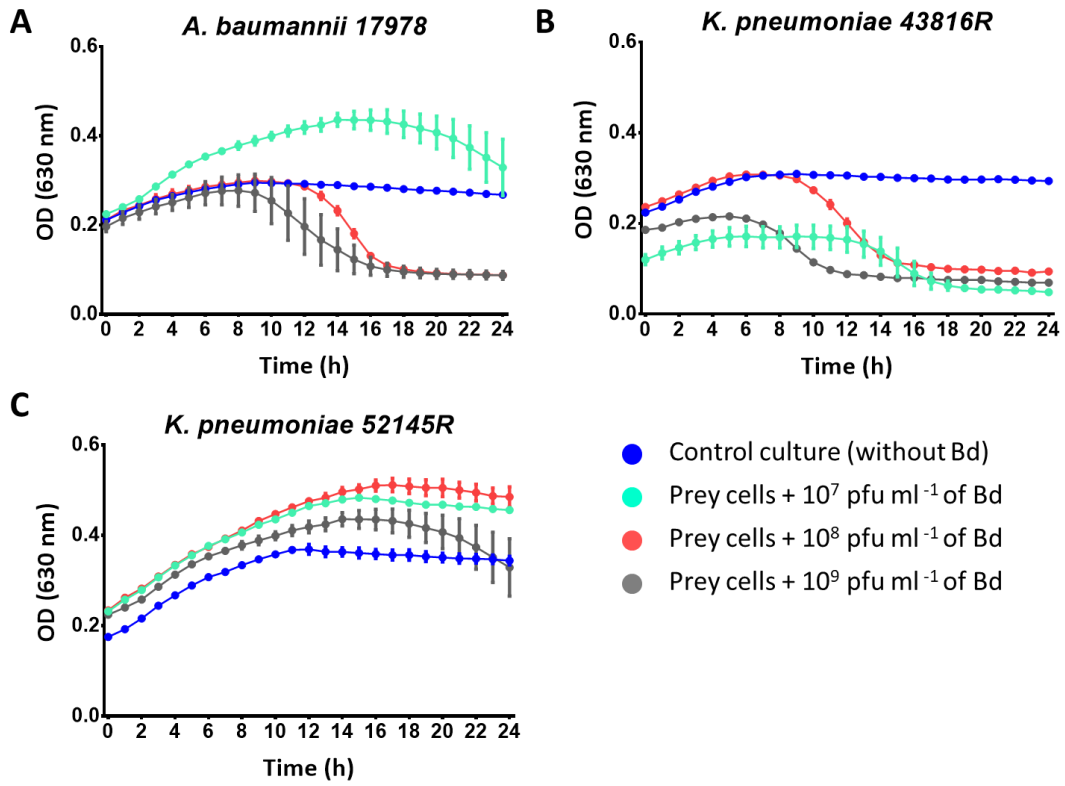

Figure 31. *B. bacteriovorus* predatory ability against gram-negative human pathogens. A) Monitorization of the lysis of *A. baumannii* 17978 cells. **B)** Monitorization of the lysis of *K. pneumoniae* 43816R cells. **C)** Monitorization of the lysis of *K. pneumoniae* 52145R cells. Prey cells were prepared at OD_{600} 0.5 and different concentrations of predator cells were evaluated (light blue: 10^7 pfu ml^{-1}, red: 10^8 pfu ml^{-1}, grey: 10^9 pfu ml^{-1}). Dark blue represents the viability curve of the control prey culture (without predator). Bd: *B. bacteriovorus* HD100 cells.

The susceptibility of different strains of *K. pneumoniae* and *A. baumannii* has been previously tested using different strains of *B. bacteriovorus* (Annex 1) (Dashiff et al., 2010; Dharani et al., 2017; Guerrini et al., 1982). During this work, we wanted to evaluate the ability

to prey upon them of *B. bacteriovorus* HD100 strain. The results indicated that *A. baumannii* 17978 and *K. pneumoniae* 43816R are susceptible to predation (Figure 31A and B). The quantification of prey cell viability revealed that after 24 h of predation the population was completely decimated (data not shown). In contrast, no reduction of *K. pneumoniae* 52145R cell population was measured after the exposure with HD100 in the experimental condition tested (Figure 31C). Different strains within the same species, could possess small differences in the cell envelope of the prey cells that determine the susceptibility to predation. This finding opens new perspectives to study the specificity of the predation.

Several reports have demonstrated the susceptibility of *S. typhimurium* and *P. aeruginosa* to predatory bacteria (Atterbury et al., 2011; Iebba et al., 2014a). Thus, these pathogens were used as positive control bacteria susceptible to be preyed by HD100 strain in this evaluation. The control predation curves and the viable cell count is shown in Figures 32A and B, respectively. The case of *P. aeruginosa* will be further studied in the next section exclusively due to its impact as a pathogen in human health.

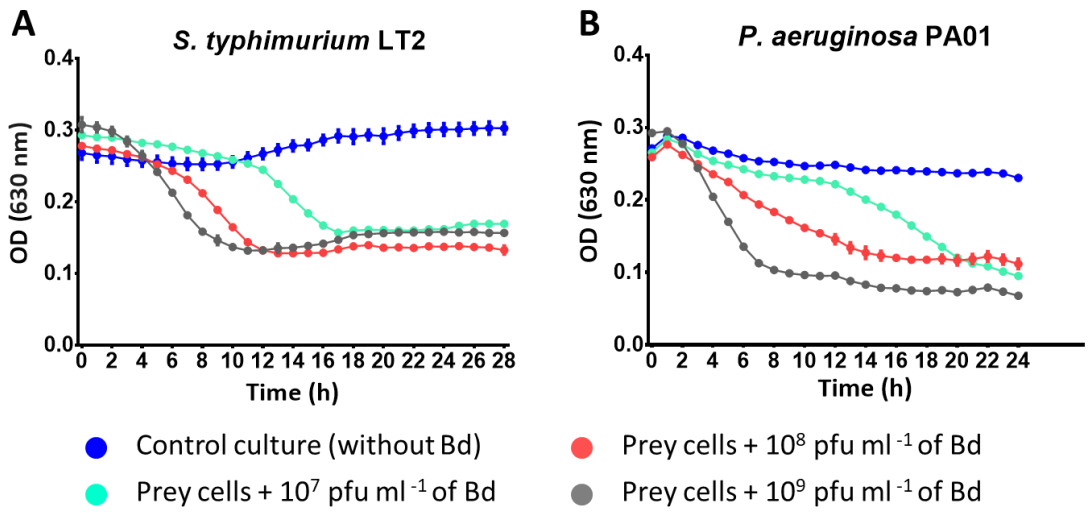

Figure 32. Monitoring the predatory ability of *B. bacteriovorus* HD100 on A) *S. typhimurium* LT2 and B) *P. aeruginosa* PAO1. Prey cells were prepared at OD_{600} 0.5 and different concentrations of predator cells were evaluated (light blue: 10^7 pfu ml^{-1}, red: 10^8 pfu ml^{-1}, grey: 10^9 pfu ml^{-1}). Dark blue represents the viability curve of the control prey culture (without predator). Bd: *B. bacteriovorus* HD100 cells.

3.3 Predatory ability of *B. bacteriovorus* HD100 against clinical *P. aeruginosa* strains isolated from cystic fibrosis patients

Cystic fibrosis is a genetic disorder caused by different mutations in the cystic fibrosis transmembrane conductance regulator (CFTR) gene that encodes a transmembrane chloride/bicarbonate transporter (Kerem et al., 1989). The respiratory disease is the most severe consequence of CF and it causes the death of around 80% of the patients due to respiratory failure and other complications. Although the life expectancy of CF patients has significantly increased due to the progress reached in treating this disease, there is still no cure. The current and future therapeutic objectives are mainly focused on correcting structural and functional defects of CFTR protein (Rafeeq and Murad, 2017), as well as the antibacterial treatment against the *P. aeruginosa* colonization.

The first multicenter study on the microbiology of CF in Spain has been recently reported. This study recruited 341 CF patients from all Spanish geography including adult and pediatric units, with an advanced disease and chronic colonization of *P. aeruginosa*. This study described the characterization of 79 *P. aeruginosa* clinical isolates in terms of population structure, antibiotic susceptibility and genetic background (López-Causapé et al., 2017). In addition, a lung microbiome analysis of these patients revealed the presence of predatory bacteria from the genera *Bdellovibrio* and *Vampirococcus*. In this section, we evaluated the susceptibility of predation by *B. bacteriovorus* HD100 of 36 of the *P. aeruginosa* strains isolates during this multicenter study. These strains have been characterized in terms of population structure, antibiotic resistance and genetic background (López-Causapé et al., 2017).

Table 11 shows the susceptibility of the different strains of *P. aeruginosa* as well as the microbiological features of each strain, and the age and weight of the patients. From the 36 strains, 21 (58.3%) showed susceptibility to be preyed by *B. bacteriovorus* HD100. The statistical analyses reveal that there are no differences in the age, the weight and the force expiratory volume (FEV_1) of the patients comparing the group of susceptible and not susceptible strains. This revealed that the condition of the patient does not determine the ability to prey. Focusing on the strain morphotype, strains with metallic and enterobacteriaceae morphotypes were susceptible to predation. Finally, it is important to remark the case of small colony variant (scv), that is a very common morphotype in the CF context (Evans, 2015). This morphotype does not present any advantage to predation: from the twelve strains found under this phenotype, *B. bacteriovorus* HD100 is able to prey on five of them.

Table 11. Clinical data of CF patients and microbiological characteristics of the *P. aeruginosa* strains. FEV_1: force expiratory volume in 1 s of the patient. ST: Sequence Type. *scv: small colony variant.

Strain	Age of the patient (years)	Weight of the patient (kg)	FEV_1	Strain morphotype*	Strain pigment	ST	Susceptibility to predation
17	30	87	102,4	metallic	no	116	+
49	20	55	20	enterobacteriaceae	no	132	+
75	33	58	64	scv	no	198	+
22	26	43	19	scv	no	253	+
68	22	49	37,12	scv	no	348	-
23	28	60	39,6	scv	red-brown	395	-
35	29	52	28	enterobacteriaceae	brown	560	+
73	38	65	56	mucoid	brown	575	+
33	14	36	40	metallic	green	617	+
48	33	.	47	scv	green	644	+
9	39	53	52	scv	no	1109	-
21	24	58	30,4	regular - mucoid	green	1228	+
56	.	.		regular	no	1251	-
26	19	.	18	enterobacteriaceae	no	1871	+
28	38	75,8	36	metallic	no	1873	+
41	20	55	77	mucoid	red-brown	1875	-
57	22	50,6	42	mucoid	no	1878	+
67	18	50	32,88	regular	no	1882	-
69	29	47	30,0	scv	no	1883	+
2	16	58,2	107	regular -mucoid	brown	1886	-
4	27	68	67	regular	green	1888	+
5	36	52	38	regular	no	1889	+
7	16	49	42	regular	no	1891	+
20	21	63	82,1	mucoid	brown	1895	-
24	20	48	40,5	scv	green	1896	+
25	24	63,5	69	regular	green	1897	-

Strain	Age of the patient (years)	Weight of the patient (kg)	FEV_1	Strain morphotype*	Strain pigment	ST	Susceptibility to predation
34	28	70	35	scv	green	1901	-
36	22	56	53	mucoid	red-brown	1902	-
46	33	68	48	scv	green	1905	-
47	32	81	48,6	enterobacteriaceae	no	1906	+
51	25	59	50,9	scv	no	1907	-
52	30	75,6	30,9	scv	no	1908	-
53	16	49,2	69,1	regular	no	1909	+
54	18	69,7	71,4	mucoid	no	1910	+
59	15	41	62,42	regular	no	1913	-
3	18	73	106	regular	green	4887	+

3.4 *B. bacteriovorus* HD100 as a biocontrol agent in aquaculture

Aquaculture, beyond doubt, is the fastest growing food-producing sector in the world. Its important role is to provide aquatic animal protein to balance out the deficit in the wild fisheries. Likewise, its socio-economic role in providing livelihood opportunities and economic security, particularly for the less-developed regions in the world, is being recognized (Rohana et al, 1999). The threat of disease has now become a primary constraint and risk to the growth of this sector. The importance of prevention and control of disease risks as a measure to reduce production losses in commercial and small-scale aquaculture systems has thus received increased attention (Mazid and Banu, 2002). In particular, outbreaks caused by fish pathogens such as *A. hydrophyla* or *Y. ruckeri* among others are considered to be a major problem to fish farming and quality, leading to severe losses on the production (Cao et al., 2012). These infections are now partially controlled by fish farmers with direct application of antibiotics such as terramycin and florfenicol. However, antibiotic treatment is cost-prohibitive to farmers in many undeveloped and developing countries, and antibiotic use may be detrimental to the environment and human health (Harikrishnan et al., 2010). The intrinsic ability to lyse gram-negative prey cells of BALOs suggests a crucial role in reducing or eliminating the incidence of fish pathogens. Therefore, in this section, we have selected some pathogenic strains that cause health and economic problems in aquaculture (Mazid and Banu, 2002) and the ability of *B. bacteriovorus* HD100 to reduce the population was evaluated.

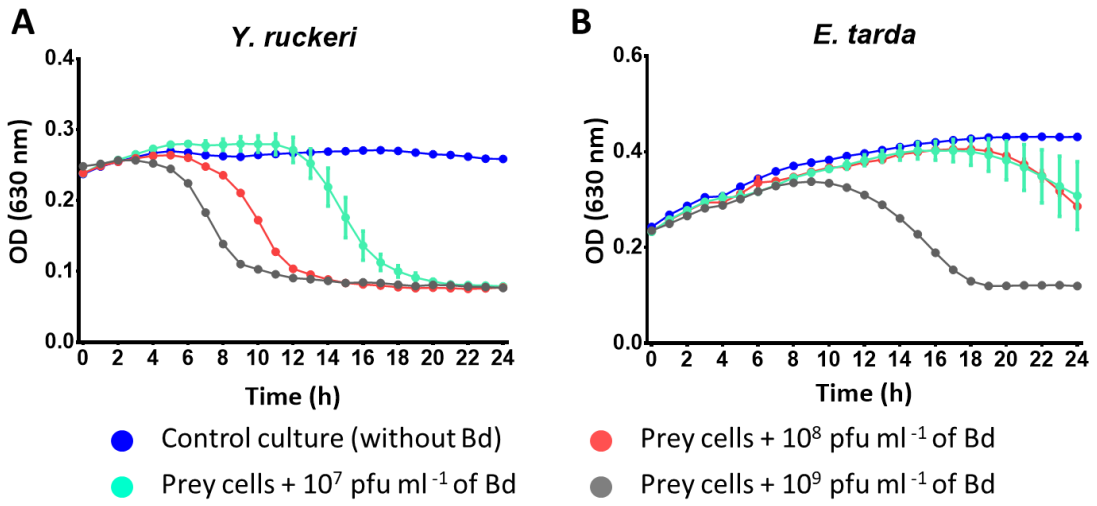

Figure 33. Monitoring the predation of *B. bacteriovorus HD100* upon aquaculture pathogens on multiwell system. A) *Y. ruckeri*. **B)** *E. tarda.* Prey cells were prepared at OD_{600} 0.5 and different concentrations of predator cells were evaluated (light blue: 10^7 pfu ml^{-1}, red: 10^8 pfu ml^{-1}, grey: 10^9 pfu ml^{-1}). Dark blue represents the viability curve of the control prey culture (without predator). Bd: *B. bacteriovorus* HD100 cells.

The present study indicated that *B. bacteriovorus* HD100 could significantly reduce the cell density of *Y. ruckeri* and exhibited also 100% lysis rate to the tested pathogenic *E. tarda* after the inoculation at the final cell density (Figure 33A and B). Quantification of prey cell viability confirms the predation event (data not shown). However, this predator did not show any bacteriolytic activity against other tested pathogens: *A. hydrophila*, *A. salmonicida*, *F. columnare* and *E. ictaluri* (Figure 34).

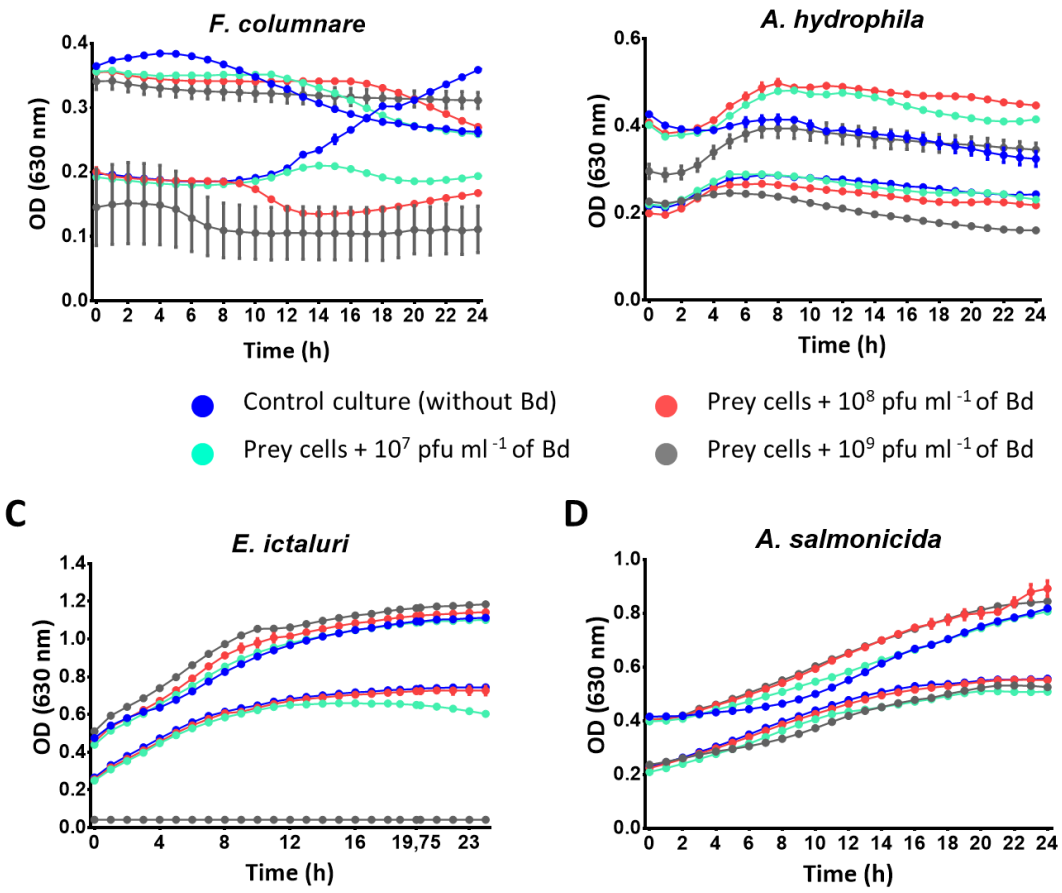

Figure 34. Monitoring the predation of *B. bacteriovorus HD100* upon aquaculture pathogens on multiwell system. A) *A. hypdrophila*, **B)** *A. salmonicida*, **C)** *F. columnare* and **D)** *E. ictaluri*. Prey cells were prepared at OD_{600} 0.5 or 1, and different concentrations of predator cells were evaluated (light blue: 10^7 pfu ml^{-1}, red: 10^8 pfu ml^{-1}, grey: 10^9 pfu ml^{-1}). Dark blue represents the viability curve of the control prey culture (without predator). Bd: *B. bacteriovorus* HD100 cells.

XI. INTEGRATED DISCUSSION

INTEGRATED DISCUSSION

1. THE METABOLIC MODEL, *i*CH457, PROVIDES METABOLIC CONTEXTUALIZATION OF THE OBLIGATE PREDATORY LIFESTYLE OF *B. BACTERIOVORUS* HD100: THE POTENTIAL FOR GROWTH IN THE ABSENCE OF PREY.

Integrative approaches combining traditional and innovative technologies are currently being addressed to establish the metabolic network of hot-spot microorganisms. This issue becomes much more challenging when it refers to predatory microorganisms such as the bacterium *B. bacteriovorus,* with its bi-phasic lifestyle. With the aim of elucidating the metabolic network wired to predator physiology and lifestyle, we implemented a computational test-bed, which provides a very useful platform for associating phenotypical relationships with predator genotype, while providing new insight on how the *B. bacteriovorus* metabolism works at the systemic level.

Although the metabolic reconstruction of *B. bacteriovorus* poses a big challenge, we are still far from availing of the level of knowledge of model organisms such as *E. coli* and *P. putida* KT2440 (*i*JO1366 and *i*JN1411), and consequently, from completing its respective GEMs. However, this predator metabolic reconstruction provides an excellent computational tool for finalising the development of this bacterium as a suitable biocatalyst for multiple biotechnological and clinical uses.

Although Rendulic et al. (Rendulic et al., 2004) had reported numerous auxotrophies in specific genes, the metabolic model allows these deficiencies in the network to be contextualised, revealing other auxotrophies or alternative metabolic routes. In general, the loss of essential biosynthetic genes is a typical characteristic of bacteria existing in nutrient-rich environments, such as lactic acid bacteria, endosymbionts or pathogens (D'Souza et al., 2014). In this sense, although *B. bacteriovorus* HD100 possesses a relatively large genome, it could also be included in this "genome streamlining" bacterial group because it directly employs whole molecules from the cytoplasm of the prey, which provides a crowded compartment comprising all the metabolites that support life (Golding and Cox, 2006; Rittenberg and Langley, 1975; Vendeville et al., 2011). With regard to the production of the biomass building blocks, it is noteworthy that most amino acids suffer a total lack of biosynthesis pathways. In contrast, *B.*

bacteriovorus is fully equipped with the biosynthetic routes for nucleotides and fatty acids. Keeping in mind the macromolecular composition of the cytoplasm of a prokaryotic cell as the natural growth niche of *B. bacteriovorus* (50 % proteins, 20 % RNA, 10 % lipids, 20 % remaining components), it is easy to speculate why the transporter system of amino acids is widely represented. While the factors driving *de novo* synthesis or the uptake of the biomass building blocks are still unknown, it is likely that these processes are extremely regulated and only activated in the absence of intermediates.

In addition, the presence of these complete metabolic pathways determines the potential ability of the predator to survive and grow without prey, as predicted by the model. On supplying the model with a rich medium based on amino acids, the simulation provided key information on the growth and generation of biomass, but why the biosynthetic pathways of amino acids are incomplete is still unknown.

Importantly, this potentially independent growth might be associated with its role as a balancer of bacterial population either in aquatic and soil environments or in the intestine of healthy individuals, because survival is not uniquely dependent on the predation event.

Comparison of the essential reactions between *B. bacteriovorus* and *P. putida* (a free-living microorganism) has revealed that the group of reactions pertaining exclusively to the predator mainly comprises transporters and amino acids and nucleotide metabolic pathways, consequently reflecting the reduction of biosynthetic pathways.

Moreover, the development of *i*CH457, *i*CHAP and *i*CHGP provides a framework, as well as testable reaction mechanisms, for a better understanding of the physiological and metabolic versatility of BALOs and other predatory bacteria and of their domestication for different applications. Briefly, during AP, *B. bacteriovorus* invests most of its resources in ATP generation, presumably in order to fuel the flagellum to search for new prey. In contrast, GP is characterized by the biosynthesis of biomass building blocks. *i*CH457 has demonstrated the inactivation of metabolic pathways in order to re-route the carbon flux distribution. For instance, the decarboxilative phase of the TCA cycle is completely inoperative when glutamate is used as a carbon and energy source.

2. RATIONAL SWITCH BETWEEN AP AND GP: RICH MEDIUM TRIGGERS ACTIVATION OF THE METABOLISM OF *B. BACTERIOVORUS* HD100

Growth of some *B. bacteriovorus* strains in rich media, such as PYE, promotes their development in HI derivative strains. Since these variants do not need prey to complete their

life cycle, cultivation of the HD100 strain could axenically constitute a good opportunity to better understand their physiology and metabolism during the growth phase. Previous research has suggested the survival and likely size increase of predator cells under rich medium conditions (Dwidar et al., 2017). The present thesis describes for the first time the independent growth of *B. bacteriovorus* HD100 characterized in terms of metabolic efficiency (ATP, biomass and nucleotide production). The results of the present thesis are in good agreement with previous data and model predictions, and indicate that this predator is metabolically active in rich medium, a phenomenon similar to the GP phase in the absence of prey. That is to say, BdQ cells have the capability to grow (understood as biomass generation) and to replicate their genome like they do inside the bdelloplast due to the fact that PYE simulates the cytoplasm of the prey cell. In accordance with previous HI predator studies, and in relation to the development rate of BdQ cells, only a small portion of the total population is capable of supporting the axenic growth and of yielding a heterogeneous population (Figure 11A) (Roschanski et al., 2011). Analysis of the sequence of the *hit* locus *bd0801* has confirmed the wild type genotype in this region (Figure 12).

Another crucial finding of our research involves optimization of the PYE to PYE10 medium in order to obtain a more homogeneous population of quiescent cells of HD100, which would provide more reliable results in physiological and metabolic studies. Importantly, modulating the concentration of the composition of the media (PYE10 vs CAV medium) enables us to rationally control the metabolism of the predator: ATP, nucleotide and biomass production. This fact highlights the potential use of this predatory bacterium in biotechnological and clinical research, because predator growth can be controlled.

Although amino acids have been proposed as major carbon sources (Hespell, 1976), the consumption of each individual molecule has not been reported to date. In the present thesis, we employed a minimal medium, CAV, strictly comprising amino acids, in order to analyze their uptake. Glutamate, aspartate, alanine, glycine, serine, threonine, proline and valine were proposed as the metabolites most commonly chosen by the predator. The exclusive use of amino acids had previously been tested in *B. bacterivorous* 109D and glutamate enabled more efficient growth of the predator (Ishiguro, 1974). In our study we go one step further, feeding *B. bacteriovorus* with a mixture of the 20 amino acids in saturated concentrations. This analysis revealed a clear preference for glutamate; once this metabolite is depleted, the remaining amino acids are consumed.

Glutamate is a key metabolite involved in anapletoric reactions. Glutamate deshydrogenase directly fuels the TCA cycle with α-ketoglutarate, as described in Chapter 1. This reaction provided an excellent source of reducing equivalents, crucial metabolites for the anabolic reactions, thus highlighting the preferential usage of glutamate.

These carbon sources should presumably be deaminized by the predator to obtain the respective carboxylic acid that might be channeled into substrate oxidation pathways in order for it to be finally directed towards the nucleotide synthesis. Indeed, the biosynthesis of nucleotides resulting from feeding the predator with amino acids as the sole carbon source (CAV medium) confirms the presence of an active and robust *de novo* nucleotide metabolism in *B. bacteiovorus*. In view of these conclusions, the predatory capability of *B. bacteriovorus* HD100 against *P. putida* KT2440 was evaluated in rich medium (LB), resulting in a more efficient predation, due to the "energization" of the AP cells (data not shown). Similar results should be expected if we supplement the Hepes buffer with amino acids in terms of predation efficiency, opening new opportunities for further optimization of the predatory medium composition

Based on the genome annotation, the predator has been described as possessing numerous systems for the uptake of amino acids and peptides (Barabote et al., 2007) as a result of its lifestyle, but their substrate specificity has not been reported to date. Although there is a need for targeted experiments to accurately elucidate the transporters and their mechanisms, herein we employ metabolic uptake analyses to demonstrate the presence of, at least, specific transporters for the eight metabolized amino acids present in CAV.

With regard to the growth cycle of the BdQ10 cells, there is a need for more in-depth study of this elongated predatory bacterium in order to understand its incapability to sept after replicating its genome. In this sense, and due to the obligated predatory nature of this strain, the key signal factor/molecule driving the division of the filamentous cells to complete the lifecycle might be i) part of the prey's metabolic arsenal, or ii) starvation following depletion of the prey nutrient content. In this sense, supplementation with *P. putida* extract has been attempted, but with no success to date (data not shown).

Chapters 1 and 2 of this thesis provided a new platform for *B. bacteriovorus* to be used as a chassis in biotechnology, based upon the new metabolic capabilities identified. However, to completely develop this predator as an efficient tool, we need to overcome the limitations associated with its manipulation in the laboratory. Among other factors, there is a need for improvement of the cultivability, detection and quantification of predator cells and of the narrow repertory of genetic tools and the availability of the omic data.

3. PREDATORY BACTERIA AS A BIOTECHNOLOGICAL TOOL BASED ON THEIR LYTIC CAPABILITY

The culture of *B. bacteriovorus* in laboratory requires two-membered cultures, due to the obligate intraperiplasm predatory lifestyle (Lambert et al., 2003) of the species. These procedures require careful and laborious manipulation, which affects the accuracy of the detection and quantification of *B. bacteriovorus* in different samples (Davidov et al., 2006). All this hinders our work with these predatory bacteria, and alternative methodologies have therefore been sought, such as the FISH and qPCR molecular techniques. These culture-independent techniques provide more sensitive quantification due to the specificity of probe hybridization or oligonucleotides. The FISH assay presents several limitations resulting from the mutual dependence of the fluorescence signal and the template concentration, which is affected by the prey and the growth phase of *Bdellovibrio*. Consequently, this FISH technology is recommended when *B. bacteriovorus* concentration is at least 10^5 pfu ml^{-1} (Khaled K. Mahmoud et al., 2007). However, the qPCR method is not affected by the aforementioned restrictions, and has been shown to constitute an effective tool for detection and quantification of specific groups of bacteria in complex samples.

During this thesis, we developed a precise method based on a qPCR assay to quantify *B. bacteriovorus* HD100 from whole cells, in which no pretreatments such as DNA extraction, retrotranscription or RNAse addition are necessary. This system provides a useful and rapid protocol for monitoring the genome number of *B. bacteriovorus* growing axenically and in co-culture. As previously mentioned, this qPCR system will contribute to enhancing the applicability of predators in different fields.

B. bacteriovorus has long been proposed as an alternative to antibiotics, given its ability to decimate gram-negative bacterial populations (Atterbury et al., 2011; Dashiff et al., 2010; Kadouri and O'Toole, 2005; Kadouri and Tran, 2013; Sockett, 2009b; Sockett and Lambert, 2004). Moreover, the *B. bacteriovorus* HD100 genome sequence, published in 2004 (Rendulic et al., 2004), pointed to the vast amount of hydrolytic enzymes (biocatalysts) suitable for numerous industrial applications (Martínez et al., 2013, 2012). Due to its lytic activity, *B. bacteriovorus* HD100 represents a highly promising candidate to be developed for biotechnological uses. Within this framework, herein we highlight *B. bacteriovorus* as a potential lytic tool for intracellular bio-product recovery. This original cell breakage methodology is based on the use of the predator as an external living-cell lytic agent. However, in contrast with phage restrictions, which are species-specific, a fact that limits the range of applicability (Fidler and Dennis, 1992;

Hori et al., 2002; Martínez et al., 2011; Resch et al., 1998; Yu and Hederstedt, 1995), *Bdellovibrio* strains present the advantage of preying upon a wide range of gram-negative bacteria (Jurkevitch and Davidov, 2006; Sockett, 2009a). Our previous studies have demonstrated the ability of *B. bacteriovorus* HD100 to prey upon *P. putida* KT2440 accumulating mcl-PHA and to release the 50% of the biopolymer granules into the extracellular medium after the predation event (Martínez et al., 2013). This result motivated us to evaluate the potential use of the predator as a novel downstream chassis in the recovery of intracellular products such as PHAs.

Moreover, the usefulness of this biological system for optimizing the PHA downstream process in well-established PHA producers has been demonstrated. The downstream procedure consists of a simple predator addition to the PHA producer culture, thus causing the release of the intracellular biopolymer into the culture medium. Given the broad prey range of *B. bacteriovorus*, the cell breakage procedure has been successfully applied in different bacterial species for the collection of other interesting intracellular biopolymers, such as PHB produced by a recombinant strain of *E. coli, C. necator* H16 and *R. rubrum*.

Nonetheless, in order to be more competitive *Bdellovibrio* spp. needs to be engineered to increase the efficiency of extraction, and biopolymer degradation during the recovery process must be avoided. Using the Bd3709 or Bd2637 mutant strains, which present no mcl-PHA or PHB depolymerase activity, the optimum conditions were established for recovery of up to 80% of the total mcl-PHA (or PHB) content following predation. Surprisingly, both the Bd3709 and the Bd2637 mutants killed more prey cells compared to the wild type strain. Although there is a need for additional experiments, it can speculated that mcl-PHA and scl-PHA depolymerase deletion had a major impact on predator fitness and killing capacity, thus rendering predators more aggressive.

Apart from enhancing the mutant strains, we also demonstrated the efficacy of the bio-based lytic system at high prey cell densities such as OD_{600} 30 and OD_{600} 160, highlighting *B. bacteriovorus* as an optimal lytic chassis for large-scale production of such natural products.

Previous data on the wild type strain HD100 preying upon *P. putida* showed that PHA degradation confers upon the predator ecological advantages in terms of motility and predation efficiency, but it does not increase biomass or the number of predator cells (Martínez et al 2013). In contrast with these results, predation on PHB accumulating *E. coli* cells provided *B. bacteriovorus* with fitness benefits in terms of number of progeny, whereas mean swimming speed was similar. The hydrolytic products derived from PHB degradation might be catabolized for synthesis of biomass building blocks via a putative R-3-hydroxyacyl CoA synthase (*Bd1803*)

[EC 6.2.1.3 (http://www.genome.jp/kegg-bin/show_pathway?bba00071)], followed by the action of a putative 3-hydroxyacyl-CoA isomerase to yield S-3-hydroxyacyl-CoA (*Bd1836*) [EC 5.1.2.3 (http://www. genome.jp/kegg-bin/show_pathway?bba00650)]. Finally, 3-hydroxyacyl-CoA dehydrogenase would convert S-3-hydroxybutyryl-CoA to acetoacetyl-CoA (*Bd1836*) [EC 1.1.1.35 (http://www.genome.jp/kegg-bin/show_ pathway?bba00650)], which channels into the central metabolism, thus accounting for the increase in predator progeny following predation on PHB-accumulating *E. coli*. The species *B. bacteriovorus* has also been demonstrated to use the intermediate metabolites it acquires from the prey (Kuenen et al., 1975; Rubi et al., 1986); mcl-PHA and PHB may therefore have acted as extra carbon sources. These metabolites might become incorporated into the fatty acid pathway and the secondary metabolism, consequently improving the predation capacity of the bacterium.

In summary, the present study further highlights the potential application of predatory bacteria as external living-cell lytic agents with the capability to prey on a wide variety of gram-negative bacteria for the production of industrially relevant compounds

4. *B. BACTERIOVORUS* HD100 HAS A WIDE PREY RANGE INCLUDING HUMAN AND FISH PATHOGENS

Several published studies describe the possible use of BALOs as biological control agents in both environmental and medical microbiological settings (Hobley et al., 2006; Westergaard and Kramer, 1977). Our thesis compiles an evaluation of the capacity for predation of *B. bacteriovorus* HD100 upon different pathogens for prevention and control of bacterial diseases in clinics and in the environment.

In view of the increasing antibiotic resistance among clinical pathogens, the use of *B. bacteriovorus* has been suggested as a 'living-antibiotic' (Negus et al., 2017; Rendulic et al., 2004; Sockett and Lambert, 2004). Interestingly, the dual foraging strategy exhibited by *B. bacteriovorus* on *S. aureus* (epibiotic) and *P. aeruginosa* (periplasmic) (Iebba et al., 2014a), could significantly reduce the bacterial loads and biofilms of both gram-negative and gram-positive bacteria. We further evaluated this dual capacity, establishing that the HD 100 strain was unable to prey upon two other gram-positive bacteria: *S. pneumonie* and *S. pyogenes.* Moreover, when the susceptibility to predation was assessed against some strains of the ESKAPE pathogenic group, we found that *K. pneumoniae* 52145R was resistant to predation under these experimental conditions. Strikingly, the other strain of *K. pneumoniae* tested in this chapter (43816R) was susceptible to predation. This specificity could contribute to elucidating why the predator is unable to complete the predatory cycle and moreover, to identifying the resistance factors.

As bdellovibrios has been reported to be capable of eradicating bacterial pathogen populations in aquaculture systems (Li et al., 2014b; Zhou et al., 2009), herein we tested its ability to kill some of the most harmful pathogenic bacteria in fish farming. In the results section, we demonstrated that upon exposure to a high titer of *B. bacteriovorus* cells, reduction of *Y. ruckeri* and *E. tarda* was achieved within the first 24 hours of attack. These bacterial pathogens are very common in aquaculture, causing different skin diseases that affect *Salmo salar*, *Salmo trutta*, *Pangasius hypophthalmus* and *Oreochromis* spp. (Li et al., 2012). The consequences of these infections have a severe economic impact on fish farming due to losses of production and quality of the final product (Cao et al., 2010). As antibiotic treatment is cost-prohibitive to farmers, the use of predatory bacteria constitutes an attractive alternative.

Another interesting finding of these analyses involves the ability of *B. bacteriovorus* HD100 to prey upon clinical *P. aeruginosa* strains isolated from CF patients. As these strains do not come from a laboratory collection, which means they are not adapted to laboratory

conditions, their phenotype and genotype are likely closer to those of the potential candidates that BALOs would encounter as a living antibiotic. The clinical isolates from sputum are classically all derived from the same bacterial strain, which could coexist exhibiting different morphologies. The clinical isolate *P. aeruginosa* can be found with different morphologies: mucoid, regular, enterobacteriaceae and small colony variants (scv) (Evans, 2015). Scv has been associated with a worse and persistent clinical condition. This scv phenotype allows the bacterium to survive under adverse environmental conditions as a resistant form. From the thirty-six *P. aeruginosa* strains tested in this thesis, twelve exhibit the scv morphotype (33%) (Table 13). Considering the features of the scv phenotype, one would expect all these strains to be resistant to predation. However, the predator is able to prey on five of them, suggesting that the modifications in the cell wall that determine this phenotype are not linked to the viability of predation events.

Regarding the resistance to predation of some of the bacterial strains evaluated in our research, the specific mechanism of the biology of predatory bacteria, as well as the key factor governing prey specificity remain unknown. Attachment of the predator to the prey's outer membrane is believed to constitute an essential first step and apparently determines the feasibility of predation. In this sense, few studies focusing on the prey cell membrane have been reported. For instance, it has been described that *mcr-1* encoding a phosphoethanolamine transferase, which leads to the addition of phosphoethanolamine moiety on lipid A, is in part responsible for the specificity of the prey outer membrane. The mechanism would reduce the affinity of cationic chemicals and would alter the negatively charged LPS phosphates (Dharani et al., 2017). Therefore, in order to increase our understanding of how this predator behaves and why some gram-negative strains are resistant, this *mrc-1* should be evaluated. This would provide better knowledge of the use of BALOs as a "living antibiotic".

Likewise, numerous analyses of the composition and integrity of LPS in prey cells have also been conducted. The α-Proteobacteria have different LPS that could inhibit or slow predation. In this context, *E. coli* and *Salmonella* sp. of "rough" mutants, defective and altered in LPS production, present an initial lag in predation, which is eventually overcome; this suggests an adaptative population of *B. bacteriovorus*, and that LPS may not be the only factor influencing successful predation (Gray and Ruby, 1990; Schelling and Conti, 1986; Varon and M. Shilo, 1969).

Finally, it becomes clear that *B. bacteriovorus* has attracted much attention recently both for its basic biology, as well as for its potential applications in medicine, industry, and agriculture. Consequently, tools that allow control of this unique bacterium should make it more amenable

as a microbial chassis for synthetic biology applications. On considering the development of predators as a platform for biotechnological purposes, the predatory ability plays a vital role. Traditionally, the double-layer method of the co-culture was used to monitor the capacity to decimate the bacterial population. As has been pointed out, this method is laborious; it is time-consuming and limits the use of predators. In order to increase the efficiency of the predator systems, in the present thesis we establish a method for monitoring the predation event by measuring the OD_{630}. This approach represents a great improvement and provides faster and more reliable data for the implementation of *B. bacteriovorus* as a biotechnological and clinical chassis. The dependence of *Bdellovibrio* cells on prey bacteria for its survival makes it more challenging and some considerations on the use of predatory bacteria should be taken into account. For example, in applications related with human health, such as medicine or food industry. As *B. bacteriovorus* requires a host to grow and replicate, it likely limits its propagation when the potential host is present. Surprisingly, however, 1 in $10^6 – 10^7$ cells can grow in the absence of prey cells when provided with nutrient-rich media. This may pose a problem if *B. bacteriovorus* is used as a therapeutic agent and administered to patients, as the predatory bacterium could potentially take over once the gram-negative pathogens have been eradicated. This risk can be addressed with the design of strictly predatory mutants (Hobley et al., 2012).

XII. CONCLUSIONS

CONCLUSIONS

1- This thesis reports the first curated genome-scale model of *B. bacteriovorus* HD100 metabolism, *i*CH457. The construction of specific phase models, *i*CHAP and *i*CHGP has revealed the metabolic pathway driving each phase of the life cycle.

2- Metabolic simulations performed in *i*CH457, *i*CHAP and *i*CHGP reiteratively suggest that, based on its genetic and metabolic capabilities, the predator should be able to grow autonomously, in the absence of the prey.

3- Experimental validations in an undefined rich medium such as PYE10 demonstrate the activation of the *B. bacteriovorus* HD100, promoting the growth in terms of biomass generation, ATP production, and nucleotide biosynthesis. However, division of the predator cells was not detected.

4- The cultivation of the predator in PYE10 rich medium stimulates the generation of a population of *B. bacteriovorus* HD100, called BdQ10, homogeneous in their cell size, with an average length of 1.3110 ± 0.0391 µm.

5- Although BdQ10 cells are metabolically active, they maintain the wild type genotype regarding the *hit* mutations in the loci *bd0810* and *bd3464* and are unable to generate progeny in the absence of the prey.

6- GC-Q-TOF-MS analyses confirm the amino acids as the major utilizable carbon source among all the metabolites present in PYE10 medium. The quantification of the consumption rate of amino acids from PYE10 has provided the design of the rational defined medium CAV used for growing *B. bacteriovorus* HD100.

7- CAV medium stimulates the activation of the metabolism of *B. bacteriovorus* HD100 cells in terms of ATP production and nucleotides biosynthesis. The preference of glutamate as carbon and energy source from a mixture of amino acids was confirmed.

8- *B. bacteriovorus* HD100 has been developed as an efficient biological lytic system for the recovery of intracellular bioproducts, such as PHAs, even for high cell density cultures. Moreover, this system can be used to prey upon different PHA-producing bacteria, expanding its utility.

9- *B. bacteriovorus* HD100 is able to prey on different nosocomial pathogens such as *S. aureus*, *P. aeruginosa* PAO1, *S. typhimurium* LT2, *K. pneumoniae* 43816R and *A. baumannii* 17978. Besides, 21 clinical *P. aeruginosa* strains from CF patients are susceptible to predation, highlighting the use of *B. bacteriovorus* HD100 as a living antibiotic.

10- The fish farm pathogens *E. tarda* and *Y. ruckeri* are susceptible to predation by *B. bacteriovorus* HD100.

XIII. REFERENCES

REFERENCES

Albrich, W.C., Monnet, D.L., Harbarth, S., 2004. Antibiotic Selection Pressure and Resistance in *Streptococcus pneumoniae* and *Streptococcus pyogenes*. Emerg. Infect. Dis. 10, 514–517. doi:10.3201/eid1003.030252

Ames, J., MacLeod, G., 1985. Volatile components of a Yeast Extract Composition. J. Food Sci. 50, 9–10.

Atterbury, R.J., Hobley, L., Till, R., Lambert, C., Capeness, M.J., Lerner, T.R., Fenton, A.K., Barrow, P., Sockett, R.E., 2011. Effects of orally administered *Bdellovibrio bacteriovorus* on the well-being and *Salmonella* colonization of young chicks. Appl. Environ. Microbiol. 77, 5794–5803. doi:10.1128/AEM.00426-11

Aziz, R.K., Devoid, S., Disz, T., Edwards, R.A., Henry, C.S., Olsen, G.J., Olson, R., Overbeek, R., Parrello, B., Pusch, G.D., Stevens, R.L., Vonstein, V., Xia, F., 2012. SEED Servers: High-Performance Access to the SEED Genomes, Annotations, and Metabolic Models. PLoS One 7, 1–10. doi:10.1371/journal.pone.0048053

Baker, M., Negus, D., Raghunathan, D., Radford, P., Moore, C., Clark, G., Diggle, M., Tyson, J., Twycross, J., Sockett, E., n.d. Measuring and modelling the response of *Klebsiella pneumoniae* KPC prey to *Bdellovibrio bacteriovorus* predation, in human serum and defined buffer. doi:10.1038/s41598-017-08060-4

Barabote, R.D., Rendulic, S., Schuster, S.C., Saier, M.H., 2007. Comprehensive analysis of transport proteins encoded within the genome of *Bdellovibrio bacteriovorus*. Genomics 90, 424–46. doi:10.1016/j.ygeno.2007.06.002

Becker, S.A., Palsson, B.O., 2008. Context-specific metabolic networks are consistent with experiments. PLoS Comput. Biol. 4. doi:10.1371/journal.pcbi.1000082

Berger, J., Stacey, P.B., Bellis, L., Johnson, M.P., 2001. A mammalian predator-prey inbalance; grizzly bear and wolf extinction affect avian neotropical migrants. Ecol. Appl. 11, 947–960.

Bonarius, H.P.J., Schmid, G., Tramper, J., 1997. Flux analysis of underdetermined metabolic networks: The quest for the missing constraints. Trends Biotechnol. 15, 308–314. doi:10.1016/S0167-7799(97)01067-6

Bordbar, A., Monk, J.M., King, Z.A., Palsson, B.O., 2014. Constraint-based models predict

metabolic and associated cellular functions. Nat. Rev. Genet. 15, 107–120. doi:10.1038/nrg3643

Brodie, E.D., 1999. Predator-Prey Arms Races Asymmetrical selection on predators and prey may be reduced when prey are dangerous.

Caballero, J.D.D., Vida, R., Cobo, M., Máiz, L., Suárez, L., Galeano, J., Baquero, F., Canton, R., Del Campo, R., 2017. Individual Patterns of Complexity in Including Predator Bacteria , over a 1-Year Period 8, e00959-17. doi:10.1128/mBio.00959-17

Cao, H., He, S., Wang, H., Hou, S., Lu, L., Yang, X., 2012. *Bdellovibrios*, potential biocontrol bacteria against pathogenic Aeromonas hydrophila. Vet. Microbiol. 154, 413–418. doi:10.1016/j.vetmic.2011.07.032

Cao, H.P., He, S., Lu, L.Q., Hou, L.D., 2010. Characterization and Phylogenetic Analysis of the Bitrichous Pathogenic *Aeromonas hydrophila* Isolated from Diseased Siberian sturgeon (*Acipenser baerii*). Isr. J. Aquac. 62, 181–188.

Capeness, M.J., Lambert, C., Lovering, A.L., Till, R., Uchida, K., Chaudhuri, R., Alderwick, L.J., Lee, D.J., Swarbreck, D., Liddell, S., Aizawa, S.-I., Sockett, R.E., 2013. Activity of *Bdellovibrio Hit* Locus Proteins, Bd0108 and Bd0109, Links Type IVa Pilus Extrusion/Retraction Status to Prey-Independent Growth Signalling. doi:10.1371/journal.pone.0079759

Chang, K.L., Ho, P.C., 2014. Gas chromatography time-of-flight mass spectrometry (GC-TOF-MS)-based metabolomics for comparison of caffeinated and decaffeinated coffee and its implications for Alzheimer's disease. PLoS One 9. doi:10.1371/journal.pone.0104621

Chanprateep, S., 2010. Current trends in biodegradable polyhydroxyalkanoates. J. Biosci. Bioeng. 110, 621–632. doi:10.1016/j.jbiosc.2010.07.014

Chanyi, R.M., Koval, S.F., 2014. Role of type IV Pili in predation by *Bdellovibrio bacteriovorus*. PLoS One 9. doi:10.1371/journal.pone.0113404

Chen, C.-Y., Yen, S.-H., Chung, Y.-C., 2014. Combination of photoreactor and packed bed bioreactor for the removal of ethyl violet from wastewater. Chemosph. J. 117, 494–501. doi:10.1016/j.chemosphere.2014.08.069

Clarholm, M., 1984. Microbes as predators or prey, Current perspectives on microbial ecology.

Coburn, B., Sekirov, I., Finlay, B.B., 2007. Type III secretion systems and disease. Clin. Microbiol. Rev. 20, 535–549. doi:10.1128/CMR.00013-07

Corno, G., Jürgens, K., 2006. Direct and indirect effects of protist predation on population size structure of a bacterial strain with high phenotypic plasticity. Appl. Environ. Microbiol. 72, 78–86. doi:10.1128/AEM.72.1.78

Cotter, T.W., Thomashow, M.F., 1992. A conjugation procedure for *Bdellovibrio bacteriovorus* and its use to identify DNA sequences that enhance the plaque-forming ability of a spontaneous host-independent mutant. J. Bacteriol. 174, 6011–6017.

Cotter, T.W., Thomashow, M.F., 1992. Identification of a *Bdellovibrio bacteriovorus* genetic locus, hit, associated with the host-independent phenotype. J. Bacteriol. 174, 6018–24.

Czárá, T.L., Hoekstra, R.F., Pagie, L., Levin, S.A., 2002. Chemical warfare between microbes promotes biodiversity. pnas 99, 786–790.

D'Souza, G., Waschina, S., Pande, S., Bohl, K., Kaleta, C., Kost, C., 2014. Less is more: selective advantages can explain the prevalent loss of biosynthetic genes in bacteria. Evolution (N. Y). 68, 2559–2570. doi:doi:10.1111/evo.12468

Dashiff, A., Junka, R.A., Libera, M., Kadouri, D.E., 2010. Predation of human pathogens by the predatory bacteria *Micavibrio aeruginosavorus* and *Bdellovibrio bacteriovorus*. J. Appl. Microbiol. 110, 431–444. doi:10.1111/j.1365-2672.2010.04900.x

Davidov, Y., Friedjung, A., Jurkevitch, E., 2006. Structure analysis of a soil community of predatory bacteria using culture-dependent and culture-independent methods reveals a hitherto undetected diversity of *Bdellovibrio*-and-like organisms. Environ. Microbiol. 8, 1667–1673. doi:10.1111/j.1462-2920.2006.01052.x

Davidov, Y., Jurkevitch, E., 2009. Predation between prokaryotes and the origin of eukaryotes. BioEssays 31, 748–757. doi:10.1002/bies.200900018

Davidov, Y., Jurkevitch, E., 2004. Diversity and evolution of *Bdellovibrio*-and-like organisms (BALOs), reclassification of *Bacteriovorax starrii* as *Peredibacter starrii* gen. nov., comb. nov., and description of the Bacteriovorax-Peredibacter clade as Bacteriovoracaceae fam. nov. Int. J. Syst. Evol. Microbiol. 54, 1439–1452. doi:10.1099/ijs.0.02978-0

de Eugenio, L.I., Escapa, I.F., Morales, V., Dinjaski, N., Galán, B., García, J.L., Prieto, M. a, 2010. The turnover of medium-chain-length polyhydroxyalkanoates in *Pseudomonas putida* KT2442 and the fundamental role of PhaZ depolymerase for the metabolic balance. Environ. Microbiol. 12, 207–21. doi:10.1111/j.1462-2920.2009.02061.x

de Eugenio, L.I., García, P., Luengo, J.M., Sanz, J.M., Román, J.S., García, J.L., Prieto, M. a, 2007.

Biochemical evidence that phaZ gene encodes a specific intracellular medium chain length polyhydroxyalkanoate depolymerase in *Pseudomonas putida* KT2442: characterization of a paradigmatic enzyme. J. Biol. Chem. 282, 4951–62. doi:10.1074/jbc.M608119200

Dharani, S., Hyun Kim, D., Shanks, R.M., Doi, Y., Kadouri, D.E., 2017. Susceptibility of colistin-resistant pathogens to predatory bacteria. doi:10.1016/j.resmic.2017.09.001

Dori-Bachash, M., Dassa, B., Peleg, O., Pineiro, S. a, Jurkevitch, E., Pietrokovski, S., 2009. Bacterial intein-like domains of predatory bacteria: a new domain type characterized in *Bdellovibrio bacteriovorus*. Funct. Integr. Genomics 9, 153–66. doi:10.1007/s10142-008-0106-7

Dori-Bachash, M., Dassa, B., Pietrokovski, S., Jurkevitch, E., 2008. Proteome-based comparative analyses of growth stages reveal new cell cycle-dependent functions in the predatory bacterium *Bdellovibrio bacteriovorus*. Appl. Environ. Microbiol. 74, 7152–62. doi:10.1128/AEM.01736-08

Dwidar, M., Im, H., Seo, J.K., Mitchell, R.J., 2017. Attack-Phase *Bdellovibrio bacteriovorus* Responses to Extracellular Nutrients Are Analogous to Those Seen During Late Intraperiplasmic Growth. Microb. Ecol. doi:10.1007/s00248-017-1003-1

Eksztejn, M., Varon, M., 1977. Elongation and Cell Division in *Bdellovibrio bacteriovorus*. Arch. Microbiol. 114, 175–181.

Elbahloul, Y., Steinbüchel, A., 2009. Large-scale production of poly(3-hydroxyoctanoic acid) by *Pseudomonas putida* GPo1 and a simplified downstream process. Appl. Environ. Microbiol. 75, 643–651. doi:10.1128/AEM.01869-08

Elbourne, L.D.H., Tetu, S.G., Hassan, K.A., Paulsen, I.T., 2017. TransportDB 2.0: A database for exploring membrane transporters in sequenced genomes from all domains of life. Nucleic Acids Res. 45, D320–D324. doi:10.1093/nar/gkw1068

Erkin Kuru, 1, 7, Carey Lambert, 2, Jonathan Rittichier, 3, 7, Rob Till, 2, Adrien Ducret, 4, 6, Adeline Derouaux, 5, 8, Joe Gray, 5, Jacob Biboy, 5, Waldemar Vo l, lmer, 5, Michael VanNieuwenhze, 3, Yves V. Brun, 4, and, R. Elizabeth Sockett, 2017. Fluorescent D -amino-acids reveal bi-cellular cell wall modifications important for *Bdellovibrio bacteriovorus* predation. Nat. Microbiol. doi:doi: 10.1038/s41564-017-0029-y

Evans, T.J., 2015. Small colony variants of *Pseudomonas aeruginosa* in chronic bacterial infection of the lung in cystic fibrosis. Future Microbiol. 10, 231–239. doi:10.2217/fmb.14.107

Feist, A.M., Henry, C.S., Reed, J.L., Krummenacker, M., Joyce, A.R., Karp, P.D., Broadbelt, L.J.,

Hatzimanikatis, V., Palsson, B.Ø., 2007. A genome-scale metabolic reconstruction for *Escherichia coli* K-12 MG1655 that accounts for 1260 ORFs and thermodynamic information. Mol. Syst. Biol. 3, 121. doi:10.1038/msb4100155

Feng, W., Sun, F., Wang, Q., Xiong, W., Qiu, X., Dai, X., Xia, P., 2017. Epidemiology and resistance characteristics of *Pseudomonas aeruginosa* isolates from the respiratory department of a hospital in China. J. Glob. Antimicrob. Resist. 8, 142–147. doi:10.1016/j.jgar.2016.11.012

Fenton, A.K., Lambert, C., Wagstaff, P.C., Sockett, R.E., 2010. Manipulating each MreB of *Bdellovibrio bacteriovorus* gives diverse morphological and predatory phenotypes. J. Bacteriol. 192, 1299–311. doi:10.1128/JB.01157-09

Fidler, S., Dennis, D., 1992. Polyhydroxyalkanoate production in recombinant *Escherichia coli*. FEMS Microbiol. Lett. 103, 231–235. doi:10.1016/0378-1097(92)90314-E

Flowers, J.J., Richards, M.A., Baliga, N., Meyer, B., Stahl, D.A., 2018. Constraint-based modelling captures the metabolic versatility of *Desulfovibrio vulgaris*. Environ. Microbiol. Rep. 10, 190–201. doi:10.1111/1758-2229.12619

Fong, S.S., Joyce, A.R., Palsson, B.Ø., 2005. Parallel adaptive evolution cultures of *Escherichia coli* lead to convergent growth phenotypes with different gene expression states. Genome Res. 15, 1365–1372.

Fuhrman, J.A., Caron, D.A., 2016. Heterotrophic Planktonic Microbes: Virus, Bacteria, Archaea, and Protozoa. doi:10.1128/9781555818821.ch4.2.2

Gallet, R., Tully, T., Evans, M.E.K., 2009. Ecological conditions affect evolutionary trajectory in a predator-prey system. Evolution (N. Y). 63, 641–651. doi:10.1111/j.1558-5646.2008.00559.x

Golding, I., Cox, E.C., 2006. Physical nature of bacterial cytoplasm. Phys. Rev. Lett. 96, 14–17. doi:10.1103/PhysRevLett.96.098102

Gray, K.M., Ruby, E.G., 1990. Prey-derived signals regulating duration of the develomental growth phase of *Bdellovibrio bacteriovorus*. J. Bacteriol. 172, 4002–4007. doi:10.1128/jb.172.7.4002-4007.1990

Green, M.R., Sambrook, J., 2012. Chapter I, Isolation and Quantification of DNA, Molecular cloning, A laborotory manual. doi:10.3724/SP.J.1141.2012.01075

Green, S.K., Schroth, M.N., Cho, J.J., Kominos, S.D., Vitanza-Jack, V.B., 1974. Agricultural Plants

and Soil as a Reservoir for *Pseudomonas aeruginosa*. Appl. Microbiol. 28, 987–991.

Guerrero, R., Pedros-Alio, C., Esteve, I., Mas, J., Chase, D., Margulis, L., 1986. Predatory prokaryotes: predation and primary consumption evolved in bacteria. Proc. Natl. Acad. Sci. U. S. A. 83, 2138–42. doi:10.1073/pnas.83.7.2138

Guerrini, F., Romano, V., Valenzi, M., Di Giulio, M., Mupo, M.R., Sacco, M., 1982. Molecular parasitism in the *Escherichia coli-Bdellovibrio bacteriovorus* system: translocation of the matrix protein from the host to the parasite outer membrane. EMBO J. 1, 1439–44.

Harikrishnan, R., Balasundaram, C., Heo, M.S., 2010. Effect of probiotics enriched diet on *Paralichthys olivaceus* infected with lymphocystis disease virus (LCDV). Fish Shellfish Immunol. 29, 868–874. doi:10.1016/j.fsi.2010.07.031

Harrison, F., 2007. Microbial ecology of the cystic fibrosis lung. Microbiology 153, 917–923. doi:10.1099/mic.0.2006/004077-0

Hawlena, D., Schmitz, O.J., 2010. Physiological Stress as a Fundamental Mechanism Linking Predation to Ecosystem Functioning. Am. Nat. 176, 537–556. doi:10.1086/656495

Heirendt, L., Arreckx, S., Pfau, T., Mendoza, S.N., Richelle, A., Heinken, A., Haraldsdóttir, H.S., Wachowiak, J., Keating, S.M., Vlasov, V., Magnusdóttir, S., Ng, C.Y., Preciat, G., Žagare, A., Chan, S.H.J., Aurich, M.K., Clancy, C.M., Modamio, J., Sauls, J.T., Noronha, A., Bordbar, A., Cousins, B.-J., El Assal, D.C., Valcarcel, L. V, Apaolaza, I., Ghaderi, S., Ahookhosh, M., Guebila, M. Ben, Kostromins, A., Sompairac, N., Le, H.M., Ma, D., Sun, Y., Wang, L., Yurkovich, J.T., Oliveira, M.A.P., Vuong, P.T., El Assal, L.P., Kuperstein, I., Zinovyev, A., Hinton, H.S., Bryant, W.A., Artacho, F.J.A., Planes, F.J., Stalidzans, E., Maass, A., Vempala, S., Hucka, M., Saunders, M.A., Maranas, C.D., Lewis, N.E., Sauter, T., Palsson, B.Ø., Thiele, I., Fleming, R.M.T., 2007. Creation and analysis of biochemical constraint-based models: the COBRA Toolbox v3.0. Nat. Protoc. 2, 1290–1307. doi:10.1038/nprot.2007.99

Herencias, C., Prieto, M.A., Martínez, V., 2017. Determination of the predatory capability of *Bdellovibrio bacteriovorus* HD100. Bio-protocol 7, 2–10. doi:10.21769/BioProtoc.2177

Hespell, R.B., 1976. Glycolytic and Tricarboxylic Acid Cycle Enzyme Activities During Intraperiplasmic Growth of *Bdellovibrio bacteriovorus* on *Escherichia coli*. J. Bacteriol. 128, 677–680.

Hespell, R.B., Miozzari, G.F., Rittenberg, S.C., 1975. Ribonucleic acid destruction and synthesis during intraperiplasmic growth of *Bdellovibrio bacteriovorus*. J. Bacteriol. 123, 481–91.

Hespell, R.B., Rosson, R. a, Thomashow, M.F., Rittenberg, S.C., 1973. Respiration of *Bdellovibrio bacteriovorus* strain 109J and its energy substrates for intraperiplasmic growth. J. Bacteriol. 113, 1280–8.

Hobley, L., King, J.R., Sockett, R.E., 2006. *Bdellovibrio* predation in the presence of decoys: Three-way bacterial interactions revealed by mathematical and experimental analyses. Appl. Environ. Microbiol. 72, 6757–6765. doi:10.1128/AEM.00844-06

Hobley, L., Lerner, T.R., Williams, L.E., Lambert, C., Till, R., Milner, D.S., Basford, S.M., Capeness, M.J., Fenton, A.K., Atterbury, R.J., Harris, M. a T.S., Sockett, R.E., 2012. Genome analysis of a simultaneously predatory and prey-independent, novel *Bdellovibrio bacteriovorus* from the River Tiber, supports in silico predictions of both ancient and recent lateral gene transfer from diverse bacteria. BMC Genomics 13, 670. doi:10.1186/1471-2164-13-670

Hori, K., Kaneko, M., Tanji, Y., Xing, X.H., Unno, H., 2002. Construction of self-disruptive *Bacillus megaterium* in response to substrate exhaustion for polyhydroxybutyrate production. Appl. Microbiol. Biotechnol. 59, 211–216. doi:10.1007/s00253-002-0986-8

Hoskins, J., Jr, W.E.A., Blaszczak, L.C., Burgett, S., Dehoff, B.S., Estrem, S.T., Fritz, L., Fu, D., Fuller, W., Geringer, C., Gilmour, R., Glass, J.S., Khoja, H., Kraft, A.R., Lagace, R.E., Blanc, D.J.L.E., Lee, L.N., Lefkowitz, E.J., Lu, J., Matsushima, P., Mcahren, S.M., Mchenney, M., Leaster, K.M.C., Mundy, C.W., Nicas, T.I., Norris, F.H., Gara, M.O., Peery, R.B., Robertson, G.T., Rockey, P., Sun, P., Winkler, M.E., Yang, Y., Young-bellido, M., Zhao, G., Zook, C.A., Baltz, R.H., Jaskunas, S.R., Jr, P.R.R., Skatrud, P.L., Glass, J.I., 2001. Genome of the Bacterium *Streptococcus pneumoniae* Strain R6. J. Bacteriol. 183, 5709–5717. doi:10.1128/JB.183.19.5709

Iebba, V., Totino, V., Santangelo, F., Gagliardi, A., Ciotoli, L., Virga, A., Ambrosi, C., Pompili, M., De Biase, R. V., Selan, L., Artini, M., Pantanella, F., Mura, F., Passariello, C., Nicoletti, M., Nencioni, L., Trancassini, M., Quattrucci, S., Schippa, S., 2014a. *Bdellovibrio bacteriovorus* directly attacks *Pseudomonas aeruginosa* and *Staphylococcus aureus* cystic fibrosis isolates. Front. Microbiol. 5, 1–9. doi:10.3389/fmicb.2014.00280

Ishiguro, E.E., 1974. Minimum nutritional requirements for growth of host-independent derivatives of *Bdellovibrio bacteriovorus* strain 109 Davis. Can. J. Microbiol. 20, 263–265. doi:10.1139/m74-041

Jacquel, N., Lo, C.W., Wei, Y.H., Wu, H.S., Wang, S.S., 2008. Isolation and purification of bacterial poly(3-hydroxyalkanoates). Biochem. Eng. J. 39, 15–27. doi:10.1016/j.bej.2007.11.029

Jurkevitch, E., 2007. Predatory Behaviors in Bacteria-Diversity and Transitions. Microbe 2, 67–73. doi:10.1128/microbe.2.67.1

Jurkevitch, E., 2006. The Genus *Bdellovibrio*, Prokariotes. doi:10.1007/0-387-30747-8_2

Jurkevitch, E., Davidov, Y., 2006. Phylogenetic Diversity and Evolution of Predatory Prokaryotes, ACS Division of Fuel Chemistry, Preprints. doi:10.1007/7171

Jurkevitch, E., Minz, D., Ramati, B., Barel, G., 2000. Prey range characterization, ribotyping, and diversity of soil and rhizosphere *Bdellovibrio* spp. isolated on phytopathogenic bacteria. Appl. Environ. Microbiol. 66, 2365–2371. doi:10.1128/AEM.66.6.2365-2371.2000

Kadouri, D., O'Toole, G.A., 2005. Susceptibility of biofilms to *Bdellovibrio bacteriovorus* attack. Appl. Environ. Microbiol. 71, 4044–4051. doi:10.1128/AEM.71.7.4044-4051.2005

Kadouri, D.E., To, K., Shanks, R.M.Q., Doi, Y., 2013. Predatory bacteria: a potential ally against multidrug-resistant Gram-negative pathogens. PLoS One 8, e63397. doi:10.1371/journal.pone.0063397

Kadouri, D.E., Tran, A., 2013. Measurement of predation and biofilm formation under different ambient oxygen conditions using a simple gasbag-based system. Appl. Environ. Microbiol. 79, 5264–5271. doi:10.1128/AEM.01193-13

Kahar, P., Agus, J., Kikkawa, Y., Taguchi, K., Doi, Y., Tsuge, T., 2005. Effective production and kinetic characterization of ultra-high-molecular- weight poly[(R)-3-hydroxybutyrate] in recombinant *Escherichia coli*. Polym. Degrad. Stab. 87, 161–169. doi:10.1016/j.polymdegradstab.2004.08.002

Karunker, I., Rotem, O., Dori-Bachash, M., Jurkevitch, E., Sorek, R., 2013. A Global Transcriptional Switch between the Attack and Growth Forms of *Bdellovibrio bacteriovorus*. PLoS One 8, e61850. doi:10.1371/journal.pone.0061850

Kerem, B., Rommens, J.M., Buchanan, J.A., Markiewicz, D., Cox, T.K., Chakravarti, A., Buchwald, M., Tsui, L., 1989. Identification of the Cystic Fibrosis Gene: Genetic Analysis. Science (80-.). 245, 1073–1080.

King, Z.A., Lu, J., Dräger, A., Miller, P., Federowicz, S., Lerman, J.A., Ebrahim, A., Palsson, B.O., Lewis, N.E., 2016. BiGG Models: A platform for integrating, standardizing and sharing genome-scale models. Nucleic Acids Res. 44, D515–D522. doi:10.1093/nar/gkv1049

Kobayashi, D.Y., Reedy, R.M., Palumbo, J.D., Zhou, J.-M., Yuen, G.Y., 2005. A clp Gene

Homologue Belonging to the Crp Gene Family Globally Regulates Lytic Enzyme Production, Antimicrobial Activity, and Biological Control Activity Expressed by *Lysobacter* enzymogenes Strain C3 †. Appl. Environ. Microbiol. 71, 261–269. doi:10.1128/AEM.71.1.261-269.2005

Koval, S.F., Hynes, S.H., 1991. Effect of paracrystalline protein surface layers on predation by *Bdellovibrio bacteriovorus*. J. Bacteriol. 173, 2244–2249.

Koval, S.F., Hynes, S.H., Flannagan, R.S., Pasternak, Z., Davidov, Y., Jurkevitch, E., 2013. *Bdellovibrio exovorus* sp. nov., a novel predator of *Caulobacter crescentus*. Int. J. Syst. Evol. Microbiol. 63, 146–151. doi:10.1099/ijs.0.039701-0

Kuenen, J.G., Rittenberg, S.C., 1975. Incorporation of long-chain fatty acids of the substrate organism by *Bdellovibrio bacteriovorus* during intraperiplasmic growth. J. Bacteriol. 121, 1145–57.

LaMarre, a G., Straley, S.C., Conti, S.F., 1977. Chemotaxis toward amino acids by *Bdellovibrio bacteriovorus*. J. Bacteriol. 131, 201–7.

Lambert, C., Evans, K.J., Till, R., Hobley, L., Capeness, M., Rendulic, S., Schuster, S.C., Aizawa, S.I., Sockett, R.E., 2006a. Characterizing the flagellar filament and the role of motility in bacterial prey-penetration by *Bdellovibrio bacteriovorus*. Mol. Microbiol. 60, 274–286. doi:10.1111/j.1365-2958.2006.05081.x

Lambert, C., Hobley, L., Chang, C.-Y., Fenton, A., Capeness, M., Sockett, L., 2009. A predatory patchwork: membrane and surface structures of *Bdellovibrio bacteriovorus*. Advances in microbial physiology. doi:10.1016/S0065-2911(08)00005-2

Lambert, C., Morehouse, K. a, Chang, C.-Y., Sockett, R.E., 2006b. *Bdellovibrio*: growth and development during the predatory cycle. Curr. Opin. Microbiol. 9, 639–44. doi:10.1016/j.mib.2006.10.002

Lambert, C., Smith, M.C.M., Sockett, R.E., 2003. A novel assay to monitor predator-prey interactions for *Bdellovibrio bacteriovorus* 109 J reveals a role for methyl-accepting chemotaxis proteins in predation. Environ. Microbiol. 5, 127–132. doi:10.1046/j.1462-2920.2003.00385.x

Lambert, C., Socket, R.E., 2008. Laboratory maintenance of *Bdellovibrio*. Curr. Protoc. Microbiol. 1–13. doi:10.1002/9780471729259.mc07b02s9

Lerner, T.R., Lovering, A.L., Bui, N.K., Uchida, K., Aizawa, S.I., Vollmer, W., Sockett, R.E., 2012.

Specialized peptidoglycan hydrolases sculpt the intra-bacterial niche of predatory *Bdellovibrio* and increase population fitness. PLoS Pathog. 8. doi:10.1371/journal.ppat.1002524

Lewis, N.E., Nagarajan, H., Palsson, B.O., 2012. Constraining the metabolic genotype-phenotype relationship using a phylogeny of in silico methods. Nat. Rev. Microbiol. 10, 291–305. doi:10.1038/nrmicro2737

Li, H., Chen, C., Sun, Q., Liu, R., Cai, J., 2014a. *Bdellovibrio* and like organisms enhanced growth and survival of *Penaeus monodon* and altered bacterial community structures in its rearing water. Appl. Environ. Microbiol. 80, 6346–6354. doi:10.1128/AEM.01737-14

Li, S., Sun, L., Wu, H., Hu, Z., Liu, W., Li, Y., Wen, X., 2012. The intestinal microbial diversity in mud crab (*Scylla paramamosain*) as determined by PCR-DGGE and clone library analysis. J. Appl. Microbiol. 113, 1341–1351. doi:10.1111/jam.12008

Liao, Y.C., Huang, T.W., Chen, F.C., Charusanti, P., Hong, J.S.J., Chang, H.Y., Tsai, S.F., Palsson, B.O., Hsiung, C.A., 2011. An experimentally validated genome-scale metabolic reconstruction of *Klebsiella pneumoniae* MGH 78578, iYL1228. J. Bacteriol. 193, 1710–1717. doi:10.1128/JB.01218-10

Lin, B., Chen, S., Cao, Z., Lin, Y., Mo, D., Zhang, H., Gu, J., Dong, M., Liu, Z., Xu, A., 2007. Acute phase response in zebrafish upon *Aeromonas salmonicida* and *Staphylococcus aureus* infection: Striking similarities and obvious differences with mammals. Mol. Immunol. 44, 295–301. doi:10.1016/j.molimm.2006.03.001

Lin, D.M., Koskella, B., Lin, H.C., 2017. Phage therapy: An alternative to antibiotics in the age of multi-drug resistance. World J. Gastrointest. Pharmacol. Ther. doi:10.4292/wjgpt.v8.i3.162

Livak, K.J., Schmittgen, T.D., 2001. Analysis of relative gene expression data using real-time quantitative PCR and the 2(-Delta Delta C(T)) Method. Methods 25, 402–8. doi:10.1006/meth.2001.1262

Loozen, G., Boon, N., Pauwels, M., Slomka, V., Rodrigues Herrero, E., Quirynen, M., Teughels, W., 2015. Effect of *Bdellovibrio bacteriovorus* HD100 on multispecies oral communities. Anaerobe 35, 45–53. doi:10.1016/j.anaerobe.2014.09.011

López-Causapé, C., de Dios-Caballero, J., Cobo, M., Escribano, A., Asensio, Ó., Oliver, A., del Campo, R., Cantón, R., Solé, A., Cortell, I., Asensio, O., García, G., Martínez, M.T., Cols, M., Salcedo, A., Vázquez, C., Baranda, F., Girón, R., Quintana, E., Delgado, I., de Miguel, M.Á.,

García, M., Oliva, C., Prados, M.C., Barrio, M.I., Pastor, M.D., Olveira, C., de Gracia, J., Álvarez, A., Escribano, A., Castillo, S., Figuerola, J., Togores, B., Oliver, A., López, C., de Dios Caballero, J., Tato, M., Máiz, L., Suárez, L., Cantón, R., 2017. Antibiotic resistance and population structure of cystic fibrosis *Pseudomonas aeruginosa* isolates from a Spanish multi-centre study. Int. J. Antimicrob. Agents 50, 334–341. doi:10.1016/j.ijantimicag.2017.03.034

Lu, F., Cai, J., 2010. The protective effect of *Bdellovibrio*-and-like organisms (BALO) on tilapia fish fillets against *Salmonella enterica* spp. enterica serovar Typhimurium. Lett. Appl. Microbiol. 51, 625–631. doi:10.1111/j.1472-765X.2010.02943.x

Lyczak, J.B., Cannon, C.L., Pier, G.B., 2002. Lung Infections Associated with Cystic Fibrosis. Clin. Microbiol. Rev. 15, 194–222. doi:10.1128/CMR.15.2.194-222.2002

Lyczak, J.B., Cannon, C.L., Pier, G.B., 2000. Establishment of *Pseudomonas aeruginosa* infection: Lessons from a versatile opportunist. Microbes Infect. 2, 1051–1060. doi:10.1016/S1286-4579(00)01259-4

Madkour, M.H., Heinrich, D., Alghamdi, M. a, Shabbaj, I.I., Steinbüchel, A., 2013. PHA Recovery from Biomass. Biomacromolecules. doi:10.1021/bm4010244

Mahadevan, R., Bond, D.R., Butler, ‡ J E, Esteve-Nuñez, A., Coppi, M. V, Palsson, B.O., Schilling, C.H., Lovley, D.R., 2006. Characterization of Metabolism in the Fe(III)-Reducing Organism *Geobacter sulfurreducens* by Constraint-Based Modeling †. Appl. Environ. Microbiol. 72, 1558–1568. doi:10.1128/AEM.72.2.1558-1568.2006

Mahmoud, K.K., McNeely, D., Elwood, C., Koval, S.F., 2007. Design and performance of a 16S rRNA-targeted oligonucleotide probe for detection of members of the genus *Bdellovibrio* by fluorescence in situ hybridization. Appl. Environ. Microbiol. 73, 7488–93. doi:10.1128/AEM.01112-07

Mahmoud, K.K., McNeely, D., Elwood, C., Koval, S.F., 2007. Design and performance of a 16S rRNA-targeted oligonucleotide probe for detection of members of the genus *Bdellovibrio* by fluorescence in situ hybridization. Appl. Environ. Microbiol. 73, 7488–7493. doi:10.1128/AEM.01112-07

Margulis, L., 1996. Archaeal-eubacterial mergers in the origin of Eukarya: phylogenetic classification of life. Proc. Natl. Acad. Sci. U. S. A. 93, 1071–1076. doi:10.1073/pnas.93.3.1071

Martin, M.O., 2002. Predatory prokaryotes: an emerging research opportunity. J. Mol. Microbiol. Biotechnol. 4, 467–477.

Martínez, V., de la Peña, F., García-Hidalgo, J., de la Mata, I., García, J.L., Prieto, M.A., 2012. Identification and biochemical evidence of a medium-chain-length polyhydroxyalkanoate depolymerase in the *Bdellovibrio bacteriovorus* predatory hydrolytic arsenal. Appl. Environ. Microbiol. 78, 6017–26. doi:10.1128/AEM.01099-12

Martínez, V., García, P., García, J.L., Prieto, M.A., 2011. Controlled autolysis facilitates the polyhydroxyalkanoate recovery in *Pseudomonas putida* KT2440. Microb. Biotechnol. 4, 533–47. doi:10.1111/j.1751-7915.2011.00257.x

Martínez, V., Herencias, C., Jurkevitch, E., Auxiliadora Prieto, M., 2016. Engineering a predatory bacterium as a proficient killer agent for intracellular bio- products recovery: The case of the polyhydroxyalkanoates. Nat. Publ. Gr. doi:10.1038/srep24381

Martínez, V., Jurkevitch, E., García, J.L., Prieto, M.A., 2013. Reward for *Bdellovibrio bacteriovorus* for preying on a polyhydroxyalkanoate producer. Environ. Microbiol. doi:10.1111/1462-2920.12047

Matin, a, Rittenberg, S.C., 1972. Kinetics of deoxyribonucleic acid destruction and synthesis during growth of *Bdellovibrio bacteriovorus* strain 109D on *Pseudomonas putida* and *Escherichia coli*. J. Bacteriol. 111, 664–73.

McBride, M.J., 2004. Cytophaga-flavobacterium gliding motility. J. Mol. Microbiol. Biotechnol. 7, 63–71. doi:10.1159/000077870

Mcbride, Mark J, Zusman, D.R., 1996. Behavioral analysis of single cells of *Myxococcus xanthus* in response to prey cells of *Escherichia coli,* FEMS Microbiology Letters. doi:10.1111/j.1574-6968.1996.tb08110.x

Medina, A.A., Kadouri, D.E., 2009. Biofilm formation of *Bdellovibrio bacteriovorus* host-independent derivatives. Res. Microbiol. 160, 224–231. doi:10.1016/j.resmic.2009.02.001

Moldes, C., García, P., García, J.L., Prieto, M.A., 2004. In vivo immobilization of fusion proteins on bioplastics by the novel tag BioF. Appl. Environ. Microbiol. 70, 3205–3212. doi:10.1128/AEM.70.6.3205-3212.2004

Monk, J., Nogales, J., Palsson, B.O., 2014. Optimizing genome-scale network reconstructions. Nat. Biotechnol. doi:10.1038/nbt.2870

Monnappa, A.K., Dwidar, M., Seo, J.K., Hur, J.H., Mitchell, R.J., 2014. *Bdellovibrio bacteriovorus* inhibits *Staphylococcus aureus* biofilm formation and invasion into human epithelial cells. Sci Rep 4, 3811. doi:10.1038/srep03811

Moran, N.A., 2002. Minireview Microbial Minimalism: Genome Reduction in Bacterial Pathogens, Cell.

Müller, F.D., Beck, S., Strauch, E., Linscheid, M.W., 2011. Bacterial predators possess unique membrane lipid structures. Lipids 46, 1129–40. doi:10.1007/s11745-011-3614-5

Negus, D., Moore, C., Baker, M., Raghunathan, D., Tyson, J., Sockett, R.E., 2017. Predator Versus Pathogen : How Does Predatory *Bdellovibrio bacteriovorus* Interface with the Challenges of Killing Gram-Negative Pathogens in a Host Setting ? Annu. Rev. Microbiol. 71, 441–457.

Nelson, E.H., Matthews, C.E., Rosenheim, J.A.Y.A., 2004. Predators Reduce Prey Population Growth by Inducing Changes in Prey Behavior Authors (s): Erik H . Nelson , Christopher E . Matthews and Jay A . Rosenheim Published by : Wiley Stable URL : http://www.jstor.org/stable/3450359 REFERENCES Linked references 85, 1853–1858.

Neto, F.C., Pilon, A.C., Selegato, D.M., Freire, R.T., Gu, H., Raftery, D., Lopes, N.P., Castro-Gamboa, I., 2016. Dereplication of Natural Products Using GC-TOF Mass Spectrometry: Improved Metabolite Identification by Spectral Deconvolution Ratio Analysis. Front. Mol. Biosci. 3, 1–13. doi:10.3389/fmolb.2016.00059

Nguyen, N.-A.T., Sallans, L., Kaneshiro, E.S., 2008. The major glycerophospholipids of the predatory and parasitic bacterium *Bdellovibrio bacteriovorus* HID5. Lipids 43, 1053–63. doi:10.1007/s11745-008-3235-9

Nielsen, J., 2017. Systems Biology of Metabolism. Annu. Rev. Biochem. 86, 245–275. doi:10.1146/annurev-biochem-061516-044757

Nogales, J., Agudo, L., 2015. A Practical Protocol for Integration of Transcriptomics Data into Genome-Scale Metabolic Reconstructions. Hydrocarb. Lipid Microbiol. Protoc. - Springer Protoc. Handbooks 135–152. doi:10.1007/8623

Nogales, J., Gudmundsson, S., Duque, E., Luis Ramos, J., Putida, P., 2017. Expanding the computable reactome in *Pseudomonas putida* reveals metabolic cycles providing robustness. 2 3 Running Head: Metabolic Robustness Cycles in. BioRxiv May. doi:10.1101/139121

O ’brien, E.J., Monk, J.M., Palsson, B.O., 2015. Using Genome-Scale Models to Predict Biological

Capabilities. Cell 161, 971–987. doi:10.1016/j.cell.2015.05.019

Ogata, H., Goto, S., Sato, K., Fujibuchi, W., Bono, H., Kanehisa, M., 1999. KEGG: Kyoto encyclopedia of genes and genomes. Nucleic Acids Res. 27, 29–34. doi:10.1093/nar/27.1.29

Orth, J.D., 2010. What is flux balance analysis? Nat. Biotechnol. 28, 245–248. doi:doi:10.1038/nbt.1614

Orth, J.D., Conrad, T.M., Na, J., Lerman, J.A., Nam, H., Feist, A.M., Palsson, B.Ø., 2011. A comprehensive genome-scale reconstruction of *Escherichia coli* metabolism—2011. Mol. Syst. Biol. 7, 535. doi:10.1038/msb.2011.65

Otto, S., Harms, H., Wick, L.Y., 2017. Effects of predation and dispersal on bacterial abundance and contaminant biodegradation. FEMS Microbiol. Ecol. 93, 241. doi:10.1093/femsec/fiw241

Pasternak, Z., Njagi, M., Shani, Y., Chanyi, R., Rotem, O., Lurie-Weinberger, M.N., Koval, S., Pietrokovski, S., Gophna, U., Jurkevitch, E., 2013. In and out: an analysis of epibiotic vs periplasmic bacterial predators. ISME J. 1–11. doi:10.1038/ismej.2013.164

Pernthaler, J., 2005. Predation on prokaryotes in the water column and its ecological implications. Nat. Rev. Microbiol. 3, 537–546. doi:10.1038/nrmicro1252

Piñeiro, S.A., Williams, H.N., Stine, O.C., 2008. Phylogenetic relationships amongst the saltwater members of the genus *Bacteriovorax* using *rpoB* sequences and reclassification of *Bacteriovorax stolpii* as Bacteriolyticum stolpii gen. nov., comb. nov. Int. J. Syst. Evol. Microbiol. 58, 1203–1209. doi:10.1099/ijs.0.65710-0

Placzek, S., Schomburg, I., Chang, A., Jeske, L., Ulbrich, M., Tillack, J., Schomburg, D., 2017. BRENDA in 2017: New perspectives and new tools in BRENDA. Nucleic Acids Res. 45, D380–D388. doi:10.1093/nar/gkw952

Prieto, A., Escapa, I.F., Martínez, V., Dinjaski, N., Herencias, C., de la Peña, F., Tarazona, N., Revelles, O., 2016. A holistic view of polyhydroxyalkanoate metabolism in *Pseudomonas putida*. Environ. Microbiol. 18, 341–57. doi:10.1111/1462-2920.12760

Rafeeq, M.M., Murad, H.A.S., 2017. Cystic fibrosis: Current therapeutic targets and future approaches. J. Transl. Med. 15, 1–9. doi:10.1186/s12967-017-1193-9

Rendulic, S., Jagtap, P., Rosinus, A., Eppinger, M., Baar, C., Lanz, C., Keller, H., Lambert, C., Evans,

K.J., Goesmann, A., Meyer, F., Sockett, R.E., Schuster, S.C., 2004. A predator unmasked: life cycle of *Bdellovibrio bacteriovorus* from a genomic perspective. Science 303, 689–92. doi:10.1126/science.1093027

Resch, S., Gruber, K., Wanner, G., Slater, S., Dennis, D., Lubitz, W., 1998. Aqueous release and purification of poly(β-hydroxybutyrate) from *Escherichia coli*. J. Biotechnol. 65, 173–182. doi:10.1016/S0168-1656(98)00127-8

Rittenberg, S.C., Langley, D., 1975. Utilization of nucleoside monophosphates *per se* for intraperiplasmic growth of *Bdellovibrio bacteriovorus*. J. Bacteriol. 121, 1137–44.

Roca, I., Akova, M., Baquero, F., Carlet, J., Cavaleri, M., Coenen, S., Cohen, J., Findlay, D., Gyssens, I., Heure, O.E., Kahlmeter, G., Kruse, H., Laxminarayan, R., Liébana, E., López-Cerero, L., Macgowan, A., Martins, M., Rodríguez-Baño, J., Rolain, J.-M., Segovia, C., Sigauque, B., Taconelli, E., Wellington, E., Vila, J., 2015. The global threat of antimicrobial resistance: science for intervention. New Microbes New Infect. 6, 22–29. doi:10.1016/j.nmni.2015.02.007

Rogosky, A.M., Moak, P.L., Emmert, E. a B., 2006. Differential predation by *Bdellovibrio bacteriovorus* 109J. Curr. Microbiol. 52, 81–5. doi:10.1007/s00284-005-0038-6

Roschanski, N., Klages, S., Reinhardt, R., Linscheid, M., Strauch, E., 2011. Identification of genes essential for prey-independent growth of *Bdellovibrio bacteriovorus* HD100. J. Bacteriol. 193, 1745–1756. doi:10.1128/JB.01343-10

Ruby, E.G., McCabe, J.B., Barke, J.I., 1985. Uptake of intact nucleoside monophosphates by *Bdellovibrio bacteriovorus* 109J. J. Bacteriol. 163, 1087–94.

Russo, R., Chae, R., Mukherjee, S., Singleton, E., Occi, J., Kadouri, D., Connell, N., 2015. Susceptibility of Select Agents to Predation by Predatory Bacteria. Microorganisms 3, 903–912. doi:10.3390/microorganisms3040903

Santajit, S., Indrawattana, N., 2016. Mechanisms of Antimicrobial Resistance in ESKAPE Pathogens. Biomed Res. Int. 2016. doi:10.1155/2016/2475067

Schaaper, R.M., 1993. Base selection, proofreading, and mismatch repair during DNA replication in *Escherichia coli*. J. Biol. Chem. 268, 23762–23765. doi:10.1074/jbc.274.3.1306

Schäfer, a, Tauch, A., Jäger, W., Kalinowski, J., Thierbach, G., Pühler, A., 1994. Small mobilizable multi-purpose cloning vectors derived from the *Escherichia coli* plasmids pK18 and pK19: selection of defined deletions in the chromosome of *Corynebacterium glutamicum*. Gene

145, 69–73.

Schellenberger, J., Que, R., Fleming, R.M.T., Thiele, I., Orth, J.D., Feist, A.M., Zielinski, D.C., Bordbar, A., Lewis, N.E., Rahmanian, S., Kang, J., Hyduke, D.R., Palsson, B., 2011. Quantitative prediction of cellular metabolism with constraint-based models: The COBRA Toolbox v2.0. Nat. Protoc. 6, 1290–1307. doi:10.1038/nprot.2011.308

Schelling, M., Conti, S., 1986. Host receptor sites involved in the attachment of *Bdellovibrio bacteriovorus* and *Bdellovibrio stolpii*. FEMS Microbiol. Lett. 36, 319–323. doi:10.1111/j.1574-6968.1986.tb01718.x

Scherff, R.H., 2AD. Control of bacterial blight of soybean by *Bdellovibrio bacteriovorus*. Phytopathology 63, 400–402.

Scheubert, K., Hufsky, F., Petras, D., Wang, M., Nothias, L.F., Dührkop, K., Bandeira, N., Dorrestein, P.C., Böcker, S., 2017. Significance estimation for large scale metabolomics annotations by spectral matching. Nat. Commun. 8. doi:10.1038/s41467-017-01318-5

Schmidt, B.J., Ebrahim, A., Metz, T.O., Adkins, J.N., Palsson, B.Ø., Hyduke, D.R., 2013. Systems biology GIM^{3}E: condition-specific models of cellular metabolism developed from metabolomics and expression data. Bioinfo 29, 2900–2908. doi:10.1093/bioinformatics/btt493

Schoeffield, A.J., 1996. A Comparison of the Survival of Intraperiplasmic and Attack Phase *Bdellovibrios* with Reduced Oxygen. Microb. Ecol. 35–46.

Schwudke, D., Linscheid, M., Strauch, E., Appel, B., Zahringer, U., Moll, H., Muller, M., Brecker, L., Gronow, S., Lindner, B., 2003. The obligate predatory Bdellovibrio bacteriovorus possesses a neutral lipid A containing alpha-D-Mannoses that replace phosphate residues: similarities and differences between the lipid As and the lipopolysaccharides of the wild type strain *B. bacteriovorus* J. Biol. Chem. 278, 27502–12. doi:10.1074/jbc.M303012200

Schwudke, D., STRAUCH, E., KRUEGER, M., APPEL, B., 2001. Taxonomic Studies of Predatory *Bdellovibrios* Based on 16S rRNA Analysis, Ribotyping and the *hit* Locus and Characterization of Isolates from the Gut of Animals. Syst. Appl. Microbiol. 24, 385–394.

Seidler, R.J., Starr, M., 1969. Isolation and Characterization of Host-Independent *Bdellovibrios.* J. Bacteriol. 100, 769–785.

Seidler, R.J., Starr, M.P., Mandel, M., 1969. Deoxyribonucleic acid characterization of Bdellovibrios. J. Bacteriol. 100, 786–90.

Shanks, R.M.Q., Davra, V.R., Romanowski, E.G., Brothers, K.M., Stella, N. a, Godboley, D., Kadouri, D.E., 2013. An Eye to a Kill: Using Predatory Bacteria to Control Gram-Negative Pathogens Associated with Ocular Infections. PLoS One 8, e66723. doi:10.1371/journal.pone.0066723

Shatzkes, K., Chae, R., Tang, C., Ramirez, G.C., Mukherjee, S., Tsenova, L., Connell, N.D., Kadouri, D.E., 2015. Examining the safety of respiratory and intravenous inoculation of *Bdellovibrio bacteriovorus* and *Micavibrio aeruginosavorus* in a mouse model. Nat. Publ. Gr. 1–12. doi:10.1038/srep12899

Shemesh, Y., Jurkevitch, E., 2004. Plastic phenotypic resistance to predation by *Bdellovibrio* and like organisms in bacterial prey. Environ. Microbiol. 6, 12–18. doi:10.1046/j.1462-2920.2003.00530.x

Shilo, B.Y.M., Bruff, B., Bacteriology, D., Calqorrnia, U., 1965. Lysis of Gram-Negative Bacteria by Host = Independent Ectoparasitic *Bdellovibrio bacteriovorus* Isolates. J. gen. Microbiol. 40, 317–328.

Sibley, C.D., Surette, M.G., 2011. The polymicrobial nature of airway infections in cystic fibrosis: Cangene Gold Medal LectureThis article is based on a presentation by Dr. Christopher Sibley at the 60th Annual Meeting of the Canadian Society of Microbiologists in Hamilton, Ontario, on 15. Can. J. Microbiol. 57, 69–77. doi:10.1139/W10-105

Sockett, R.E., 2009a. Predatory lifestyle of *Bdellovibrio bacteriovorus*. Annu. Rev. Microbiol. 63, 523–539. doi:10.1146/annurev.micro.091208.073346

Sockett, R.E., Lambert, C., 2004. *Bdellovibrio* as therapeutic agents: a predatory renaissance? Nat. Rev. Microbiol. 2, 669–675. doi:10.1038/nrmicro959

Stolp, H., Starr, M.P., 1963. *Bdellovibrio bacteriovorus* gen. etsp. n., a predatory, ectoparasitic, and bacteriolytic microorganism. Antonie Van Leeuwenhoek 29, 217–248.

Straley, S.C., Conti, S.F., 1974. Chemotaxis in *Bdellovibrio bacteriovorus*. Jo 120, 549–551.

Straley, S.C., LaMarre, A.G., Lawrence, L.J., Conti, S.F., 1979. Chemotaxis of *Bdellovibrio bacteriovorus* toward pure compounds. J. Bacteriol. 140, 634–642.

Strittmatter, W., Weckesser, J., Salimath, P. V, Galanosl, A.C., 1983. Nontoxic Lipopolysaccharide from *Rhodopseudomonas sphaeroides* ATCC 17023, JOURNAL OF BACTERIOLOGY.

Sudesh, K., Bhubalan, K., Chuah, J.-A., Kek, Y.-K., Kamilah, H., Sridewi, N., Lee, Y.-F., 2011.

Synthesis of polyhydroxyalkanoate from palm oil and some new applications. Appl. Microbiol. Biotechnol. 89, 1373–86. doi:10.1007/s00253-011-3098-5

Sun, J., Sayyar, B., Butler, J.E., Pharkya, P., Fahland, T.R., Famili, I., Schilling, C.H., Lovley, D.R., Mahadevan, R., 2009. Genome-scale constraint-based modeling of *Geobacter metallireducens*. BMC Syst. Biol. 3, 15. doi:10.1186/1752-0509-3-15

Thiele, I., Palsson, B., 2010. A protocol for generating a high-quality genome-scale metabolic reconstruction. Nat Protoc 5, 93–121. doi:10.1038/nprot.2009.203.A

Thingstad, T.F., 2000. Elements of a theory for the mechanisms controlling abundance, diversity, and biogeochemical role of lytic bacterial viruses in aquatic systems - Thingstad - 2000 - Limnology and Oceanography - Wiley Online Library. Limnol. Oceanogr. 45, 1320–1328.

Thomashow, M.F., Rittenberg, S.C., 1978. Penicillin-induced formation of osmotically stable spheroplasts in nongrowing *Bdellovibrio bacteriovorus.* J. Bacteriol. 133, 1484–91.

Thompson, J.N., 1999. The evolution of species interactions. Sci. (washingt. D C) 284, 2116–2118. doi:10.1126/science.284.5423.2116

Tudor, J.J., Davis, J.J., Panichella, M., Zwolak, A., 2008. Isolation of predation-deficient mutants of *Bdellovibrio bacteriovorus* by using transposon mutagenesis. Appl. Environ. Microbiol. 74, 5436–5443. doi:10.1128/AEM.00256-08

Van Essche, M., Sliepen, I., Loozen, G., Van Eldere, J., Quirynen, M., Davidov, Y., Jurkevitch, E., Boon, N., Teughels, W., 2009. Development and performance of a quantitative PCR for the enumeration of *Bdellovibrionaceae*. Environ. Microbiol. Rep. 1, 228–233. doi:10.1111/j.1758-2229.2009.00034.x

Varma, A., Palsson, B., 1993. Metabolic Capabilities of *Escherichia coli:* I. Synthesis of biosynthetic precursors and cofactors. J ournal Theor. Biol. 165, 477–502.

Varma, A., Palsson, B. 0, 1994. Stoichiometric Flux Balance Models Quantitatively Predict Growth and Metabolic By-Product Secretion in Wild-Type *Escherichia coli* W3110. Appl. Environ. Microbiol. 3724–3731.

Varon, M., M. Shilo, 1969. Interaction of *Bdellovibrio bacteriovorus* and Host Bacteria. J. Bacteriol. 99, 136–141.

Vendeville, A. s, Lariviere, D., Fourmentin, E., 2011. An inventory of the bacterial macromolecular components and their spatial organization. FEMS Microbiol. Rev. 35, 395–

414. doi:10.1111/j.1574-6976.2010.00254.x

Vermeij, G.J., 1994. The Evolutionary Interaction Among Species: Selection, Escalation, and Coevolution. Annu. Rev. Ecol. Syst. 25, 219–236. doi:10.1146/annurev.es.25.110194.001251

Wan, C., Yang, X., Lee, D.J., Liu, X., Sun, S., 2014. Partial nitrification using aerobic granule continuous-flow reactor: Operations and microbial community. J. Taiwan Inst. Chem. Eng. 45, 2681–2687. doi:10.1016/j.jtice.2014.08.009

Weissbrodt, D.G., Shani, N., Holliger, C., 2014. Linking bacterial population dynamics and nutrient removal in the granular sludge biofilm ecosystem engineered for wastewater treatment. FEMS Microbiol. Ecol. 88, 579–595. doi:10.1111/1574-6941.12326

Westergaard, J.M., Kramer, T.T., 1977. *Bdellovibrio* and the intestinal flora of vertebrates. Appl. Environ. Microbiol. 34, 506–511.

Williams, P.A., Worsey, M.J., 1976. Ubiquity of plasmids in coding for toluene and xylene metabolism in soil bacteria: evidence for the existence of new TOL plasmids. J. Bacteriol. 125, 818–828.

Winstanley, C., O'brien, S., Brockhurst, M.A., 2016. *Pseudomonas aeruginosa* Evolutionary Adaptation and Diversification in Cystic Fibrosis Chronic Lung Infections. Trends Microbiol. 24, 327–337. doi:10.1016/j.tim.2016.01.008

Wurtzel, O., Dori-Bachash, M., Pietrokovski, S., Jurkevitch, E., Sorek, R., Ben-Jacob, E., 2010. Mutation Detection with Next-Generation Resequencing through a Mediator Genome. PLoS One 5. doi:10.1371/journal.pone.0015628

Yu, J.U.N., Hederstedt, L., 1995. The cytochrome bc complex (menaquinone : cytochrome c reductase) in *Bacillus subtilis* has a nontraditional subunit organization . J. Bacteriol. 177, 6751–6760.

Zhang, Y.-H.P., 2011. Substrate channeling and enzyme complexes for biotechnological applications. Biotechnol. Adv. 29, 715–725. doi:10.1016/j.biotechadv.2011.05.020

Zheng, G., Wang, C., Williams, H.N., Pineiro, S.A., 2008. Development and evaluation of a quantitative real-time PCR assay for the detection of saltwater *Bacteriovorax*. Environ. Microbiol. 10, 2515–2526. doi:10.1111/j.1462-2920.2008.01676.x

Zhou, Q., Li, K., Jun, X., Bo, L., 2009. Role and functions of beneficial microorganisms in

sustainable aquaculture. Bioresour. Technol. 100, 3780–3786. doi:10.1016/j.biortech.2008.12.037

Zimmerman, S.B., Trach, S. 0, 1991. Estimation of Macromolecule Concentrations and Excluded Volume Effects for the Cytoplasm of *Escherichia coli*. J. Mol. Bid 222, 599–620.

XIV. ANNEXX

ANNEX 1. PREY RANGE OF *BDELLOVIBRIO* AND LIKE ORGANISMS*

***Bdellovibrio* species**	**Susceptible prey**
B. bacteriovorus HD100	*E. coli* S17-1, *E. coli* ML35, *E. coli* strain RP3098, *E. coli* K12, *E. coli* SB3, *E. coli* 0157, *E. coli* B, *E. coli* strain MG1655, *Aggregatibacter actinomycetemcomitans*, *Aquaspirillum serpens* VHL, *Pseudomonas fluorescens*, *Pseudomonas putida*, *Pseudomonas aeruginosa*, *Pseudomonas tolaasii*, *Alcaligenes faecalis*, *Erwinia amylovora*, *Erwinia caratovora*, *S. typhimurium*, *Salmonella Enteritidis* P125109, *Shigella dysenteriae*, *Vibrio cholerae*, *Campylobacter jejuni* 4, *C. jejuni* 5, *Helicobacter pylori*, *Eikenella corrodens*, *Porphyromonas gingivalis*, *Capnocytophaga sputigena, Prevotella intermedia*, *Fusobacterium nucleatum*, *Serratia marcescens*, *Aeromonas hydrophila* ATCC 7966, *Yersinia pestis*, *S. aureus*, *K. pneumoniae* ATCC 43816, *Shigella flexneri*, *K. pneumoniae* KPC.
B. bacteriovorus 109J	*Pseudomonas fluorescens* SBW25, *P. fluorescens* PIC 105, *Pseudomonas aeruginosa* ATCC BAA-427, *P. aeruginosa* ATCC 10145, *Pseudomonas syringae*, *Pseudomonas putida* PIC 107, *E. coli* ML35, *E. coli* strain ZK2686, *E. coli* SM10-λpir, *E. coli* ZK1056, *E. coli* K-12, *E. coli* S17-1, *E. coli* strain WM3064, *E. coli* nonflagellate strain DFB225, *E. coli* PIC 336, *E. coli* DH5α, *Aquaspirillum serpens* VHL, *Acinetobacter* species ATCC 49466, *Acinetobacter* species ATCC 10153, *Acinetobacter baumannii* ATCC 19606, *A. baumannii* NCIMB 12457, *A. baumannii* ATCC BAA-747, *A. baumannii* NCIMB 12457, *Acinetobacter calcoaceticus* PIC 346, *Acinetobacter haemolyticus* ATCC 19002, *Acinetobacter lwoffii* ATCC 15309, *A. lwoffii* ATCC 17925, *Aeromonas hydrophila* PIC 191, *Aeromonas salmonicida* ATCC 33658, *Bordetella bronchiseptica* PIC 402, *Burkholderia cepacia*, *Burkholderia mallei, Campylobacter jejuni* ATCC 29428, *C. jejuni* ATCC BAA-1153, *Citrobacter freundii* NCTC 9750, *C. freundii* ATCC 43864, *C. freundii* ATCC 8090, *Enterobacter aerogenes* ATCC 13048, *E. aerogenes* ATCC 35029, *E. aerogenes* ATCC 51697, *E. aerogenes* NCIMB, *Enterobacter amnigenus* ATCC 51816, *Enterobacter cloacae* ATCC 700323, *E. cloacae* ATCC 35030, *E. cloacae* ATCC 49141, *Enterobacter gergoviae* ATCC 33028, *Enterococcus faecalis* PIC 522B, *Klebsiella pneumoniae* ATCC 33495, *K. pneumoniae* ATCC BAA-1706, *K. pneumoniae* ATCC BAA-1705, *K. pneumoniae* ATCC 43816, *K. pneumoniae* ATCC 13883, *K. pneumoniae* 6 clinical isolates, *Listonella anguillarum* ATCC 14181, *Morganella morganii* ATCC 25829, *M. morganii* ATCC 25830, *M. morganii* PIC 329, *Proteus mirabilis* ATCC 35659, *P. mirabilis* ATCC 43071, *P. mirabilis* ATCC 25933, *P. mirabilis* NCIMB 13283, *P. mirabilis* ATCC 7002, *P. mirabilis* PIC 366, *Proteus morganii* PIC 3661, *Proteus rettgeri* ATCC 9250, *Proteus vulgaris* ATCC 33420, *P. vulgaris* ATCC 49132, *P. vulgaris* ATCC 8427, *P. vulgaris* NCTC 4636, *P. vulgaris* PIC 365, *Salmonella enterica* PIC 371, *Serratia marcescens* PIC 361, *Shigella flexneri* PIC 387, *Shigella sonnei* PIC 388, *Yersinia pestis*, *Yersinia enterocolitica* PIC 330, *Yersinia pseudotuberculosys* PIC 399, *Vibrio angulara* PIC 232, *Vibrio cholerae* EL Tor, PIC 234, *Aggregatibacter actinomycetemcomitans, Eikenella corrodens*, *Porphyromonas gingivalis*, *Capnocytophaga sputigena, Prevotella intermedia*, *Fusobacterium nucleatum, Moraxella bovis* hemolytic strain Epp63-300, *Moraxella bovis* nonhemolytic strain 12040577, *Serratia marcescens, Aquaspirillum serpensVHL.*

***Bdellovibrio* species**	**Susceptible prey**
B. bacteriovorus 6-5-S	*Aquaspirillum serpens* VHL
B. bacteriovorus DM7C, DM8A and DM11A	*Burkholderia cenocepacia* K56-2, *B. cenocepacia* J2315,
B. bacteriovorus strain H16	*V. cholerae* strain GYL*, V. cholerae* strain LD081008B-1*, Vibrio alginolyticus* strain BYK0834*, V. alginolyticus* strain BYK00019, *Vibrio harveyi* strain ZL0022, *V. harveyi* strain BYK00034, *Vibrio vulnificus* strain BYK000965*, Vibrio parahaemolyticus* strain ZL0025, *V. parahaemolyticus* strain ZL0040*, Vibrio anguillarum* strain BYK0638
Micavibrio aeruginosavorus ARL13	*Klebsiella pneumoniae*, *Pseudomonas aeruginosa*, *Pseudomonas* spp., *Burkholderia mallei,*
B.exovorus KL8	*Caulobacter crescentus* CB2A, *E. coli* ML35,
B.exovorus JSS	*Burkholderia cenocepacia* K56-2, *Caulobacter crescentus*
Halophilic BALOs	*Vibrio parahaemolyticus* strain P-5, *Vibrio vulnificus* FLA042, *Vibrio alginolyticus* zouA
Bacteriovorax stolpii	*Vibrio parahaemolyticus*
Peredibacter starrii	*Vibrio parahaemolyticus*
BD2GS	*Salmonella enterica* spp. enterica serovar Typhimurium
Bdellovibrio strain F16	*Aeromonas hydrophila* strain S1
BDH12	*Vibrio parahaemolyticus* strain SH06
BDHSH06	*Vibrio parahaemolyticus* strain SH06
Bdellovibrio BdC1	*Aeromonas hydrophila* strain J-1

*Prey susceptibility for predatory bacteria since 2007.

REFERENCES RELATED TO ANNEX 1

Atterbury, R.J., Hobley, L., Till, R., Lambert, C., Capeness, M.J., Lerner, T.R., Fenton, A.K., Barrow, P., Sockett, R.E., 2011. Effects of orally administered *Bdellovibrio bacteriovorus* on the well-being and Salmonella colonization of young chicks. Appl. Environ. Microbiol. 77, 5794–5803. doi:10.1128/AEM.00426-11

Baker, M., Negus, D., Raghunathan, D., Radford, P., Moore, C., Clark, G., Diggle, M., Tyson, J., Twycross, J., Sockett, E., n.d. Measuring and modelling the response of *Klebsiella pneumoniae* KPC prey to *Bdellovibrio bacteriovorus* predation, in human serum and defined buffer. doi:10.1038/s41598-017-08060-4

Boileau, M.J., Clinkenbeard, K.D., Iandolo, J.J., 2011. Assessment of *Bdellovibrio bacteriovorus* 109J killing of *Moraxella bovis* in an in vitro model of infectious bovine keratoconjunctivitis. Can. J. Vet. Res. 75, 285–291.

Boileau, M.J., Mani, R., Breshears, M.A., Gilmour, M., Taylor, J.D., Clinkenbeard, K.D., 2016. Efficacy of *Bdellovibrio bacteriovorus* 109J for the treatment of dairy calves with experimentally induced infectious bovine keratoconjunctivitis. Am. J. Vet. Res. 77, 1017–1028. doi:10.2460/ajvr.77.9.1017

Borgnia, M.J., Subramaniam, S., Milne, J.L.S., 2008. Three-dimensional imaging of the highly bent architecture of *Bdellovibrio bacteriovorus* by using cryo-electron tomography. J. Bacteriol. 190, 2588–96. doi:10.1128/JB.01538-07

Butan, C., Hartnell, L.M., Fenton, A.K., Bliss, D., Sockett, R.E., Subramaniam, S., Milne, J.L.S., 2011. Spiral architecture of the nucleoid in *Bdellovibrio bacteriovorus*. J. Bacteriol. 193, 1341–1350. doi:10.1128/JB.01061-10

Cao, H., An, J., Zheng, W., He, S., 2015. *Vibrio cholerae* pathogen from the freshwater-cultured whiteleg shrimp Penaeus vannamei and control with *Bdellovibrio bacteriovorus*. J. Invertebr. Pathol. 130, 13–20. doi:10.1016/j.jip.2015.06.002

Cao, H., He, S., Wang, H., Hou, S., Lu, L., Yang, X., 2012. *Bdellovibrios*, potential biocontrol bacteria against pathogenic *Aeromonas hydrophila*. Vet. Microbiol. 154, 413–418. doi:10.1016/j.vetmic.2011.07.032

Chanyi, R.M., Ward, C., Pechey, A., Koval, S.F., 2013. To invade or not to invade: two approaches to a prokaryotic predatory life cycle. doi:10.1139/cjm-2013-0041

Chauhan, A., Williams, H.N., 2008. Biostimulation of estuarine microbiota on substrate coated agar slides: A novel approach to study diversity of autochthonous *Bdellovibrio*- and like organisms. Microb. Ecol. 55, 640–650. doi:10.1007/s00248-007-9307-1

Chen, H., Athar, R., Zheng, G., Williams, H.N., 2011. Prey bacteria shape the community structure of their predators. ISME J. 5, 1314–1322. doi:10.1038/ismej.2011.4

Chu, W.H., Zhu, W., 2010. Isolation of *bdellovibrio* as biological therapeutic agents used for the treatment of *Aeromonas hydrophila* infection in fish. Zoonoses Public Health 57, 258–264. doi:10.1111/j.1863-2378.2008.01224.x

Dashiff, A., Junka, R.A., Libera, M., Kadouri, D.E., 2010. Predation of human pathogens by the predatory bacteria *Micavibrio aeruginosavorus* and *Bdellovibrio bacteriovorus*. J. Appl. Microbiol. 110, 431–444. doi:10.1111/j.1365-2672.2010.04900.x

Dashiff, A., Kadouri, D.E., 2009. A New Method for Isolating Host-Independent Variants of *Bdellovibrio bacteriovorus* Using E. coli Auxotrophs. Open Microbiol. J. 3, 87–91. doi:10.2174/1874285800903000087

Dashiff, A., Keeling, T.G., Kadouri, D.E., 2011. Inhibition of Predation by *Bdellovibrio bacteriovorus* and *Micavibrio aeruginosavorus* via Host Cell Metabolic Activity in the Presence of Carbohydrates . Appl. Environ. Microbiol. 77, 2224–2231. doi:10.1128/aem.02565-10

Dori-Bachash, M., Dassa, B., Peleg, O., Pineiro, S. a, Jurkevitch, E., Pietrokovski, S., 2009. Bacterial intein-like domains of predatory bacteria: a new domain type characterized in *Bdellovibrio bacteriovorus*. Funct. Integr. Genomics 9, 153–66. doi:10.1007/s10142-008-0106-7

Dori-Bachash, M., Dassa, B., Pietrokovski, S., Jurkevitch, E., 2008. Proteome-based comparative analyses of growth stages reveal new cell cycle-dependent functions in the predatory bacterium *Bdellovibrio bacteriovorus*. Appl. Environ. Microbiol. 74, 7152–62. doi:10.1128/AEM.01736-08

Evans, K.J., Lambert, C., Sockett, R.E., 2007. Predation by *Bdellovibrio bacteriovorus* HD100 requires type IV pili. J. Bacteriol. 189, 4850–9. doi:10.1128/JB.01942-06

Fenton, A.K., Lambert, C., Wagstaff, P.C., Sockett, R.E., 2010. Manipulating each *MreB* of *Bdellovibrio bacteriovorus* gives diverse morphological and predatory phenotypes. J. Bacteriol. 192, 1299–311. doi:10.1128/JB.01157-09

Iebba, V., Totino, V., Santangelo, F., Gagliardi, A., Ciotoli, L., Virga, A., Ambrosi, C., Pompili, M.,

De Biase, R. V., Selan, L., Artini, M., Pantanella, F., Mura, F., Passariello, C., Nicoletti, M., Nencioni, L., Trancassini, M., Quattrucci, S., Schippa, S., 2014. *Bdellovibrio bacteriovorus* directly attacks *Pseudomonas aeruginosa* and *Staphylococcus aureus* cystic fibrosis isolates. Front. Microbiol. 5, 1–9. doi:10.3389/fmicb.2014.00280

Iida, Y., Hobley, L., Lambert, C., Fenton, A.K., Sockett, R.E., Aizawa, S.-I., 2009. Roles of Multiple Flagellins in Flagellar Formation and Flagellar Growth Post Bdelloplast Lysis in *Bdellovibrio bacteriovorus*. J. Mol. Biol. 394, 1011–1021. doi:10.1016/j.jmb.2009.10.003

Kadouri, D.E., To, K., Shanks, R.M.Q., Doi, Y., 2013. Predatory bacteria: a potential ally against multidrug-resistant Gram-negative pathogens. PLoS One 8, e63397. doi:10.1371/journal.pone.0063397

Kaneshiro, E.S., Hunt, S.M., Watanabe, Y., 2008. *Bacteriovorax stolpii* proliferation and predation without sphingophosphonolipids. Biochem. Biophys. Res. Commun. 367, 21–25. doi:10.1016/j.bbrc.2007.12.059

Koval, S.F., Hynes, S.H., Flannagan, R.S., Pasternak, Z., Davidov, Y., Jurkevitch, E., 2013. *Bdellovibrio exovorus* sp. nov., a novel predator of *Caulobacter crescentus*. Int. J. Syst. Evol. Microbiol. 63, 146–151. doi:10.1099/ijs.0.039701-0

Lambert, C., Chang, C., Capeness, M.J., Sockett, R.E., 2010. The First Bite — Profiling the Predatosome in the Bacterial Pathogen *Bdellovibrio*. PLoS One 5. doi:10.1371/journal.pone.0008599

Li, H., Liu, C., Chen, L., Zhang, X., Cai, J., 2011. Biological characterization of two marine *Bdellovibrio*-and-like organisms isolated from Daya bay of Shenzhen, China and their application in the elimination of *Vibrio parahaemolyticus* in oyster. Int. J. Food Microbiol. 151, 36–43. doi:10.1016/j.ijfoodmicro.2011.07.036

Loozen, G., Boon, N., Pauwels, M., Slomka, V., Rodrigues Herrero, E., Quirynen, M., Teughels, W., 2015. Effect of *Bdellovibrio bacteriovorus* HD100 on multispecies oral communities. Anaerobe 35, 45–53. doi:10.1016/j.anaerobe.2014.09.011

Lu, F., Cai, J., 2010. The protective effect of *Bdellovibrio*-and-like organisms (BALO) on tilapia fish fillets against *Salmonella enterica* spp. enterica serovar Typhimurium. Lett. Appl. Microbiol. 51, 625–631. doi:10.1111/j.1472-765X.2010.02943.x

Mahmoud, K.K., Koval, S.F., 2010. Characterization of type IV pili in the life cycle of the predator bacterium *Bdellovibrio*. Microbiology 156, 1040–1051. doi:10.1099/mic.0.036137-0

Mahmoud, K.K., McNeely, D., Elwood, C., Koval, S.F., 2007. Design and performance of a 16S rRNA-targeted oligonucleotide probe for detection of members of the genus *Bdellovibrio* by fluorescence in situ hybridization. Appl. Environ. Microbiol. 73, 7488–93. doi:10.1128/AEM.01112-07

Markelova, N.Y., 2010. Predacious bacteria, *Bdellovibrio* with potential biocontrol. Int. J. Hyg. Environ. Health 213, 428–431.

Markelova, N.Y., 2010. Interaction of *Bdellovibrio bacteriovorus* with bacteria *Campylobacter jejun*i and *Helicobacter pylori.* Microbiology 79, 777–779. doi:10.1134/S0026261710060093

Markelova, N.Y., 2007. Survival strategy of *Bdellovibrio*. Microbiology 76, 769–774. doi:10.1134/s0026261707060173

McNeely, D., Chanyi, R.M., Dooley, J.S., Moore, J.E., Koval, S.F., 2016. Biocontrol of *Burkholderia cepacia* complex bacteria and bacterial phytopathogens by *Bdellovibrio bacteriovorus.* Can. J. Microbiol. 63, 350–358. doi:10.1139/cjm-2016-0612

Medina, A. a, Shanks, R.M., Kadouri, D.E., 2008. Development of a novel system for isolating genes involved in predator-prey interactions using host independent derivatives of *Bdellovibrio bacteriovorus* 109J. BMC Microbiol. 8, 33. doi:10.1186/1471-2180-8-33

Medina, A.A., Kadouri, D.E., 2009. Biofilm formation of *Bdellovibrio bacteriovorus* host-independent derivatives. Res. Microbiol. 160, 224–231. doi:10.1016/j.resmic.2009.02.001

Monnappa, A.K., Dwidar, M., Seo, J.K., Hur, J.H., Mitchell, R.J., 2014. *Bdellovibrio bacteriovorus* inhibits Staphylococcus aureus biofilm formation and invasion into human epithelial cells. Sci Rep 4, 3811. doi:10.1038/srep03811

Morehouse, K.A., Hobley, L., Capeness, M., Sockett, R.E., 2011. Three *motAB* stator gene products in *Bdellovibrio bacteriovorus* contribute to motility of a single flagellum during predatory and prey-independent growth. J. Bacteriol. 193, 932–943. doi:10.1128/JB.00941-10

Nguyen, N.-A.T., Sallans, L., Kaneshiro, E.S., 2008. The major glycerophospholipids of the predatory and parasitic bacterium *Bdellovibrio bacteriovorus* HID5. Lipids 43, 1053–63. doi:10.1007/s11745-008-3235-9

Park, S., Kim, D., Mitchell, R.J., Kim, T., 2011. A microfluidic concentrator array for quantitative predation assays of predatory microbes. Lab Chip 11, 2916–2923. doi:10.1039/c1lc20230h

Pineiro, S.A., Stine, O.C., Chauhan, A., Steyert, S.R., Smith, R., Williams, H.N., 2007. Global survey of diversity among environmental saltwater *Bacteriovoracaceae*. Environ. Microbiol. 9, 2441–2450. doi:10.1111/j.1462-2920.2007.01362.x

Piñeiro, S.A., Williams, H.N., Stine, O.C., 2008. Phylogenetic relationships amongst the saltwater members of the genus *Bacteriovorax* using *rpoB* sequences and reclassification of *Bacteriovorax stolpii* as *Bacteriolyticum stolpi*i gen. nov., comb. nov. Int. J. Syst. Evol. Microbiol. 58, 1203–1209. doi:10.1099/ijs.0.65710-0

Richards, G.P., Fay, J.P., Dickens, K.A., Parent, M.A., Soroka, D.S., Boyd, E.F., 2012. Predatory bacteria as natural modulators of *Vibrio parahaemolyticus* and *Vibrio vulnificus i*n seawater and oysters. Appl. Environ. Microbiol. 78, 7455–7466. doi:10.1128/AEM.01594-12

Roschanski, N., Klages, S., Reinhardt, R., Linscheid, M., Strauch, E., 2011. Identification of genes essential for prey-independent growth of *Bdellovibrio bacteriovorus* HD100. J. Bacteriol. 193, 1745–1756. doi:10.1128/JB.01343-10

Roschanski, N., Strauch, E., 2010. Assessment of the Mobilizable Vector Plasmids pSUP202 and pSUP404.2 as Genetic Tools for the Predatory Bacterium *Bdellovibrio bacteriovorus*. doi:10.1007/s00284-010-9748-5

Russo, R., Chae, R., Mukherjee, S., Singleton, E., Occi, J., Kadouri, D., Connell, N., 2015. Susceptibility of Select Agents to Predation by Predatory Bacteria. Microorganisms 3, 903–912. doi:10.3390/microorganisms3040903

Russo, R., Kolesnikova, I., Kim, T., Gupta, S., Pericleous, A., Kadouri, D., Connell, N., 2018. Susceptibility of Virulent *Yersinia pestis* Bacteria to Predator Bacteria in the Lungs of Mice. Microorganisms 7, 2. doi:10.3390/microorganisms7010002

Saxon, E.B., Jackson, R.W., Bhumbra, S., Smith, T., Sockett, R.E., 2014a. *Bdellovibrio bacteriovorus* HD100 guards against *Pseudomonas tolaasii* brown-blotch lesions on the surface of post-harvest *Agaricus bisporus* supermarket mushrooms. BMC Microbiol. 14, 163. doi:10.1186/1471-2180-14-163

Saxon, E.B., Jackson, R.W., Bhumbra, S., Smith, T., Sockett, R.E., 2014b. *Bdellovibrio bacteriovorus* HD100 guards against Pseudomonas tolaasii brown-blotch lesions on the surface of post-harvest Agaricus bisporus supermarket mushrooms. BMC Microbiol. 14. doi:10.1186/1471-2180-14-163

Shanks, R.M.Q., Davra, V.R., Romanowski, E.G., Brothers, K.M., Stella, N. a, Godboley, D.,

Kadouri, D.E., 2013. An Eye to a Kill: Using Predatory Bacteria to Control Gram-Negative Pathogens Associated with Ocular Infections. PLoS One 8, e66723. doi:10.1371/journal.pone.0066723

Shatzkes, K., Chae, R., Tang, C., Ramirez, G.C., Mukherjee, S., Tsenova, L., Connell, N.D., Kadouri, D.E., 2015. Examining the safety of respiratory and intravenous inoculation of *Bdellovibrio bacteriovorus* and *Micavibrio aeruginosavorus* in a mouse model. Nat. Publ. Gr. 1–12. doi:10.1038/srep12899

Shatzkes, K., Singleton, E., Tang, C., Zuena, M., Shukla, S., Gupta, S., Dharani, S., Onyile, O., Rinaggio, J., Connell, N.D., Kadouri, D.E., 2016. Predatory Bacteria Attenuate *Klebsiella pneumoniae* Burden in Rat Lungs. MBio 7, 1–9. doi:10.1128/mbio.01847-16

Shatzkes, K., Singleton, E., Tang, C., Zuena, M., Shukla, S., Gupta, S., Dharani, S., Rinaggio, J., Kadouri, D.E., Connell, N.D., 2017. Examining the efficacy of intravenous administration of predatory bacteria in rats. Sci. Rep. 7, 1–11. doi:10.1038/s41598-017-02041-3

Silva, P.H.F., Oliveira, L.F.F., Cardoso, R.S., Ricoldi, M.S.T., Figueiredo, L.C., Salvador, S.L., Palioto, D.B., Furlaneto, F.A.C., Messora, M.R., 2019. The impact of predatory bacteria on experimental periodontitis. J. Periodontol. doi:10.1002/JPER.18-0485

Steyert, S.R., Messing, S.A.J., Amze, L.M., Gabelli, S.B., Pi??eiro, S.A., 2008. Identification of *Bdellovibrio bacteriovorus* HD100 Bd0714 as a nudix dGTPase. J. Bacteriol. 190, 8215–8219. doi:10.1128/JB.01009-08

Steyert, S.R., Pineiro, S.A., 2007. Development of a novel genetic system to create markerless deletion mutants of *Bdellovibrio bacteriovorus.* Appl. Environ. Microbiol. 73, 4717–4724. doi:10.1128/AEM.00640-07

Tudor, J.J., Davis, J.J., Panichella, M., Zwolak, A., 2008. Isolation of predation-deficient mutants of *Bdellovibrio bacteriovorus* by using transposon mutagenesis. Appl. Environ. Microbiol. 74, 5436–5443. doi:10.1128/AEM.00256-08

Van Essche, M., Quirynen, M., Sliepen, I., Loozen, G., Boon, N., Van Eldere, J., Teughels, W., 2011. Killing of anaerobic pathogens by predatory bacteria. Mol. Oral Microbiol. 26, 52–61. doi:10.1111/j.2041-1014.2010.00595.x

Van Essche, M., Sliepen, I., Loozen, G., Van Eldere, J., Quirynen, M., Davidov, Y., Jurkevitch, E., Boon, N., Teughels, W., 2009. Development and performance of a quantitative PCR for the enumeration of *Bdellovibrionaceae*. Environ. Microbiol. Rep. 1, 228–233.

doi:10.1111/j.1758-2229.2009.00034.x

Volle, C.B., Ferguson, M.A., Aidala, K.E., Nu, M.E., 2008. Quantitative Changes in the Elasticity and Adhesive Properties of *Escherichia coli* ZK1056 Prey Cells During Predation by *Bdellovibrio bacteriovorus* 109J 8102–8110.

Wand, H., Vacca, G., Kuschk, P., Krü Ger, M., Kä Stner, M., 2006. Removal of bacteria by filtration in planted and non-planted sand columns. doi:10.1016/j.watres.2006.08.024

Wen, C.Q., Lai, X.T., Xue, M., Huang, Y.L., Li, H.X., Zhou, S.N., 2009. Molecular typing and identification of *Bdellovibrio*-and-like organisms isolated from seawater shrimp ponds and adjacent coastal waters. J. Appl. Microbiol. 106, 1154–1162. doi:10.1111/j.1365-2672.2008.04081.x

Williams, H.N., Turng, B.F., Kelley, J.I., 2009. Survival response of *Bacteriovorax* in surface biofilm versus suspension when stressed by extremes in environmental conditions. Microb. Ecol. 58, 474–484. doi:10.1007/s00248-009-9499-7

Willis, A.R., Moore, C., Mazon-Moya, M., Krokowski, S., Lambert, C., Till, R., Mostowy, S., Sockett, R.E., 2016. Injections of Predatory Bacteria Work Alongside Host Immune Cells to Treat *Shigella* Infection in Zebrafish Larvae. Curr. Biol. 26, 3343–3351. doi:10.1016/j.cub.2016.09.067

Zheng, G., Wang, C., Williams, H.N., Pineiro, S.A., 2008. Development and evaluation of a quantitative real-time PCR assay for the detection of saltwater *Bacteriovorax*. Environ. Microbiol. 10, 2515–2526. doi:10.1111/j.1462-2920.2008.01676.x

ANNEX 2. SUMMARY OF THE THERAPEUTIC ASSESSMENT OF BALOS AVAILABLE IN THE LITERATURE.

Table 1. Summary of the animal model and human cell lines used for test the potencial use of BALOs as therapeutic agents.

Predatory species	**Type of predation**	**Prey species**	**Animal model / cell line**	**Disease**	**Reference**
B. bacteriovorus Bd-17	Periplasmic predation	*Pseudomonas glycinea*	Soybean	Bacterial blight	Scherff, 1972
B. bacteriovorus HD100	Periplasmic predation	*Salmonella* Enteritis P12109	Chicken	Cecal inflamation due to *Salmonella* action	Atterbury et al., 2011
B. bacteriovorus HD100 *B. bacteriovorus* 109J	Periplasmic predation	*S. marcescens* *P. aeruginosa*	Human corneal-limbal epitheliar cells *Galleria mellonella* (wax moth)	Ocular infections	Shanks et al., 2013

Predatory species	**Type of predation**	**Prey species**	**Animal model / cell line**	**Disease**	**Reference**
BALO strain BDHSH06		*Vibrio parahaemolyticus* strain SH06	*Penaeus monodon* (black tiger shrimp)	Aquatic disease in aquacultures by opportunistic and pathogenic bacteria	Li et al., 2014
B. bacteriovorus HD100	Periplasmic predation	*Escherichia coli* K12	*Caenorhabditis elegans*	Control bacterial infections	Emmert et al., 2014
		Enterobacter aerogenes ATCC 13048			
		Pantoea agglomerans LS005			
		Salmonella enterica serovar Typhimurium LT2			
B. bacteriovorus HD100	Periplasmic predation	*Klebsiella pneumoniae* ATCC 43826 (for predator growth in flask)	Mouse	No pathogenic infection	Shatzkes et al., 2015
B. bacteriovorus 109J					
M.aeruginosavorus ARL-13	epibiotic predation				

Predatory species	**Type of predation**	**Prey species**	**Animal model / cell line**	**Disease**	**Reference**
B. bacteriovorus H16	Periplasmic predation	*V. cholerae* strain GYL, *V. cholerae* strain LD081008B-1, *Vibrio alginolyticus* strain BYK0834, *V. alginolyticus* strain BYK00019, *Vibrio harveyi* strain ZL0022, *V. harveyi* strain BYK00034, *Vibrio vulnificus* strain BYK000965, *Vibrio parahaemolyticus* strain ZL0025, *V. parahaemolyticus* strain ZL0040, *Vibrio anguillarum* strain BYK0638	*Penaeus vannamei* (Whiteleg shrimp)	Skin disease (leg yellowing)	Cao et al., 2015
B. bacteriovorus HD100	Periplasmic predation	*E. coli* O157:H7, *Salmonella*	*Cattle*		Page et al., 2015
B. bacteriovorus HD100 *B. bacteriovorus* 109J *M.aeruginosavorus* ARL-13	Periplasmic predation epibiotic predation	*P. aeruginosa*	Rabit/human keratocytes/corneal stromal keratocytes	Ocular inoculation of the predatory bacteria	Romanowski et al., 2016

Predatory species	**Type of predation**	**Prey species**	**Animal model / cell line**	**Disease**	**Reference**
B. bacteriovorus HD100 *B. bacteriovorus* 109J *M. aeruginosavorus* ARL-13	Periplasmic predation Epibiotic predation	*E.coli* WM3064	Human keratinocytes (HaCaT), human liver epithelial cells (HepG2) (ATCC® HB-8065™), and human kidney epithelial cells (HK-2) (ATCC®CRL-2190™)		Gupta et al., 2016
B. bacteriovorus HD100 *B. bacteriovorus* 109J *M.aeruginosavorus* ARL-13	Periplasmic predation epibiotic predation	*K. pneumoniae* ATCC 43816	Rats	Lung infection (intranasal inoculation)	Shatzkes et al., 2016
B. bacteriovorus HD100	Periplasmic predation	*Shigella* infection	Zebrafish	Brain infection	Willis et al., 2016

Predatory species	**Type of predation**	**Prey species**	**Animal model / cell line**	**Disease**	**Reference**
B. bacteriovorus HD100 *M. aeruginosavorus* ARL-13	Periplasmic predation	*K. pneumoniae* ATCC 43816	Rats	Liver/ blood/	Shatzkes et al., 2017
	epibiotic predation				
B. bacteriovorus HD100	Periplasmic predation	*E. coli* *K. pneumoniae* *S. enterica*		Blood/human serum	Im H et al., 2017
B. bacteriovorus HD100	Periplasmic predation	*K. pneumoniae*		Human serum	Baker et al., 2017
B. bacteriovorus HD100 *M. aeruginosavorus*	Periplasmic predation /epibiotic predation	clinically relevant *mcr-1*-positive prey strain		Free swimming and biofilms of prey cells	Dharani et al., 2017
B. bacteriovorus HD100	Periplasmic predation	Natural periodontitis microbiota	Rats	Periodontitis	Silv et al., 2019

ANNEX 3. REACTIONS INCLUDED IN THE METABOLIC NETWORK THAT WERE REANNOTATED

Table 3. Specific characterization of some ORF included into the *i*CH457 metabolic network with the initial identification based on genome annotation. [(1)]

Rendulic *et al.,* 2004. The abreviations used during this thesis are the standard used in the platform BIGG (http://bigg.ucsd.edu/; (King *et al*., 2016)).

ORF	Previous annotation [(1)]	Specific Annotation in *i*CH457	Reannotation in *i*CH457	Reaction Name	Reaction Formula in *i*CH457	EC number
Bd0950	acetyltransferase	UDP 2,3-diamino-2,3-dideoxy-D-glucose acyltransferase		UGLCPAT2	pentdACP[c] + pmanpGlcpN140[c] -> h[c] + ACP[c] + pmanpGlcpN140N150[c]	
		UDP 2,3-diamino-2,3-dideoxy-D-glucose acyltransferase		UGLCPAT4	tridACP[c] + uGlcpN131[c] -> h[c] + ACP[c] + uGlcpN131N130[c]	
Bd2174	Butyryl-CoA dehydrogenase	acyl CoA dehydrogenase hexanoyl CoA		ACOAD2f	fad[c] + hxcoa[c] <=> fadh2[c] + hx2coa[c]	1.3.99.3
		acyl CoA dehydrogenase octanoyl CoA		ACOAD3f	fad[c] + occoa[c] <=> fadh2[c] + oc2coa[c]	1.3.99.3

ORF	Previous annotation [1]	Specific Annotation in *i*CH457	Reannotation in *i*CH457	Reaction Name	Reaction Formula in *i*CH457	EC number
Bd1973	Butyryl-CoA dehydrogenase	acyl CoA dehydrogenase hexanoyl CoA		ACOAD2f	fad[c] + hxcoa[c] <=> fadh2[c] + hx2coa[c]	1.3.99.3
Bd1852	Enoyl-CoA hydratase		Methylmalonyl-CoA decarboxylase	MMCD	h[c] + mmcoa_S[c] -> co2[c] + ppcoa[c]	4.1.1.41
		methylglutaconyl CoA hydratase		MGCH	h2o[c] + 3mgcoa[c] -> hmgcoa[c]	4.2.1.18
Bd1836	3-hydroxyacyl-CoA dehydrogenase		methylglutaconyl CoA hydratase	MGCH	h2o[c] + 3mgcoa[c] -> hmgcoa[c]	4.2.1.18
		3 hydroxyacyl CoA dehydrogenase acetoacetyl CoA		HACD1i	nad[c] + 3hbcoa[c] -> h[c] + aacoa[c] + nadh[c]	1.1.1.35
Bd1850	3-hydroxyacyl-CoA dehydrogenase	3 hydroxyacyl CoA dehydrogenase acetoacetyl CoA		HACD1i	nad[c] + 3hbcoa[c] -> h[c] + aacoa[c] + nadh[c]	1.1.1.35

ORF	Previous annotation [1]	Specific Annotation in *i*CH457	Reannotation in *i*CH457	Reaction Name	Reaction Formula in *i*CH457	EC number
Bd2095	Acetyl-CoA C-acetyltransferase		3 ketoacyl CoA thiolase	KAT1	aacoa[c] + coa[c] -> 2 accoa[c]	2.3.1.9
				KAT2	coa[c] + 3ohcoa[c] -> accoa[c] + btcoa[c]	2.3.1.9
				KAT3	coa[c] + 3oocoa[c] -> accoa[c] + hxcoa[c]	2.3.1.9
				KAT4	coa[c] + 3odcoa[c] -> accoa[c] + occoa[c]	2.3.1.9
				KAT5	coa[c] + 3oddcoa[c] -> accoa[c] + dcacoa[c]	2.3.1.9
				KAT6	coa[c] + 3otdcoa[c] -> accoa[c] + ddcacoa[c]	2.3.1.9
				KAT7	coa[c] + 3ohdcoa[c] -> accoa[c] + tdcoa[c]	2.3.1.9
				KAT8	coa[c] + 3oodcoa[c] -> accoa[c] + pmtcoa[c]	2.3.1.9
Bd0404	Acetyl-CoA C-acetyltransferase		3 ketoacyl CoA thiolase	KAT1	aacoa[c] + coa[c] -> 2 accoa[c]	2.3.1.9

ORF	Previous annotation [1]	Specific Annotation in *i*CH457	Reannotation in *i*CH457	Reaction Name	Reaction Formula in *i*CH457	EC number
Bd1835	Acetyl-CoA C-acetyltransferase		3 ketoacyl CoA thiolase	KAT2	coa[c] + 3ohcoa[c] -> accoa[c] + btcoa[c]	2.3.1.9
				KAT3	coa[c] + 3oocoa[c] -> accoa[c] + hxcoa[c]	2.3.1.9
				KAT4	coa[c] + 3odcoa[c] -> accoa[c] + occoa[c]	2.3.1.9
				KAT5	coa[c] + 3oddcoa[c] -> accoa[c] + dcacoa[c]	2.3.1.9
				KAT6	coa[c] + 3otdcoa[c] -> accoa[c] + ddcacoa[c]	2.3.1.9
				KAT7	coa[c] + 3ohdcoa[c] -> accoa[c] + tdcoa[c]	2.3.1.9
				KAT8	coa[c] + 3oodcoa[c] -> accoa[c] + pmtcoa[c]	2.3.1.9
			2 Methylacetyl CoA thiolase	MACCOAT	coa[c] + 2maacoa[c] -> accoa[c] + ppcoa[c]	2.3.1.16/ 2.3.1.9
Bd1201	Acetyltransferase		3 Methylbutanoyl CoA acceptor 2 3 oxidoreductase	MBCOAi	fad[c] + ivcoa[c] -> fadh2[c] + 3mb2coa[c]	1.3.8.4/ 1.3.8.7/ 1.3.99.10

ORF	Previous annotation [1]	Specific Annotation in *i*CH457	Reannotation in *i*CH457	Reaction Name	Reaction Formula in *i*CH457	EC number
Bd2728	Oxoglutarate dehydrogenase	2 Oxoadipatelipoamde 2 oxidoreductase decarboxylating and acceptor succinylating		OXOADLR	h[c] + lpam[c] + 2oxoadp[c] -> co2[c] + S_gtrdhdlp[c]	1.2.4.2
Bd3795	Cystathionine gamma-lyase	O-succinylhomoserine lyase (L-cysteine)		SHSL1	cys_L[c] + suchms[c] -> cyst_L[c] + h[c] + succ[c]	4.2.99.9
Bd0796	Phosphopyruvate hydratase		enolase	ENO	2pg[c] <=> h2o[c] + pep[c]	4.2.1.11
Bd2266	Aldehyde dehydrogenase	aldehyde dehydrogenase (acetaldehyde, NAD)		ALDD2xi	nad[c] + h2o[c] + acald[c] <=> 2 h[c] + nadh[c] + ac[c]	1.2.1.3
		beta-Aminopropion aldehyde:NAD+ oxidoreductase		BAMPPALDOX	h2o[c] + nad[c] + bamppald[c] -> 2 h[c] + nadh[c] + ala_B[c]	

ANNEX 4. DEFINITION OF *IN SILICO* MEDIA

1. DEFINITION OF *IN SILICO* RICH MEDIUM

The rich medium described below is based on the *in silico* LB medium described previously (Nogales et al., 2017) and also on conditional essential genes of *Bdellovibrio*. The default Exchange reactions were constrained as follow.

Oxygen: `model=changeRxnBounds(model,'EX_o2(e)',-10,'l')`

Amino acids

```
model=changeRxnBounds(model,'EX_val_L(e)',-5,'l')
model=changeRxnBounds(model,'EX_leu_L(e)',-5,'l')
model=changeRxnBounds(model,'EX_ile_L(e)',-5,'l')
model=changeRxnBounds(model,'EX_ser_L(e)',-5,'l')
model=changeRxnBounds(model,'EX_thr_L(e)',-5,'l')
model=changeRxnBounds(model,'EX_ala_L(e)',-5,'l')
model=changeRxnBounds(model,'EX_aps_L(e)',-5,'l')
model=changeRxnBounds(model,'EX_glu_L(e)',-5,'l')
model=changeRxnBounds(model,'EX_met_L(e)',-5,'l')
model=changeRxnBounds(model,'EX_pro_L(e)',-5,'l')
model=changeRxnBounds(model,'EX_arg_L(e)',-5,'l')
model=changeRxnBounds(model,'EX_trp_L(e)',-5,'l')
model=changeRxnBounds(model,'EX_asn_L(e)',-5,'l')
model=changeRxnBounds(model,'EX_phe_L(e)',-5,'l')
model=changeRxnBounds(model,'EX_tyr_L(e)',-5,'l')
model=changeRxnBounds(model,'EX_cys_L(e)',-5,'l')
model=changeRxnBounds(model,'EX_gly(e)',-5,'l')
model=changeRxnBounds(model,'EX_lys_L(e)',-5,'l')
model=changeRxnBounds(model,'EX_gln_L(e)',-5,'l')
```

Amino acids from dipeptides

The mayor carbon and energy source for *Bdellovibrio* are amino acid from the breakdown of proteins, preferentially dipeptides of alanine (Odelson et al., 1982)

```
model=changeRxnBounds(model,'EX_ALAHIS',-5,'l')
model=changeRxnBounds(model,'EX_ALAMET',-5,'l')
model=changeRxnBounds(model,'EX_ALAASN',-5,'l')
model=changeRxnBounds(model,'EX_ALAPRO',-5,'l')
model=changeRxnBounds(model,'EX_ALAARG',-5,'l')
model=changeRxnBounds(model,'EX_ALAPHE',-5,'l')
model=changeRxnBounds(model,'EX_ALATYR',-5,'l')
model=changeRxnBounds(model,'EX_ALATRP',-5,'l')
model=changeRxnBounds(model,'EX_ALAASP',-5,'l')
model=changeRxnBounds(model,'EX_ALALYS',-5,'l')
model=changeRxnBounds(model,'EX_ALAALA',-5,'l')
model=changeRxnBounds(model,'EX_ALAGLU',-5,'l')
model=changeRxnBounds(model,'EX_ALATHR',-5,'l')
model=changeRxnBounds(model,'EX_ALACYS',-5,'l')
model=changeRxnBounds(model,'EX_ALAGLY',-5,'l')
model=changeRxnBounds(model,'EX_ALAILE',-5,'l')
model=changeRxnBounds(model,'EX_ALASER',-5,'l')
model=changeRxnBounds(model,'EX_ALAVAL',-5,'l')
model=changeRxnBounds(model,'EX_ALAGLN',-5,'l')
```

Vitamins. This medium only provides the auxotrophic metabolites of *B. bacteriovorus* HD100.

Folic Acid (B9): `model=changeRxnBounds(model,'EX_thf(e)',-0.1,'l')`

Pantotenate: `model=changeRxnBounds(model,'EX_ptth(e)',-0.1,'l')`

Piridoxal phosphate: `model=changeRxnBounds(model,'EX_pdx5p(e)',-0.1,'l')`

Biotine (B8): `model=changeRxnBounds(model,'EX_btn(e)',-0.1,'l')`

Lipoate: `model=changeRxnBounds(model,'EX_lipoate(e)',-0.1,'l')`

2. DEFINITION OF *IN SILICO* MINIMAL MEDIUM

In order to define an *in silico* minimal medium, the lower bounds of several exchange reactions were constrained as follows and only the essential reactions have been included.

Oxygen: `model=changeRxnBounds(model,'EX_o2(e)',-10,'l')`

Essential amino acids

```
model=changeRxnBounds(model,'EX_val_L(e)',-0.1,'l')
model=changeRxnBounds(model,'EX_leu_L(e)',-0.1,'l')
model=changeRxnBounds(model,'EX_ile_L(e)',-0.1,'l')
model=changeRxnBounds(model,'EX_ser_L(e)',-0.1,'l')
```

Dipeptides. The rest of amino acid will be providing in form of dipeptides

```
model=changeRxnBounds(model,'EX_ALAHIS',-0.1,'l')
model=changeRxnBounds(model,'EX_ALACYS',-0.1,'l')
model=changeRxnBounds(model,'EX_ALAMET',-0.1,'l')
model=changeRxnBounds(model,'EX_ALAASN',-0.1,'l')
model=changeRxnBounds(model,'EX_ALAPRO',-0.1,'l')
model=changeRxnBounds(model,'EX_ALAARG',-0.1,'l')
model=changeRxnBounds(model,'EX_ALAPHE',-0.1,'l')
model=changeRxnBounds(model,'EX_ALATYR',-0.1,'l')
model=changeRxnBounds(model,'EX_ALATRP',-0.1,'l')
```

Threonine and glycine will be obtained from serine. Aspartic acid and lysine will be obtained from asparagine. Tyrosine will be obtained from phenylalanine.

Vitamins. This medium only provides the auxotrophic metabolites of *B. bacteriovorus* HD100.

Folic Acid (B9): `model=changeRxnBounds(model,'EX_thf(e)',-0.1,'l')`

Pantotenate: `model=changeRxnBounds(model,'EX_ptth(e)',-0.1,'l')`

Piridoxal phosphate: `model=changeRxnBounds(model,'EX_pdx5p(e)',-0.1,'l')`

Biotine (B8): `model=changeRxnBounds(model,'EX_btn(e)',-0.1,'l')`

Lipoate: `model=changeRxnBounds(model,'EX_lipoate(e)',-0.1,'l')`

Definition of *in silico* CAV medium to simulate the growth of BdQ10

In the following, a detailed *in silico* composition of the CAV medium used to verify the possible growth of *Bdellovibrio* cells in CAV medium axenically with *i*CH457 metabolic model, is described. The default Exchange reactions were constrained as follow

Oxigen: `model=changeRxnBounds(model,'EX_o2(e)',-10,'l')`

Amino acids

The amount of each amino acid is select based on the experimental data obtained from the target analysis by GC-MS.

```
model=changeRxnBounds(model,'EX_ala_L(e)',-0.018,'l')
model=changeRxnBounds(model,'EX_val_L(e)',-0.011,'l')
model=changeRxnBounds(model,'EX_leu_L(e)',-0.011,'l')
model=changeRxnBounds(model,'EX_ile_L(e)',-0.01,'l')
model=changeRxnBounds(model,'EX_pro_L(e)',-0.004,'l')
model=changeRxnBounds(model,'EX_gly(e)',-0.01,'l')
model=changeRxnBounds(model,'EX_ser_L(e)',-0.02,'l')
model=changeRxnBounds(model,'EX_thr_L(e)',-0.009,'l')
model=changeRxnBounds(model,'EX_asp_L(e)',-0.02,'l')
model=changeRxnBounds(model,'EX_glu_L(e)',0.012,'l')
model=changeRxnBounds(model,'EX_phe_L(e)',-0.0064,'l')
model=changeRxnBounds(model,'EX_lys_L(e)',-0.0032,'l')
model=changeRxnBounds(model,'EX_arg_L(e)',-0.0028,'l')
model=changeRxnBounds(model,'EX_trp_L(e)',-0.001,'l')
model=changeRxnBounds(model,'EX_tyr_L(e)',-0.00248,'l')
```

Dipeptides

Conditional essential genes found in Barabote et al., 2009.

```
model=changeRxnBounds(model,'EX_ALAHIS',-0.0001,'l')
model=changeRxnBounds(model,'EX_ALACYS',-0.0001,'l')
model=changeRxnBounds(model,'EX_ALAMET',-0.0001,'l')
model=changeRxnBounds(model,'EX_ALAASN',-0.0001,'l')
model=changeRxnBounds(model,'EX_ALATYR',-0.01,'l')
model=changeRxnBounds(model,'EX_ALATRP',-0.01,'l')
```

Vitamins. This medium only provides the auxotrophic metabolites of *B. bacteriovorus* HD100.

Folic Acid (B9): `model=changeRxnBounds(model,'EX_thf(e)',-0.1,'l')`

Pantotenate: `model=changeRxnBounds(model,'EX_ptth(e)',-0.1,'l')`

Piridoxal phosphate: `model=changeRxnBounds(model,'EX_pdx5p(e)',-0.1,'l')`

Biotine (B8): `model=changeRxnBounds(model,'EX_btn(e)',-0.1,'l')`

Lipoate: `model=changeRxnBounds(model,'EX_lipoate(e)',-0.1,'l')`

3. OTHER CHEMICALS INCLUDED IN ALL THE MEDIA BASED ON NOGALES ET AL., 2017

Reaction Name	Reaction Description	Lower bond ($mmol \cdot gDW^{-1} \cdot h^{-1}$)	Lower bond ($mmol \cdot gDW^{-1} \cdot h^{-1}$)
EX_co2(e)	Exchange of CO_2	-30	1000
EX_fe2(e)	Exchange of Fe_2	-30	1000
EX_h(e)	Exchange of H	-50	1000
EX_h2o(e)	Exchange of H_2O	-30	1000
EX_hco3(e)	Exchange of HCO_3	-30	1000
EX_na1(e)	Exchange Na	-30	1000
EX_nh4(e)	Exchange NH_4	-30	1000
EX_pi(e)	Exchange Pi	-30	1000
EX_so4(e)	Exchange SO_4	-30	1000

ANNEX 5. SPECIFIC METABOLIC CONTENT IN *i*CHAP AND *i*CHGP.

AP		**GP**	
Abbr.	**Reaction name**	**Abbr.**	**Reaction name**
ACONTa	aconitase half reaction A Citrate hydro lyase	ACACCT	acetyl-CoA:acetoacetyl-CoA transferase
ACONTb	aconitase half-reaction B Isocitrate hydro lyase	ACOAD20	acyl CoA dehydrogenase 2 methylbutnoyl CoA
ACS	acetyl CoA synthetase	ACOADH2	acyl CoA dehydrogenase Isobutiryl CoA
ADA	Adenosine deaminase	ADSL1r	adenylsuccinate lyase
ADD	adenine deaminase	ADSL2r	adenylosuccinate lyase
ADPT	adenine phosphoribosyltransferase	AGPAT120	1 tetradecanoyl sn glycerol 3 phosphate O acyltransferase n C120
AGM3Pt2pp	GlcNAc anhMurNAc tripeptide transport in via proton symport periplasm	AGPAT140	1 tetradecanoyl sn glycerol 3 phosphate O acyltransferase n C140
AGM4Pt2pp	GlcNAc anhMurNAc tetrapeptide transport in via proton symport periplasm	AGPAT141	1 tetradec 7 enoyl sn glycerol 3 phosphate O acyltransferase n C141
AGMt2pp	GlcNAc anhMurNAc transport in via proton symport periplasm	AGPAT160	1 hexadecanoyl sn glycerol 3 phosphate O acyltransferase n C160
AKP1	alkaline phosphatase Dihydroneopterin	AGPAT161	1 hexadec 7 enoyl sn glycerol 3 phosphate O acyltransferase n C161
ASP1DC	aspartate 1-decarboxylase	AGPAT180	1 octadecanoyl sn glycerol 3 phosphate O acyltransferase n C180

AP		GP	
Abbr.	**Reaction name**	**Abbr.**	**Reaction name**
ASPTA	aspartate transaminase	AGPAT181	1 octadec 7 enoyl sn glycerol 3 phosphate O acyltransferase n C181
CATpp	catalase periplasm	AICART	phosphoribosylaminoimidazolecarboxamide formyltransferase
CDAPPA120	CDP-Diacylglycerol pyrophostatase (n-C12:0)	ASPO4	L-aspartate oxidase
CDAPPA140	CDP-Diacylglycerol pyrophosphatase (n-C14:0)	CBPS	carbamoyl phosphate synthase glutamine hydrolyzing
CDAPPA141	CDP-Diacylglycerol pyrophostatase (n-C14:1)	CCGS	7 cyano 7 carbaguanine synthase
CDAPPA160	CDP-Diacylglycerol pyrophostatase (n-C16:0)	CDGS	7 deaza 7 carboxyguanine synthase
CDAPPA161	CDP-Diacylglycerol pyrophostatase (n-C16:1)	CYTD	cytidine deaminase
CDAPPA180	CDP-Diacylglycerol pyrophostatase (n-C18:0)	CYTK1	cytidylate kinase CMP
CDAPPA181	CDP-Diacylglycerol pyrophostatase (n-C18:1)	CYTK2	cytidylate kinase dCMP
CHORS	chorismate synthase	DCYTD	deoxycytidine deaminase
CYTDK2	cytidine kinase (GTP)	DHNAOT	1 4 dihydroxy 2 naphthoate octaprenyltransferase
DURIPP	deoxyuridine phosphorylase	DHORD1	dihydroorotic acid dehydrogenase quinone8
ECOAE	3 hydroxyacyl CoA dehydratase 3 hydroxybutanoyl CoA	DTMPK	dTMP kinase

AP		GP	
Abbr.	**Reaction name**	**Abbr.**	**Reaction name**
ECOAH12	3 hydroxyacyl CoA dehydratase 3 hydroxyisobutyryl CoA	FGLU	formimidoylglutamase
ECOAH9	2 Methylprop 2 enoyl CoA 2 Methylbut 2 enoyl CoA	GARFT	phosphoribosylglycinamide formyltransferase
GLYOX	hydroxyacylglutathione hydrolase	GLUK	Glucokinase
GPDDA2	Glycerophosphodiester phosphodiesterase Glycerophosphoethanolamine	HEMEOS	Heme O synthase
GPDDA4	Glycerophosphodiester phosphodiesterase Glycerophosphoglycerol	HISD	histidase
HACD1	3-hydroxyacyl-CoA dehydrogenase (acetoacetyl-CoA)	HISTP	histidinol phosphatase
HACD2i	3 hydroxyacyl CoA dehydrogenase 3 oxohexanoyl CoA	HSTPTr	histidinol phosphate transaminase
HACD3i	3 hydroxyacyl CoA dehydrogenase 3 oxooctanoyl CoA	MACACI	maleylacetoacetate isomerase
HACD4i	3 hydroxyacyl CoA dehydrogenase 3 oxodecanoyl CoA	MBCOAi	3 Methylbutanoyl CoA acceptor 2 3 oxidoreductase
HACD5i	3 hydroxyacyl CoA dehydrogenase 3 oxododecanoyl CoA	MCTP1App	murein crosslinking transpeptidase 1A A2pm D ala periplasm

AP		GP	
Abbr.	**Reaction name**	**Abbr.**	**Reaction name**
HACD6i	3 hydroxyacyl CoA dehydrogenase 3 oxotetradecanoyl CoA	MCTP1Bpp	murein crosslinking transpeptidase 1B A2pm A2pm periplasm
HACD7i	3 hydroxyacyl CoA dehydrogenase 3 oxohexadecanoyl CoA	MCTP2App	murein crosslinking transpeptidase 1A A2pm D ala periplasm
HACD9	3 hydroxyacyl CoA dehydrogenase 2 Methylacetoacetyl CoA	ME1	malic enzyme (NAD)
HXAND	hypoxanthine dehydrogenase	MOAT	3-deoxy-D-manno-octulosonic acid transferase
MDDCP1pp	murein D D carboxypeptidase murein5px4p periplasm	MOAT2	3-deoxy-D-manno-octulosonic acid transferase
MDDCP2pp	murein D D carboxypeptidase murein5px4px4p periplasm	OCOAT1	3 oxoacid CoA transferase Succinyl CoA acetoacetate
MDDCP3pp	murein D D carboxypeptidase murein5p5p periplasm	OCTDPS	Octaprenyl pyrophosphate synthase
MDDCP4pp	murein D D carboxypeptidase murein5p4p periplasm	PRAGSr	phosphoribosylglycinamide synthase
MDDCP5pp	murein D D carboxypeptidase murein5p3p periplasm	PRAIS	phosphoribosylaminoimidazole synthase
MICITDr	2 methylisocitrate dehydratase	RHACOAR100	3R 3 Hydroxyacyl CoANADP oxidoreductase

AP		GP	
Abbr.	**Reaction name**	**Abbr.**	**Reaction name**
NADH10	NADH dehydrogenase (menaquinone-8 & 0 protons)	RHACOAR120	R Hydroxyacyl CoANADP oxidoreductase
PEPCK_re	phosphoenolpyruvate carboxykinase GTP	RHACOAR140	3R 3 Hydroxyacyl CoANADP oxidoreductase
PHETA1	phenylalanine transaminase	RHACOAR80	3R 3 Hydroxyacyl CoANADP oxidoreductase
PPS	phosphoenolpyruvate synthase	U23GAAT	UDP-3-O-(3-hydroxymyristoyl)glucosamine acyltransferase
RNTR4	ribonucleoside triphosphate reductase UTP	UAGPT3	UDP N acetylglucosamine N acetylmuramyl pentapeptide pyrophosphoryl undecaprenol N acetylglucosamine transferase
SSALy	succinate semialdehyde dehydrogenase NADP	UDCPDP	undecaprenyl diphosphatase
UPPRT	uracil phosphoribosyltransferase	ALAASPabcpp	L-Alaninylaspartate (alaasp) transport outer membrane
URIK2	uridine kinase (GTP:Uridine)	ALAGLUabcpp	L-Alaninylglutamate (LalaLglu) transport outer membrane
XAND	xanthine dehydrogenase	ALAHISabcpp	L-Alaninylhistidine (Ala-His) transport outer membrane
CLt3_2pp	chloride transport out via proton antiport (2:1) (periplasm) (ClcA)	ALAMETabcpp	L-AlaninylMethionine (Ala-Met) transport outer membrane
SPMDabcpp	spermidine transport via ABC system (periplasm)	ALAPROabcpp	L-AlaninylProline (Ala-Pro) transport outer membrane

AP		GP	
Abbr.	**Reaction name**	**Abbr.**	**Reaction name**
PTRCabcpp	putrescine transport via ABC system (periplasm)	ALAARGabcpp	L-AlaninylArginine (Ala-Arg) transport outer membrane
PPTabcpp	phosphonate-transporting ATPase	ALACYSabcpp	L-AlaninylCysteine (Ala-Cys) transport outer membrane
CA2abc	calcium transport via ABC system	ALAILEabcpp	L-AlaninylIsoleucine (Ala-Ile) transport outer membrane
Cuabcpp	Copper ABC transporter (periplasm)	ALALYSabcpp	L-AlaninylLysine (Ala-Lys) transport outer membrane
Agabcpp	Ag ABC transporter (periplasm)	ALAPHEabcpp	L-AlaninylPhenylalanine (Ala-Phe) transport outer membrane
Cu2abcpp	Copper2+ ABC transporter (periplasm)	ALASERabcpp	L-AlaninylSerine (Ala-Ser) transport outer membrane
MG2tpp	magnesium (+2) transport in via diffusion	ALATRPabcpp	L-Alaninyltryptophan (Ala-Trp) transport outer membrane
ACOAHi	acetyl-CoA hydrolase	ALAASNabcpp	L-AlaninylAsparagine (Ala-Asn) transport outer membrane
PTHK	pantetheine kinase	ALAGLNabcpp	L-AlaninylGlutamine (Ala-Gln) transport outer membrane
PANTS	pantothenate synthase	PPIuabcpp	phosphate transport via ABC system (uptake, periplasm)
PNTK	pantothenate kinase	GLYCL	Glycine Cleavage System
PPNCL2	phosphopantothenate cysteine ligase	LYSMOX	Lysine N6 monooxygenase
		ARBTNS	aerobactin synthase
		DB4PS	3,4-Dihydroxy-2-butanone-4-phosphate synthase

AP		GP	
Abbr.	**Reaction name**	**Abbr.**	**Reaction name**
		OGMEACPR	3-Oxo-glutaryl-[ACP] methyl ester reductase
		OPMEACPR	3-Oxo-pimeloyl-[ACP] methyl ester reductase
		4HTHRS	4 Hydroxy L threonine synthase
		RBFSa	riboflavin synthase a
		HOMt2pp	L-homoserineserine efflux via proton symport
		THRt2pp	L-threonine efflux transport via proton antiport (periplasm)
		CYSTRS	Cysteinyl-tRNA synthetase
		TRPO2	L-Tryptophan:oxygen 2,3-oxidoreductase (decyclizing)
		PRFGS	phosphoribosylformylglycinamidine synthase
		VALabcpp	L valine transport via ABC system periplasm
		LEUabcpp	L leucine transport via ABC system periplasm
		THRabcpp	L threonine transport via ABC system periplasm
		GLNabcpp	L-glutamine transport via ABC system (periplasm)
		G3PAT120	glycerol 3 phosphate acyltransferase C120

AP		GP	
Abbr.	**Reaction name**	**Abbr.**	**Reaction name**
		G3PAT140	glycerol 3 phosphate acyltransferase C140
		G3PAT141	glycerol 3 phosphate acyltransferase C141
		G3PAT160	glycerol 3 phosphate acyltransferase C160
		G3PAT161	glycerol 3 phosphate acyltransferase C161
		G3PAT161	glycerol 3 phosphate acyltransferase C161
		G3PAT180	glycerol 3 phosphate acyltransferase C180
		G3PAT181	glycerol 3 phosphate acyltransferase C181
		GTPCII2	GTP cyclohydrolase II (25drapp)
		MPTG	murein polymerizing transglycosylase
		MPTG2	murein polymerizing transglycosylase 2 (three linked units)
		NNDPR	nicotinate-nucleotide diphosphorylase (carboxylating)
		BACCL	biotin-[acetyl-CoA-carboxylase] ligase
		LIPAMPL	Lipoyl-adenylate protein ligase
		LIPATPT	Lipoate-ATP adenylate transferase
		LYSTRS	Lysyl-tRNA synthetase
		PHETRS	Phenylalanyl-tRNA synthetase

ANNEX 6. Q-TOF-MS CHROMATOGRAMS

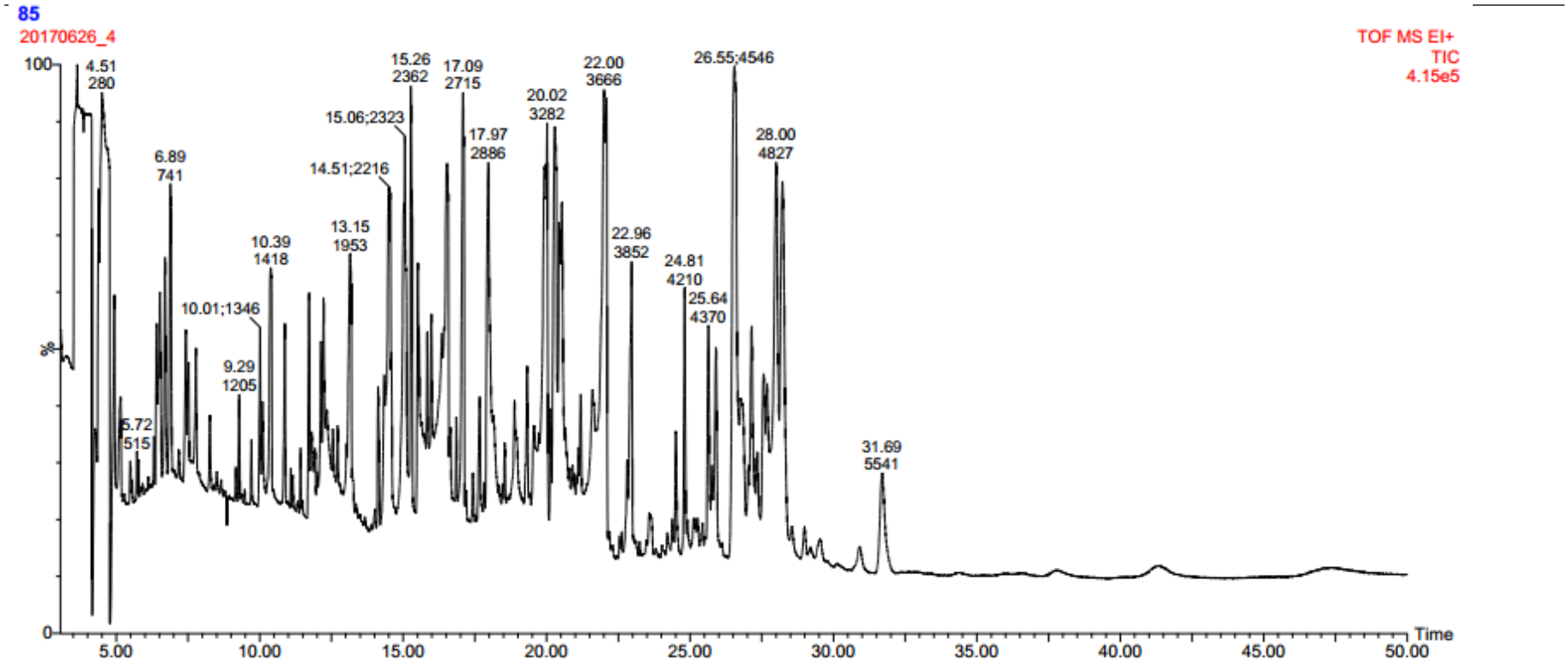

Figure 35. GC-QTOF-MS chromatograms of PYE10 at time 0

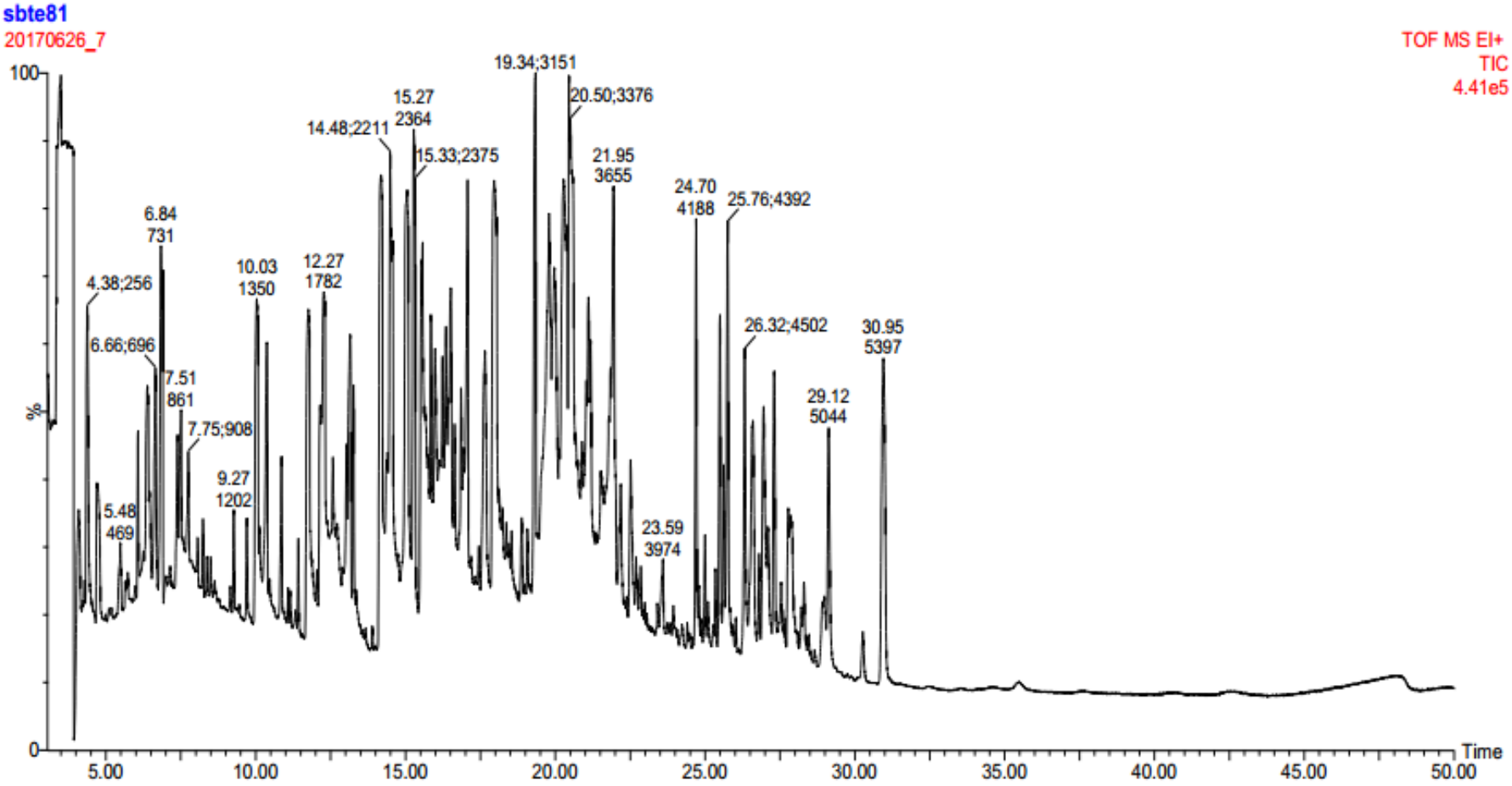

Figure 36. GC-QTOF-MS chromatograms of PYE10 at 48h

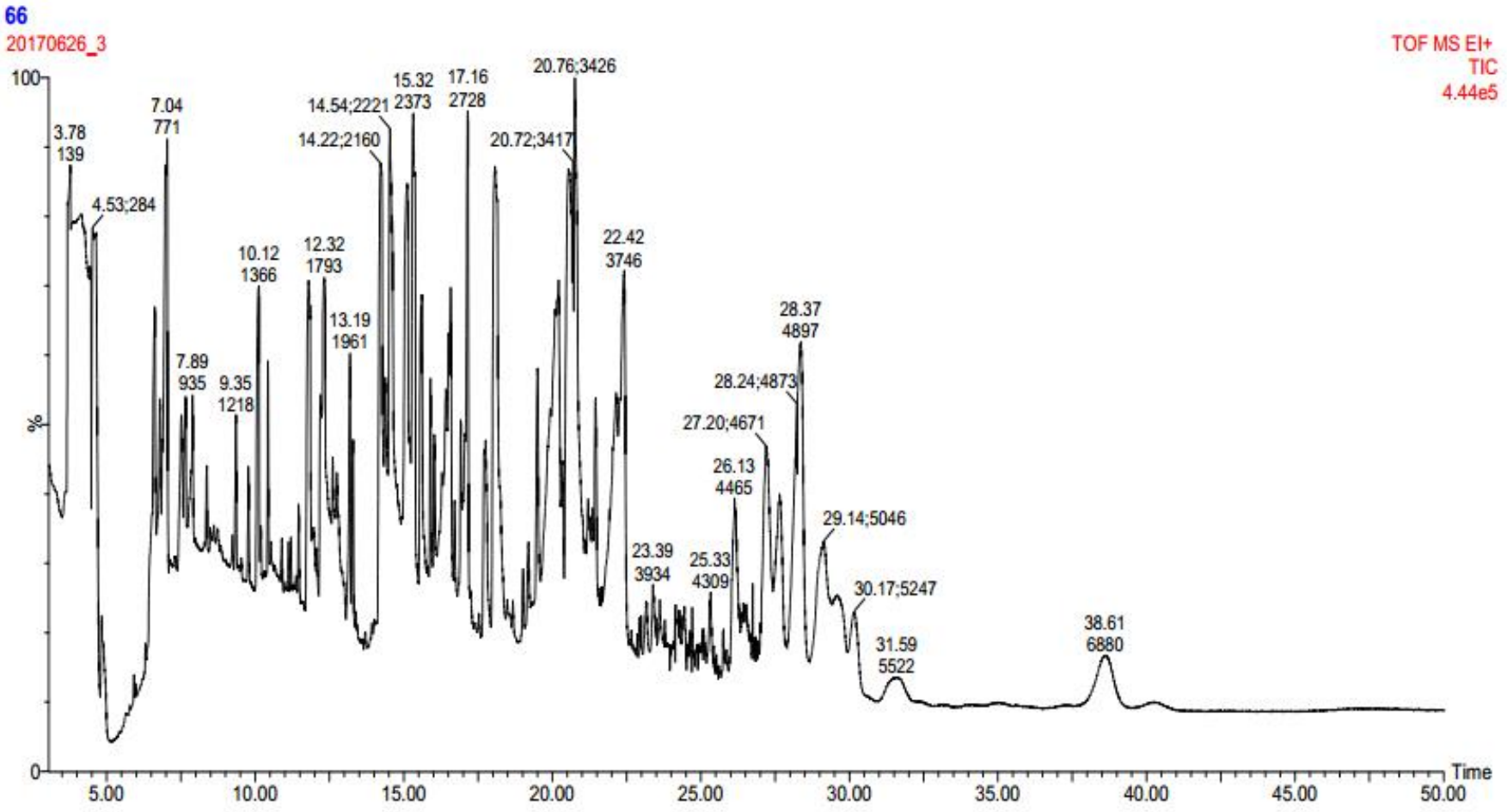

Figure 37. GC-QTOF-MS chromatograms of the supernatant of PYE10 with Bd after 48h.

Table 14. **Retention time of the compounds identified in the GC-QTOF-MS analysis.** Different retention times could be detected for the same compound due to the number of silyl groups attached to that compound.

Metabolite	RT (min)
5,6-dihydro-3-(hydroxymethyl)-2-methyl-1,4-oxathiin	6,386
ethylamine	6,454
carbodiimide	6,836
ethylene glycol	7,389
1,3,3-trimethyloxindole	7,508
silane	7,751
acetic acid	9,704
L-valine	10,035 ; 13,146
alanine	10,371
glycine	10,862
L-norvaline	12,722
serine	14,184; 16,133; 16,515
phosphate	14,484
L-threonine	15,058; 17,073
glycine	15,275
butanedioic acid	15,538
propanoic acid	15,569
fumaric acid	16,35
L-methionine	17,652
malic acid	19,342
L-proline	19,853
L-glutamic acid	20,272
rythronic acid	20,458
phenylalanine	20,551
1-H-indole-2-acetic acid	21,037
10-hydroxybenzoflavine	21,182
glutamine	21,946

Metabolite	RT (min)
arabinofuranose	22,51
phosphoric acid	24,701
D-altrose	25,497
ornithine	26,323
arabinohexanoic acid	26,597
tyrosine	26,954
D-glucose	27,099
D-galactose	27,305
D-mannitol	27,776; 27,894
alpha-D-mannopyranoside	27,843
D-gluconic acid	29,124
hexadecanoic acid	30,27
inositol	30,949